CO_2 Injection for Enhanced Gas Condensate Recovery

An Experimental and Theoretical Study

Ifeanyi Seteyeobot

Submitted for the degree of Doctor of Philosophy

Heriot-Watt University

School of Energy Geoscience Infrastructure and Society

October 2023

ABSTRACT

CO_2 injection in gas condensate reservoirs has been identified as a viable technique for alleviating condensate banking and enhancing gas condensate recovery (EGCR) favoured due to prospects of storing CO_2 in long terms. Multiple-contact miscibility (MCM) with vaporising method is recommended to extract maximum gas condensate and avoid leaving precious gas condensate fractions behind.

The research involves extensive PVT and core flood tests using CO_2 and a binary gas condensate fluid sample across a range of core permeabilities. Steady-state CO_2-condensate relative permeability data is gathered to improve H-n-P CO_2 injection simulations for enhanced gas condensate recovery and CO_2 storage. The Schlumberger E300 compositional simulator was employed to simulate incremental H-n-P CO_2 injection, shut-in, and production cycles, mirroring laboratory experiments. The simulation results emphasize the importance of using accurate CO_2-GC kr data and accounting for compositional changes during H-n-P CO_2 injection.

In the following chapters, a practical framework was suggested based on the results to accurately identify and quantify the effects of CO_2-GC interaction during CO_2 injection for enhanced gas condensate recovery. Furthermore, the miscibility pressure of CO_2 and gas condensate sample was optimised to enhance the swelling and vaporisation mechanism and determine the best injection scenarios at pressures below and above the dew point for optimal gas condensate recovery and CO_2 storage purposes. The hydrocarbon recovery efficiency of the suggested injection technique for EGCR was tested on high to ultra-low permeability core samples. The recovery efficiency of this optimised plan was observed to surpass the conventional H-n-P CO_2 injection albeit with five times less the volume of CO_2 required during the conventional injection approach. The volume of injected CO_2 was constrained by pressure limits over which the variation in maximum condensate saturation is minimal. Results indicate that condensate recovery significantly improves, reaching 69.7% after the fourth H-n-P CO_2 injection cycle, with 49.5% additional condensate recovery post primary depletion phase and 48.6% cumulative CO_2 storage. At the end of the proposed H-n-P CO2 injection, the total gas produced had an 85.9% and a 14.1% hydrocarbon and CO2 content respectively.

The experimental data reported in this thesis allow bridging the gap between conflicting reports on the CO_2-GC fluid interactions at pressures below and above the dew point pressure (P_{Dew}) and provides a solid cornerstone to design optimised H-n-P CO_2 injection scenarios for EGCR and CO_2 storage purposes.

DEDICATION

To my Family and Especially my Beloved Parents Who taught me" Everything Happens for a Reason"

To my Father Elder Sebas Seteyeobot who gave all to ensure that I become who I am today.

ACKNOWLEDGEMENT

First and foremost, I would like to express my deep gratitude to my supervisor Professor. Mahmoud Jamiolahmady for his technical guidance, encouragement, and support throughout my thesis work. I wish to express my gratefulness to Professor. Gillian, E. Pickup, and Professor Eric Mackay who kindly accepted to be my mentor during the first review of my PhD studies. I would also like to thank Professor. Phillip Jaeger for his precious technical comments which shaped my research.

The technical suggestions and input of Dr. Hosein Doryanidaryuni, Adam Sisson, and Shawn Ireland for improving this thesis are also much appreciated. I also wish to express my warmest thanks to Prof. Eric Mackay and Seyed Shariatipour for their time to review my PhD thesis and providing valuable technical comments. This study was conducted at Heriot-Watt University as a part of the Gas condensate research programme which was sponsored by Saudi Aramco and Petroleum Trust Development Funds whose financial support is gratefully acknowledged.

Finally, I would like to express my sincere gratitude to Dr. Shokoufeh Aghabozorgi Nafchi for sharing her valuable knowledge and experience with me during my studies.

I could not have accomplished so much without the help and support from you all. Thank you very much.

TABLE OF CONTENTS

LIST OF FIGURES

LIST OF TABLES

GLOSSARY

Σ: Summation

BIC: Binary Interaction Coefficient

CCE: Constant Composition Expansion

CO_2-GC: CO_2- Gas Condensate

EGCR: Enhanced Gas Condensate Recovery

EOS: Equation of State

FCM: First Contact Miscibility

FCMP: First Contact Miscibility Pressure, psi

GC: Gas Condensate

GHG: Greenhouse Gas

H-n-P: Huff and Puff Injection

HPHT: High Pressure High Temperature

IFT: Interfacial Tension (mN/m)

LDO: Liquid Dropout, Fraction, or Percentage (%)

LDO_{Max}: Maximum Liquid Dropout, Fraction, or Percentage (%)

LDO_{ref}: Maximum Liquid Saturation @ 0%SCCO2 Injection

LSAT: Liquid Saturation, Fraction, or Percentage

$LSAT_{x\%CO2}$: Maximum Liquid Saturation @ x% of CO2 Injected

$LSAT_{ref:}$ Liquid Saturation @ Reference CO_2 injection Point

MCM: Multiple Contact Miscibility

MMP: Minimum Miscibility Pressure, psi

NIST: National Institute of Standards and Technology

PVT: Pressure Volume Temperature (refers to thermodynamic properties of the fluid)

P_{Dew}: Dew Point Pressure, psi

S_{ci}: Initial Condensate Saturation

VIFT: Vanishing Interfacial Tension (mN/m)

V_{CO2_Cum}: Cumulative Volume of CO_2, %,

V_{CO2_Inj}: Volume of CO_2 Injected, scc.

V_{CO2_Prod}: Volume of CO_2 Produced, scc.

LIST OF PUBLICATIONS

- Seteyeobot, I., Jamiolahmady, M., & Jaeger, P., "*An Experimental Study of the Effects of* CO_2 *Injection on Gas-Condensate Recovery and* CO_2 *Storage in Gas-Condensate Reservoirs"*. Paper presented at the SPE Annual Technical Conference and Exhibition, Dubai, UAE, September 21–23, 2021.

- Seteyeobot I, & Jamiolahmady, M., "*Experimental Measurement and Equation of State Modelling of* CO_2 *and a Gas Condensate Binary Mixture"*. Paper presented at the 82nd EAGE Annual Conference and Exhibition, Amsterdam, Netherlands, September 2021.

- Seteyeobot, I, Jamiolahmady, M., Molokwu, V., & Jaeger, P., "*Comparison of Experimental and Simulation Study of a Novel* CO_2 *H-n-P Injection Technique for Improved Gas Condensate Recovery and* CO_2 *Storage in Gas Condensate Reservoirs"*. Paper presented at SPE Annual Technical Conference and Exhibition, Houston, Texas, USA, October 2-5, 2022.

Chapter 1 - Introduction

1.1 Background

The process of hydrocarbon exploration and exploitation is an environmentally invasive and expensive process. Following the energy crisis in 1979, the interventions aiming to enhance hydrocarbon recovery attracted significant attention in both academia and industry. The research in this area slowed down with advances in exploration and drilling techniques which broadened the access to abundant hydrocarbon resources. However, a growing interest to reduce carbon footprint of energy resources encouraged endeavours in this field recently. One of effective methods for improving hydrocarbon recovery is CO2 injection which can also contribute to meeting net-zero goals by permanent storage of the captured CO2 in the reservoir.

Enhanced hydrocarbon recovery is mainly referred to as EOR (enhanced oil recovery) emphasising on the use of such methods for reducing residual oil in the reservoir. However, these methods can be applied to gas reservoirs too, specifically gas condensate reservoirs. These reservoirs exist initially as a single-phase gas system but as the pressure declines below dew point pressure, the heavier fraction of the gas condenses and form a liquid phase. With further reduction in reservoir pressure, the gas condensate saturation builds up reaching mobility and a two-phase flow of gas and condensates can be observed in the reservoir. Condensates are typically low-viscosity liquids in ambient conditions, so they are often used to dilute highly viscous heavier oils that cannot otherwise be efficiently transported via pipelines. The increased use of condensate as diluent significantly increased its price in certain regions (Lewis, 2013). Methods aimed to prevent formation of gas condensates or to increase the recovery of gas condensates are known as Enhanced Gas Condensate Recovery (EGCR).

Commonly, gas-condensate reservoirs occur naturally at pressures ranging from about 3000-8500 psi and temperatures of 200-400 ^{o}F, exhibiting gas-oil ratios in the range of 5000-100,000 SCF/bbl and liquid with specific gravity equal to or greater than 45^{o} API (Craft & Hawkins, 1959). With recent advances in exploration of deeper formations, the potential to encounter gas and gas condensate reservoirs is very likely. In addition, early carefully designed intervention plans for the depleting reservoirs prevents loss of valuable condensates in the reservoir. Therefore, enhanced gas condensate recovery has attracted significant attention recently. Also, as mentioned earlier, it is ideal to use CO_2 gas for

such purposes as a cheaper alternative to lean gas and to alleviate meeting the global net-zero targets.

The phase diagram of a typical gas condensate fluid is shown in Figure 1.1 which clearly describes the phase changes throughout the life of the reservoir. In this phase diagram determination of cricondentherm (the highest temperature of phase envelope above which a liquid cannot be formed) is very important. In this case it is equal to 250°F.

Depletion of hydrocarbon reservoirs is mainly an iso-thermal process with declining pressure. Depending on the initial reservoir temperature and the cricondentherm of the gas condensate fluid, the two-phase gas and condensate flow may form or not. As observed in below figure, if the initial reservoir temperature is higher than cricondentherm, the isothermal depletion of the reservoir does not intersect with the phase envelope resulting in a single-phase gas reservoir (path shown from A to A_1).

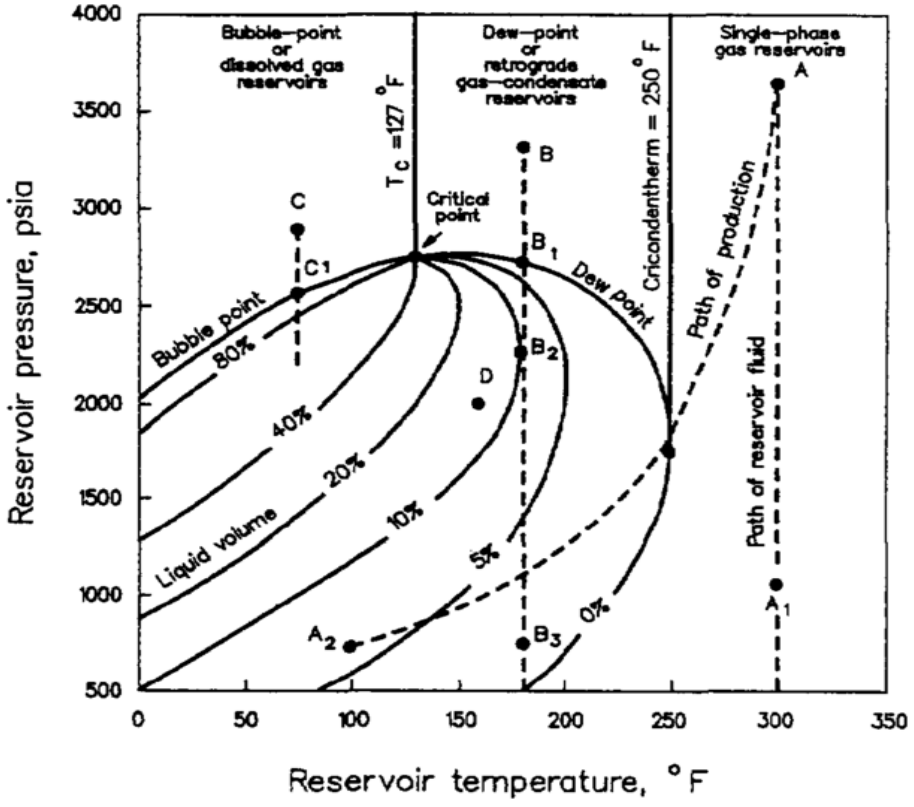

Figure 1.1: Classification of Reservoir Fluid (AAPG Wiki, January 2014).

However, if the initial reservoir temperature is more than critical temperature and below cricondentherm, the reservoir fluid is a single-phase gas at point B (above the dew point pressure). As pressure drops from point B to B_3, some of the gas begins to condense when the system pressure reaches the dew point pressure at point B_1. As pressure drops further, some of this condensate evaporates, and if the total composition remains the same, a second dew point may be observed with further pressure reduction at point B_2.

The observation of a second dew point is unlikely in the reservoir as the composition does not remain constant due to production of lighter components. If the reservoir temperature happen to be very low (below the critical temperature of the gas condensate), the reservoir initial condition would be a single-phase oil reservoir and a typical depletion of an oil reservoir with a bubble point is expected. Hence, an adequate understanding of the phase diagram and precise determination of critical temperature and cricondentherm cannot be overemphasized for accurate simulations of the gas condensates bearing reservoirs.

The fluid flow behaviour of gas condensate reservoirs is attributed to the pore size distribution of the condensate phase and the variation of the interfacial tension (IFT) between the gas and condensate phases. Small changes in pressure can cause significant changes in the IFT of gas and condensate. As capillary pressure is a direct function of IFT, the capillary trapping and loss of gas condensates is higher at high IFTs. In addition to the loss of valuable condensate fraction in the reservoir, the formed liquid phase gradually becomes mobile and migrates towards the wellbore (called gas condensate banking). An accumulation of gas condensates at the areas near wellbore reduces the gas productivity index of the well significantly. So, the benefits of EGCR methods is two folded: first preventing the loss of valuable condensates and second, maintaining high gas productivity index by vaporising or mobilising the gas condensate bank.

The gradual build-up and accumulation of condensate in these reservoirs significantly decreases the gas relative permeability at the near-wellbore region. This phenomenon makes the fluid composition and flow behaviour in these reservoirs different from those in conventional gas-oil systems. It has been established that gas productivity loss is more significant in low-permeability gas condensate reservoirs, necessitating a detailed study of low-permeability samples (Phillips & Charles, 1987).

It was also observed by Afidick et al. (1994) that to accurately determine the performance and productivity of a gas condensate reservoir, it is mandatory to obtain accurate descriptions of the effect of phase change and liquid saturation on that gas condensate reservoir. The transition of a gas condensate reservoir to a two-phase system is generally believed to occur in three or two distinct flow regions. The three regions concept stipulates; the near-wellbore area consisting of mobile oil and gas phases referred to as region 1, a slight distance away from the near-wellbore region where mobile gas and immobile condensate exist, referred to as region 2, and farther into the reservoir where pressure is higher than the saturation pressure and only single-phase gas exists, referred to as region 3. Condensate is believed to be immobile in region 2 because its saturation

at this point is lower than the critical condensation saturation. Figure 1.2 shows the coexistence of these different flow regions and also illustrates their dependence on pressure variation.

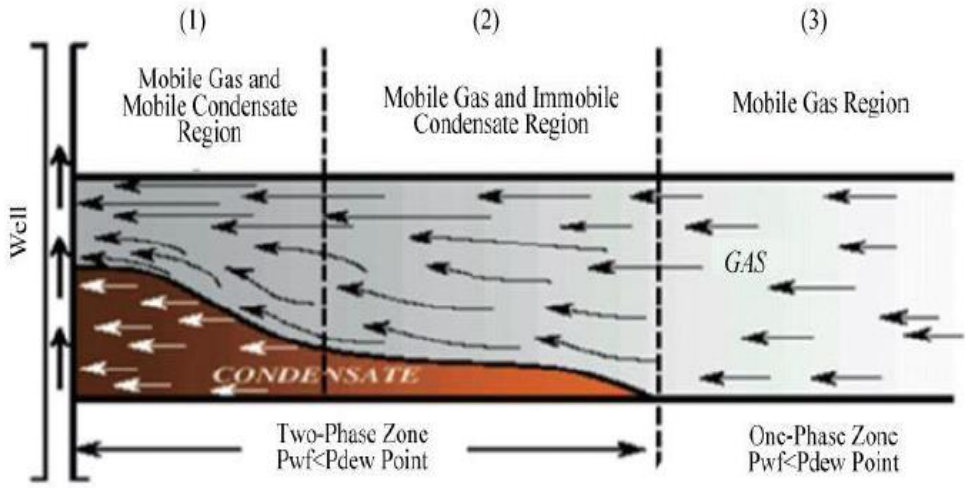

Figure 1.2: Schematic gas condensate flow behaviour in three regions (Roussennac, 2001).

This concept of immobile condensate in region 2 has been debunked by (Danesh et al., 1991) & (Jamiolahmady et al., 2010) in separate experimental studies showing that accumulated condensate is not immobile but instead has low mobility. At the early stages of depletion below Pdew, this very low mobility may behave as equivalent to zero mobility, but it will affect well productivity in the longer term as condensate will accumulate at the bottom of the reservoir due to gravity and can only be captured by assigning a low but non-zero condensate mobility value. In other words, there are only two regions, a single-phase region and a two-phase region separated by the P_{Dew} boundary.

Henderson et al. (1996) performed several core flood experiments on a sandstone core using gas condensate fluids to measure the steady-state relative permeability. At the same time, varying the condensate-to-gas ratios (CGR), velocity, and interfacial tension (IFT) to determine their effects on the relative permeability of the system. Results from this study show that the relative permeability of the gas and condensate phases were, directly and inversely, proportional to velocity and IFT, respectively (Henderson et al., 1996, 1998). Following these findings, Jamiolahmady et al., developed a generalised correlation to describe better the relationship between the relative permeability, velocity, and IFT for condensing fluids (Jamiolahmady et al., 2009).

Wheaton & Zhang (2000) stated that the effect of condensate banking problem is more significant in low-permeability gas condensate reservoirs. As the pressure drop at the

near-wellbore region is generally large, the condensate dropout and accumulation rate will also be relatively high.

Condensate build-up will result in more productivity loss as the condensate accumulates further into the reservoir with time. This has been identified in both low and high-permeability reservoirs where the preferential flow for gas in the presence of condensate significantly changes the composition of the in-situ fluid and produced stream (Al-anazi et al., 2002; Chunmei Shi, 2005; Jamiolahmady et al., 2006; Ghahri et al., 2015; Khazam et al., 2017 and Hassan et al., 2019).

The exploration and exploitation of gas condensate reservoirs is on the increase. Hence the demand for sustainable recovery techniques to maximise the production of the gas and condensate fractions from these deep-lying reservoirs is also on the rise. The common methods employed to address this include immiscible and miscible gas flooding of hydrocarbon gases like methane and most recently, non-hydrocarbon gases like carbon dioxide (CO_2) and nitrogen (N_2) to prevent or alleviate condensate formation during the production cycle of gas condensate reservoirs.

The injection of non-hydrocarbon gases for enhanced gas condensate recovery (EGCR), especially CO_2 injection, has been investigated and proven as a viable enhanced recovery technique (Marokane et al., 2002; Sheng et al., 2016; Ding et al., 2019; Zhang et al., 2020; Ashwani Kumar, 2020; Samuel, 2020; Mohsin et al., 2021; Seteyeobot et al., 2021; Reis & Carvalho, 2022). Considering the high level of miscibility of supercritical CO_2 with gas condensate fluids under reservoir conditions, it favours the recovery mechanism/s that governs the EGCR process.

1.2 Problem Statement

One of the most significant issues that occur during the production of a gas condensate reservoir is the dropout and accumulation of condensate. This liquid phase is composed of valuable heavier components of the reservoir fluid (Fevang & Whitson, 1996; Ahmed et al., 1998; Wheaton & Zhang, 2000; Miller et al., 2010; Seteyeobot et al., 2016; Sayed et al., 2016; Seteyeobot et al., 2021). Considering that Danesh et al. (1989); Jamiolahmady et al., (2007, 2008, 2010) from their experimental studies already established that during liquid dropout, the formed condensate is not immobile but will have low mobility without a critical condensate saturation. This low mobility may be insignificant in the short term but will affect well productivity in the longer term. Hence, it is important to consider the evolution of the pressure difference that exists between the

bottom hole flowing pressure and the reservoir pressure and its impact on condensate drop-out and accumulation with time when applying any injection techniques.

Laboratory studies by Henderson et al. (2001) and Jamiolahmady et al., (2009) have also demonstrated that the flow behaviour of gas and condensate is complicated by interactions of viscous, capillary, and inertial forces due to coupling (an increase in kr with a decrease in IFT or an increase in velocity) and inertia (a decrease in kr by an increase in velocity). The effects of inertia and coupling which can be significant and causes variations on the relative permeability (kr) data of gas condensate systems were also studied at the pore level for various rocks with permeabilities about 10 mD and above by (Jamiolahmady, 2000) and a generalised correlation proposed to express the effect of coupling and inertia on gas and condensate fluid mobility (Jamiolahmady, 2009).

Condensate recovery can be achieved by revaporization. This enhanced recovery can be attained by implementing the H-n-P injection technique which is primarily governed by vaporising mechanism. This involves the injection of miscible gases like CO_2 or N_2 into depleted gas condensate reservoirs to repressurise them back above the dew point pressure, followed by a soaking period, hence vaporising the condensate into the gas phase (huff stage). The second stage which is the puff stage involves gradual pressure depletion which will cause the already vapourised condensate to be produced in the produced gas stream. The H-n-P gas injection technique is more efficient for improving condensate recovery when compared to the immiscible gas flood technique (Meng et al., 2015; Sheng, 2015).

It has been proven experimentally by Meng & Sheng, (2016b) that at some point during the H-n-P injection process, both the vaporising and condensing mechanism may occur simultaneously. This occurrence depends on the composition of the injection stream and can adversely influence the productivity of such a system. Produced gas or hydrocarbon gas mixture (lean gas) has been mostly used as injection gas during H-n-P injection. The conventional H-n-P injection requires large volumes of injection gas to repressurise the reservoir above the dew point over several H-n-P circles. Considering the high level of interaction and miscibility of the injected gas and reservoir fluid, the composition of the production stream would have a high volume of the injected gas.

In more common scenarios where the injection gas is either a single or multi-component hydrocarbon gas, the composition of the produced fluid may not be of great concern. However, when a non-hydrocarbon gas like CO_2 is injected for EGCR, the composition of the produced stream becomes important. The conventional H-n-P CO_2

technique has been identified to be an efficient approach for condensate alleviation. The high volume of CO_2 production usually associated with this process is unacceptable and has significantly limited its implementation with only a handful of pilot projects tested on the field scale. With CO_2 classified as a harmful greenhouse gas, it becomes valuable to design and implement a H-n-P CO_2 injection technique where the volume of injected CO_2 is optimised such that a lesser volume of CO_2 is injected and produced while ensuring that the recovery mechanism and recovery potential remain efficient and comparable to the conventional H-n-P CO_2 injection technique.

1.3 Research Goals

CO_2 injection provides additional and favourable changes in phase and fluid flow behaviour, making it economically more attractive compared to other injection gases. However, to make an informed decision on the injection of CO_2 for the benefit of gas and condensate recovery and CO_2 storage, adequate phase and flow behaviour analysis is required for a clear understanding of CO_2 interaction with the reservoir fluid to quantify and forecast its performance.

This research has been focused on conducting appropriate experimental CO_2/Gas condensate phase behaviour, unsteady-state core flood, and steady-state relative permeability tests to determine the CO_2/gas-condensate interaction level and quantify the condensing/vaporising mechanisms governing the recovery process during H-n-P CO_2 injection for EGCR and CO_2 storage. Accordingly, a practically attractive framework to quantify the advantages of CO_2 injection, which helps in screening a suitable target reservoir and is lacking from previous studies, has been proposed. In this process, attempts have been made to optimise the amount of CO_2 injected to capitalize on the benefits of EGCR and CO_2 storage during H-n-P CO_2 injection.

Considering the previous conflicting reports in literature regarding the trend and level of CO_2/Gas-Condensate interactions. The results obtained from this experimental analysis enhance the accuracy of forecasting or quantifying the recovery efficiency of the H-n-P injection method for EGCR and CO_2 storage by addressing the following questions:

I. Can a practical framework following a combined experimental and theoretical approach be developed to identify and quantify the level and effect of CO_2-GC interaction on the recovery mechanism during CO_2 injection for enhanced condensate recovery?
II. Can the CO_2-GC miscibility pressure be optimised to enhance the governing swelling/vaporisation mechanism?

III. How does injection pressure, injection volume, and injection rates impact the recovery potential of condensate during H-n-P CO_2 injection?

IV. What are the impacts of resident fluid composition and reservoir rock properties on the recovery mechanism?

V. Can the amount of CO_2 injected be optimised to capitalise on the benefits of EGCR and storage of CO_2 under various injection scenarios?

1.4 Aims and Objectives

Based on the issues discussed in the previous sections, the major aims and objectives of this research study is outline below.

I. Determine the level of CO_2/gas-condensate interaction, quantify the condensing/vaporising mechanisms governing the recovery process during H-n-P CO_2 injection for EGCR and CO_2 storage purposes by designing and conducting appropriate experimental phase behaviour (CCE, swelling, shrinkage, and miscibility) tests, and a systematic H-n-P CO_2 injection technique, which will be based on injecting CO_2 at the maximum liquid drop-out of the corresponding CO_2-gas-condensate fluid mixture.

II. Highlight the importance of EOS tuning in compositional modeling especially as the fluid composition varies significantly in the reservoir and in cases where the injected fluid is different from the resident fluid and particularly when the injected fluid is CO_2.

III. Perform routine and special laboratory PVT tests to generate appropriate data set for tuning an EOS model which will be applied both for phase behaviour prediction and quantifying the level of interaction between CO_2 and a gas condensate system prior to designing a systematic CO_2 injection for enhanced recovery.

IV. Perform simulation study complements and generalises the core flood experimental results of the proposed H-n-P CO_2 injection technique by confirming the dominant governing mechanisms and the importance of using appropriate CO_2-gas-condensate kr data while accounting for the effect of compositional changes on gas and condensate mobility.

1.5 Thesis Outline

Chapter 1 presents an introductory overview of CO_2 injection in gas condensate reservoirs to mitigate condensate buildup and for CO_2 storage. It outlines the challenges associated with the recovery process, prior endeavors to tackle these challenges, the rationale behind this research, the objectives, aims, and research goals, as well as an outline of the thesis structure.

Chapter 2 presents the literature review in sections, which focuses on CO_2 and gas condensate reservoirs. These sections include a detailed review of gas condensate reservoirs, condensate banking and treatment methods, CO_2 injection in gas condensate reservoirs considering H-n-P CO_2 injection technique, CO_2 resident fluid interaction, chemical injection, wettability, interfacial tension, and lastly, CO_2 storage in gas condensate.

Chapter 3 presents the experimental set up and procedures designed to accurately measure the phase behaviour properties, EOS modelling, and tuning for the binary gas condensate fluid with and without CO_2 added. The procedure applied in measuring the interfacial tension, the level of interaction, and miscibility for the studied $CO_2$and gas condensate system is also discussed. The emphasis is on the effect of CO_2 on the dew point pressure, liquid dropout, miscibility, swelling, revaporisation capability, and mobility when injected at pressures above and below the measured dew point pressure (P_{Dew}) of gas condensate systems. This chapter concludes with a thorough analysis of observed data and a discussion of the results.

Chapter 4 begins by presenting the concept behind the design and implementation of the systematic H-n-P CO_2 injection method, experimental setup, procedures followed and data acquisition system, and data analysis for condensate recovery from all three tested core samples. Lastly, a comparison is made between the recovery efficiency obtained for the pre- and post-CO_2 injection scenarios, natural depletion scenarios, and the CO_2 production profile of the newly developed method and the convention H-n-P CO_2 method.

Chapter 5 presents a core scale numerical simulation that attempts to compliment and generalize the observed core flood experimental results by appropriate sensitivity and history matching analysis. It will be discussed that the numerical model is only able to correctly predict the condensate recovery from primary depletion and initial CO_2 injection stages. By performing a series of sensitivity analyses, it is demonstrated that the relative permeability (kr) data has a significant effect on the cumulative gas and condensate production and that the steady-state gas and condensate relative permeability (GC-kr)

data previously measured could not adequately describe the gas and condensate mobility through the core. Therefore, this chapter includes some experimental CO_2-GC-kr that were measured using the steady state approach and fitted to Corey's model in a bid to obtain the required coefficients for adjusting kr data in the model with some level of success.

Chapter 6 presents the conclusive summary of the findings and novel contributions of this research and recommended further work.

Chapter 2 - Literature Review

When conducting a research study, it is important to establish a conceptual framework that outlines the theoretical foundation of the study and guides the research design and analysis. A critical review of literature is a necessary step in developing this conceptual framework, as it helps to identify and synthesize existing knowledge and theories related to the research question. A thorough and objective review of available literature that draws context from a range of relevant sources and the use of appropriate analytical tools to evaluate the quality and relevance of each source is presented in this chapter. This review is focused on highlighting issues related to condensate banking phenomena, the injectivity of carbon dioxide (CO_2) into gas condensate reservoirs, CO_2-condensate phase and flow behaviour, CO_2/resident fluid dynamics, recovery mechanisms, and possible use of depleted gas condensate reservoirs for CO_2 storage in the underground geological formation as an effective mean to reduce the negative impact of this greenhouse gas.

Traditional methods of recovery such as natural depletion and secondary recovery may not be as effective, so innovative tertiary/improved recovery strategies such as CO_2 injection or chemical flooding may need to be considered. Therefore, an in-depth analysis of several factors related to CO_2 injection is required to optimise recovery and storage efficiency. For example, understanding the phase and flow behaviour of the fluids in a gas condensate reservoir is important when designing injection strategies, as it can affect the mobility and displacement efficiency of the injected fluid. Knowledge of condensate banking phenomena is also important when designing recovery strategies, as it can help to identify potential issues that may arise during production including well placement and completion design. An understanding of dominant mechanisms is also important for both recovery and storage purposes.

The Injection of CO_2 into hydrocarbon reservoirs is currently and primarily being studied as a means of enhanced gas condensate recovery. The process involves injecting CO_2 into a reservoir to displace or vaporise and recover additional hydrocarbons that would otherwise be left behind at the end of implementing the conventional recovery methods.

Only a hand full of experimental studies have been conducted to investigate the effectiveness of CO_2 injection for gas and enhanced condensate recovery. These studies have typically involved laboratory experiments or small-scale field trials. On the other hand, there are several simulation studies reported in literature.

When CO_2 is injected into a depleting natural gas reservoir, it has the potential to enhance gas and condensate recovery by increasing the pressure within the reservoir, which in turn leads to an increase in the amount of recoverable condensate with the gas phase. The effectiveness of CO_2 injection for condensate recovery has been observed to be highly dependent on the fluid's interactions, the geological properties of the reservoir, such as permeability and porosity, and the pressure and temperature within the reservoir.

Overall, experimental studies have shown that the injection of CO_2 can be an effective means of enhancing gas and condensate recovery. However, there are conflicting reports about the level of benefits, therefore, further research is needed to better understand the factors that influence the effectiveness of CO_2 injection and to optimise the process during different injection scenarios and for different types of reservoir formations. In addition, the dynamics of CO_2 and resident fluid within gas condensate reservoirs are important to consider when designing for CO_2 storage processes. Understanding the interactions between CO_2 and the resident fluid, as well as the effects of CO_2 injection on the phase and flow behaviour of the reservoir fluids, can help to optimise recovery and maximise the potential of using depleted gas condensate reservoirs for CO_2 storage, which is a welcomed and critical step towards addressing the issues of achieving reduced greenhouse gas emissions.

2.1 Condensate Banking and Treatment Methods

Condensate banking is the accumulation of liquid hydrocarbon, which is trapped in the pores of the reservoir rock due to the low permeability of the reservoir. This phenomenon affects the productivity of the well and the ultimate recovery factor of the reservoir. In this sub-section, different mechanisms of condensate banking, its effects on the productivity of the well, and the methods to mitigate or alleviate its effects will be discussed. Condensate banking can occur due to several factors, such as:

1. Capillary trapping: In this type of condensate banking, the liquid hydrocarbon is trapped in the narrow pore throats of the reservoir rock due to capillary forces. This type of condensate banking occurs in rocks with small pore sizes and high capillary pressures.
2. Gravity segregation: This type of condensate banking occurs when the liquid hydrocarbon separates from the gas phase due to the difference in densities between the two phases. This is known to occur in reservoirs with high vertical permeability and low dip angles.

3. Condensation: The condensation process is a required step for the other two methods mentioned above but here, the liquid hydrocarbon is purely trapped in the reservoir due to the high level of condensation out of the gas phase after pressure drops below Pdew and primarily away from the wellbore and especially for rich gas condensate systems with high amount of liquid content.

Some common effects of Condensate Banking on productivity can include, reduced permeability, increased pressure drop, and reduced gas saturation.

Several techniques have previously been identified and are still being investigated to prevent or mitigate condensate banking in gas condensate reservoirs. Bennion et al., (2001) and El Cheikh et al., (2019) reviewed several condensate prevention and mitigation techniques implemented over the previous decade highlighting the advantages and disadvantages associated with each. These techniques include:

- Productivity enhancement techniques (PET) like acidizing, drilling horizontal wells, hydraulic fracturing, and combining any selected two.
- Pressure maintenance techniques (PMT) like gas cycling and injection of non-hydrocarbon gases (Carbon-dioxide and Nitrogen)
- Chemical injection technique (CIT)

2.2 Productivity Enhancement Techniques

Jamiolahmady et al., (2007) conducted a simulation study using the ECLIPSE 300 compositional reservoir simulator and a previously developed relative permeability correlation to investigate the effect of fluid properties and reservoir anisotropy on the productivity of gas condensate reservoirs. They focused on reservoirs produced by horizontal and slanted wells and their result shows that reservoir anisotropy, coupling, and inertia play vital roles in quantifying the gas productivity from a gas-condensate reservoir. Later, other researchers investigated the approach of utilizing horizontal wells to mitigate condensate blockage by addressing the critical question of quantifying the fraction of increased gas production corresponding to the increased formation contact depth or actual condensate banking reduction (Miller et al., 2010). This concern was discussed further in a subsequent work by (Ghahri et al., 2015) where an improved model was proposed by developing a 3D compositional finite element-based simulator using the relative permeability correlation developed earlier by (Jamiolahmady et al., 2009). They estimated the gas and condensate recovery from a horizontal well and quantified the recovery while considering important parameters like phase change, velocity, interfacial tension (IFT), and well geometries. The results of this model were in good agreement

with those of an equivalent commercial simulator for both single-phase and two-phase gas condensate flow systems. The main challenge here was quantifying, distinguishing the additional recoveries based on well geometry and the recovery mechanism that governed the process.

Table 2.1. Basic rock properties and Average Absolute Deviations and Standard Error of Estimates between measured and calculated values of krg for RC3, the proppant filled and sand packed fractures at different conditions. (Jamiolahmady et al. 2009)

Index	Core Type	IFT mNm^{-1}	AAD%-k_{rg}	SEE-k_{rg}
1	RC3 k=3.9 mD ϕ=6% β=1.55E11 m^{-1}	0.85	11.4	0.035
2		0.15	14.4	0.010
3		0.036	17.4	0.126
ALL			**14.4**	**0.093**
1	Proppant k=146 D ϕ=35.38% β=3.5E5 m^{-1}	0.85	12.2	0.029
2		0.15	20.2	0.047
ALL			**16.2**	**0.039**
1	Sand k=15 D ϕ=33.63% β=1.06E6 m^{-1}	0.85	18.2	0.053
2		0.15	17.5	0.082
ALL			**17.8**	**0.070**

Mahdiyar, et al., (2009) and Jamiolahmady, et al., (2011) performed a modelling exercise for a fractured vertical well, similar to that performed by (Panteha Ghahri et al., 2015) for horizontal and deviated well. They also proposed an equivalent wellbore radius to capture the effect of coupling and inertia on the fractured well performance, facilitating improved and more detailed simulation and evaluation of well performance.

Ghaleb et al., (2019) conducted a simulation study using analytical and numerical models to investigate the impact of hydraulic fracturing on condensate banking, concluding that this method is primarily relevant when considering long-term economic values. (Vijayvargia et al., 2019) performed a simulation study on the injection of fracturing fluid into a multiple fractured horizontal well for clean-up. Results from this work indicate that the gas production loss was significantly reduced for the naturally fractured gas reservoir while the tight gas reservoir continued to experience gas production loss.

2.3 Pressure Maintenance Techniques

Considering that the study presented in this thesis is focused on investigating the pressure maintenance technique, more emphasis will be placed on gas injection. Gas condensate reservoirs are characterised by high initial production rates, low recovery factors, and rapid pressure decline. To maintain the reservoir pressure above the dew point pressure and improve the recovery of these reservoirs, various gas injection techniques can be implemented. Gas injection has been proven to be suitable for reservoirs with permeability ranging from low to high permeability. The use of non-hydrocarbon gases has become popular in recent years. Gases like nitrogen and carbon dioxide have been injected individually and as a mixture into depleting gas condensate reservoirs for pressure maintenance. However, with the conflicting results being reported, many questions related to the recovery efficiency and best injection technique during non-hydrocarbon gas injection remain unanswered.

Moses & Wilson, (1981) performed an experimental study on the injection of nitrogen (N_2) and lean gas into depleting gas condensate reservoirs for mitigation of condensate banking. They evaluated the pressure maintenance potential during N_2 injection and observed that N_2 displaced condensate under miscible condition which was above the dew point. The recorded condensate recovery efficiency was similar relative to that observed during lean gas injection. They concluded that N_2 and resident fluid miscibility was obtainable only above dew point.

Renner et al., (1987) conducted experimental and simulation studies to investigate the miscibility envelope and recovery potential when N_2 and N_2+Buffer Gas mixture were injected into a gas condensate system. They reported that condensate recovery was significantly improved during N_2+Buffer gas injection with a condensate recovery factor of approximately 90% relative to 50% when N_2 gas was injected into a gas condensate system at similar conditions. They also performed simulations using a generalized compositional model and a modified equation of state to replicate the Coreflood experiments. The comparison between the experimental and simulated data showed a good match. However, it was observed that miscibility between the injected gas and resident fluid was obtained by a multiple-contact mixing mechanism, this mixing was easily achievable above the dew point which was the reason for the observed enhanced condensate recovery. It remains unclear the reason why the interaction between the injected gas and the resident condensate was governed by multiple-contact miscibility at P>Pdew. It was also observed that condensate recovery was significantly reduced when

the injection of N_2 and N_2+ Buffer Gas was repeated below the dew point pressure, indicating a low or zero fluid miscibility. They concluded that for efficient mitigation or alleviation of condensate banking using N_2 or N_2+Xgas mixture, the reservoir pressure must be maintained above dew point. This is somewhat contrary to the report from a phase behaviour simulation study with and without the addition of N_2 to the original fluid conducted by (Soltan Sleiman et al., 2021). They concluded that the addition of N_2 to a gas condensate system increases the dew point pressure which results in early condensate dropout from the gas phase.

Siregar et al., (1992) conducted a simulation study to investigate the results from earlier studies that claim N_2 was able to achieve similar recovery efficiency when compared to that achieved during lean gas injection. Their results show that when N_2 is injected into gas condensate systems to maintain the pressure above the dew point, the interaction between the reservoir gas and N_2 caused an early liquid dropout in the reservoir. This was because the N_2/reservoir gas mixture had a higher dew point than the initial reservoir gas. They concluded that the two major factors that lower the recovery during N_2 injection into gas condensate reservoirs compared to the recovery during methane injection are higher liquid dropout resulting from dispersion and lower evaporation capacity. Their recommendation was to perform two- and three-dimensional simulations to investigate the effect of heterogeneity and layering during N_2 and N_2-mixture injection for improved condensate recovery.

Following the results and suggested future work from (Siregar et al., 1992), a three-dimensional simulation study was conducted by (Sanger et al., 1994) using the Peng Robinsons Equation of state to describe the fluid phase behaviour of the system. The obtained results contrasted with those reported in previous studies. Their results indicated that N_2, when injected into gas condensate reservoirs, will maintain the reservoir pressure, and limit the volume of condensate dropout in the reservoir but still experience severe liquid drop out at the displacement front only where the resultant mixture has a higher P_{Dew}. This latter observation again disagrees with the miscibility mechanism reported in earlier studies. The common observation from these earlier studies indicates that appropriate fluid phase behaviour and equation of state modelling that described the fluid interaction were lacking.

A study done by (Linderman et al., 2008) has shown that nitrogen can improve the overall hydrocarbon recovery but the late-life condensate recovery factor is significantly reduced when compared to dry gas or CO_2 injections.

Subero (2009) performed numerical modelling of N_2 injection for improved gas condensate reservoirs. In this study, appropriate fluid phase behaviour, equation of state modelling, and tuning were done, and the obtained data were utilised as input data for a three-dimensional compositional simulator model. The results show that N_2 injection into gas condensate reservoirs for the purpose of condensate mitigation had no overall benefits.

Table 2.2. Dew point prediction results from PVT analysis (Subero 2009)

Nitrogen Gas and: Reservoir Fluid Mixing Ratio	Dew Point Prediction, psia
0:1	3436
1:4	5095
3:7	6075
1:1	8467

Hassanzadeh et al., (2013) and Nasriani et al., (2014) show that the swelling and re-vaporisation capability of these two non-hydrocarbon gases (N_2 and CO_2) vary significantly based on their physicochemical properties and the level of interaction and mixing with the resident fluid at reservoir conditions. Accordingly, they concluded that N_2 is best injected into an already depleted gas condensate reservoir for repressuring it above the dewpoint, which is contrary to what Renner et al. suggested, while CO_2 performed best when injected above the dew point pressure to mitigate condensate banking, again in contrast to the findings of this study. From their report, it was unclear and difficult to quantify the swelling and shrinkage potential when both gases were injected in gas condensate reservoirs either below or above the dew point.

Table 2.3. Summary of injection scenarios by (Hassanzadeh et al. 2013)

Case No.	*Injection Rate, MMSCF/day*	*Injected Fluid*	*Plateau Life Time, Years*	*Gas RF, %*	*Condensate RF, %*
1	50	C_1	16.0	42.4	37.6
2	100	C_1	18.2	47.4	41.3
3	150	C_1	21.6	52.0	44.0
4	200	C_1	27.0	54.6	45.4
5	50	CO_2	15.5	40.8	36.4
6	100	CO_2	16.7	44.2	38.9
7	150	CO_2	18.3	47.6	41.3
8	200	CO_2	20.2	50.8	43.5
9	50	N_2	16.2	42.9	38.2
10	100	N_2	18.9	48.5	42.5
11	150	N_2	22.8	53.0	45.5
12	200	N_2	28.4	54.7	46.5
13	50	Recycling	15.6	41.8	37.4
14	100	Recycling	17.8	46.5	41.2
15	150	Recycling	20.7	51.1	44.7
16	200	Recycling	25.0	54.1	47.0

El Gohary et al., (2014) also performed simulation studies on the integrated injection of nitrogen and hydrocarbon gas for EGR. Their results show that at high pressures, nitrogen expedites the liquid dropout stripping the produced well stream of heavier components, but at lower pressures, a decrease in liquid dropout is observed even with increased nitrogen concentration. This was again contrary to the observations reported by (Sadooni & Zonnouri, 2015) when they performed an experimental phase behaviour study on the interaction between nitrogen and a rich gas condensate fluid. Their results show that nitrogen had a favourable effect on liquid dropout but increased the dew point pressure of the system.

Nasiri et al., (2015) conducted a simulation study to compare the results from injecting CO_2, methane (C_1), N_2, and a binary mixture of C_1 and ethane (C_2) into a gas-condensate reservoir. They concluded that CO_2 was the most efficient of all injected gases. It required the lowest injection rate to maintain the pressure of the reservoir above its dew point pressure while yielding a relatively high amount of condensate recovery. They recommended that an experimental approach is required to investigate and fully understand the level of interaction and recovery mechanism governing the CO_2-Enhanced gas condensate recovery process.

Sayed & Al-Muntasheri, (2014) and Sayed et al., (2016) presented reviews on advancements made on several methods used to mitigate condensate formation in reservoirs, along with their advantages and disadvantages. These reviews showed that, theoretically, gas cycling and CO_2 injection into depleting gas condensate reservoirs remains the most effective method to mitigate the condensate banking problem. Still, its economic burden makes this method unfavourable, and the injection of non-hydrocarbon gases represent good and comparable alternatives to dry hydrocarbon injection.

Generally, it is safe to conclude that recent studies on the injection of non-hydrocarbon gases for improved gas and condensate recovery have shown some inconsistent results considering the injection scenarios, level of interaction, and swelling/re-vaporization potential of these gases in depleted gas condensate reservoirs.

2.4 Productivity Enhancement by Chemical Injection Technique

Usually, gas condensate reservoirs, when the pressure falls below dew point, are characterised by the appearance of a condensate bank and exhibiting a complex phase and flow behaviour around the wellbore. As a result, not only gas production is hindered by the condensate dropout but also the valuable condensate itself is lost inside the reservoir. The unique dependency of the gas and condensate relative permeability (kr) on the

velocity and interfacial tension (IFT) further complicates the well productivity calculations both in field simulation models and in simple engineering calculations. Several methods are employed to mitigate the effects of condensate banking which can be broadly classified into three categories which are pressure-maintenance techniques, productivity-improvement techniques, or chemical-injection techniques. These methods mainly focus on either keeping the reservoir pressure above the dew point, reducing the drawdown pressure required, or mobilising the condensates by altering the wettability and/or IFT.

2.4.1 Reducing Interfacial Tension

This method is based on using chemical solvents such as methanol, isopropyl alcohol, or other mixtures to reduce the capillary pressure, which if it is high results in trapping condensate inside the pores. Reduction in capillary pressures can be achieved by a reduction in IFT. Solvents like alcohol reduce the IFT and remove condensate through a multiple-contact miscible displacement (Al-Anazi, et al., 2005). The studies highlighted the importance of the volume of methanol used and its transfer rate to the gas stream on the success of the treatment. Some studies have reported an increase in end points of gas relative permeability by a factor of 1.2 to 2.5 as methanol can dissolve and displace both water and condensate accumulations (Du, et al., 2000). The success of methanol treatment depends on the phase behaviour of gas condensate fluid which is complicated by the presence of alcohol and water. Such phase behaviour investigations are usually performed by conducting constant composition expansion experiments at reservoir conditions (Bang, et al., 2010). As an example, during the experiments performed by Bang et al., the addition of methanol to a mixture of hydrocarbon and water led to the formation of a third aqueous phase and the reduction of dew point pressure. When adding isopropanol alcohol, a small third aqueous phase was formed, and hydrocarbon volume increased. They concluded that methanol preferred to mix with water over condensate, while isopropanol alcohol preferred the hydrocarbon phase over water. Another study (Kalla, et al., 2015) has shown a clear trend between improved gas-condensate relative permeability and the reduction of IFT. The use of solvents to mitigate condensate banking has been tested and found effective in sandstone and limestone reservoirs for both low and high-permeability rocks. However, this is not a permanent solution and requires repeated treatments when condensate bank reoccurs.

2.4.2 Wettability-Alteration

Wettability alteration of the rock surface from liquid-wet to intermediate or preferentially gas-wetting is considered to be one of the most effective methods to address condensate banking phenomena in the long term as it does not require repeating the treatment. The wettability of the fluid, in the presence of two immiscible fluids, is determined by the contact angle that the denser fluid makes with the rock surface. If the contact angle is acute, then the fluid is considered to be wetting whereas a non-wetting phase has a contact angle of obtuse. A neutral wetting liquid has a contact angle of 90°.

There have been several studies examining the effect of chemicals on wettability. A promising study (Wu & Firoozabadi, 2010) showed that the treated cores have a significantly lower pressure drop during the early liquid injection period, which was attributed to wettability alteration. However, when further tests were performed under high temperatures, similar chemicals did not perform as well. Several experiments were conducted by various researchers, including those performed by the HW-GCR team (Fahimpour & Jamiolahmady, 2012) showed promising results using different fluoropolymers and surfactants, which will be discussed further below.

V. Kumar et al., (2006) and Ahmadi et al., (2011) performed an experimental study to investigate the application of chemical stimulation in a gas condensate reservoir. Their results show that applying wettability alteration chemicals greatly improved the gas relative permeability and well deliverability of gas and condensate in the field.

Table 2.4. Relative permeability parameters before and after treatment (V. Kumar et al., 2006)

	Pre Treatment	Post Treatment
Nc_gas	10^{-7}	10^{-7}
S_{wr}	0	0
S_{or}	0.3	0.15
S_{gr}	0.25	0.1
k_{ro}^{o}	0.3	0.55
k_{rg}^{o}	0.45	0.7
Corey oil exponent	2	2
Corey gas exponent	3.6	3
T_w	100	100
T_o	10,000,000	10,000,000
T_g	3,000,000	3,000,000
τ_w	1.1	1.1
τ_o	2	2
τ_g	2	2

Fahimpour & Jamiolahmady (2014 and 2015) have shown that the impact of such chemical treatment reduces at lower IFT and for reservoir fluids with more lighter fluids. Accordingly, they also highlighted the importance of performing screening tests suitable for gas-condensate fluids as those performed for conventional gas-oil systems or

procedures could produce over-optimistic results. Sheng et al., (2016) conducted a comparative study between H-n-P gas injection and chemical relative permeability modification. Their result shows that the latter technique is viable, but the H-n-P gas injection technique may be preferred depending on specific economic situations and oil prices.

A recent study by (Gahrooei & Ghazanfari, 2017) has proposed the use of hydrocarbon-based chemicals containing fluorinated polymers (MariSeal 800) for wettability alteration. This is motivated by the hydrocarbon nature of the condensate bank which would result in better compatibility with the chemical. That is, it would be easier to flow back the chemical along with the hydrocarbons as the chemical would be miscible with the condensate liquid. The results of this study suggest the use of MariSeal 800 as an effective oil-based chemical for wettability alteration in gas condensate reservoirs. However, these treatments are too costly for commercial purposes (Li & Zhang, 2011) and there is still a lack of available data on successful field trials which is central for evaluating the real field performance.

Sayed et al., (2018) proposed the use of a novel chemical treatment method. The chemical was formulated using surface-modified fluorinated Silica nanoparticles explicitly designed for rock wettability alteration from oil/water-wet to neutral wettability. Core flood experiments were performed at reservoir conditions to test the efficacy of this chemical. The results indicated that this method was effective in alleviating condensate and water blockages in gas reservoirs.

Wang et al., (2018) conducted a comparative experimental study on the injection of CO_2 and methanol for the mitigation of condensate blockage in gas condensate reservoirs, and their results conclusively indicated that CO_2 injection exhibited a higher condensate removal effect and thus significantly improved the gas relative permeability of the reservoir leading to better gas and condensate recovery. Hassan et al., (2019) proposed a new technique for permanent condensate removal called ‘chemically induced-pulse fracturing by an in-situ generation of heat and pressure using thermochemical treatment and recommended further studies on a possible combination of different mitigation techniques to provide a collaborative solution for improving condensate removal significantly.

2.5 CO_2 Injection in Gas Condensate Reservoirs

The injection of CO_2 in gas condensate reservoirs has been identified as a viable injection technique for mitigating or alleviating condensate banking and enhancing gas condensate recovery while also benefiting from CO_2 storage. Supercritical CO_2 is less susceptible to gravity segregation and injectivity problems because it has a similar density to light oil and a higher viscosity value when compared to other gases resulting in good displacement efficiencies. There are also reports about favourable changes in phase behaviour and compressibility of gas-condensate-CO_2 mixtures.

CO_2 injection in gas condensate reservoirs began early on, with researchers discovering the positive impacts associated with this process. (Monger & Khakoo, 1981; Jessen & Orr, 2004) stated that CO_2 has the potential to significantly reduce the miscibility pressure in a gas condensate system and hence improve the recovery of liquid condensate. Darvish et al., (2007) performed an experimental study on the efficiency of tertiary CO_2 injection and concluded that even though CO_2 was injected at low rates, it was able to recover a significant amount of the residual condensate after initial water injection.

Kusumawati & Jamiolahmady (2009) performed a simulation study to investigate the benefits of CO_2 injection for enhanced gas recovery (EGR) and CO_2 storage. They studied the phase behaviour changes resulting from contacting the resident fluid with CO_2 and compared the recovery potential of CO_2 to that of methane (CH_4). They concluded that CO_2 injection exhibited a higher potential for condensate banking removal and enhanced gas condensate recovery (EGCR) and recommended experimental studies should be done to validate their results. The intermediate gas contains heavier fraction ($C_{10}H_{22}$) than the lean gas, therefore it was expected that the intermediate gas would form more condensate than the lean gas. By injecting CO_2, the condensate formed inside the reservoir would be re-vapourised by the CO_2 and flow together with the leaner gas stream resulting in the increase in condensate production Figure 2.1

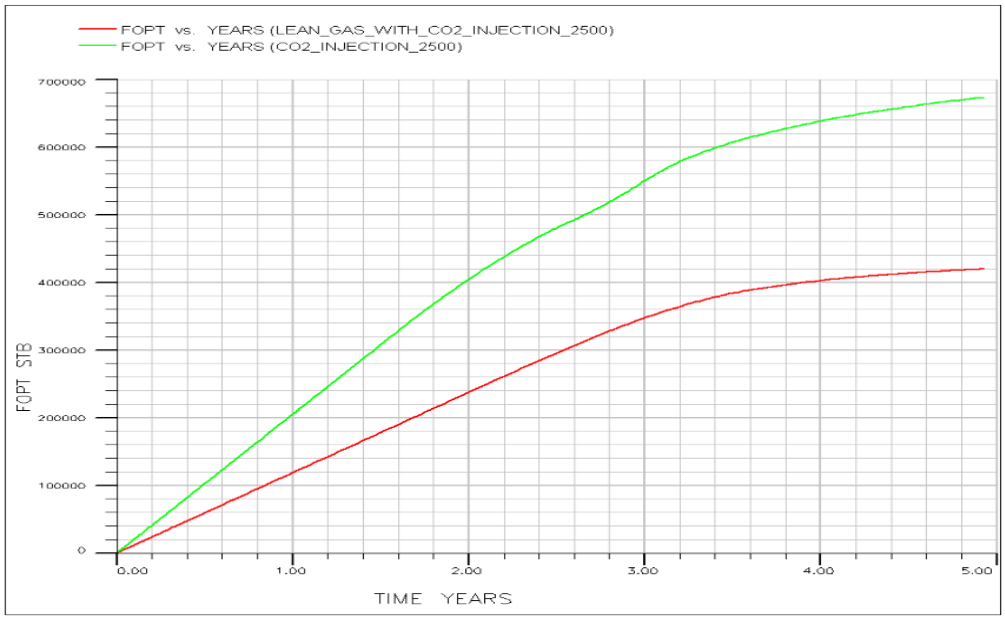

Figure 2.1: Total condensate production for lean gas and CO_2 injection for condensate alleviation. (Kusumawati & Jamiolahmady, 2009)

Mogbo (2011) conducted a simulation study to evaluate miscibility and predict the additional hydrocarbon recovery during CO_2 injection for enhanced gas condensate recovery. Results from this study indicated that the injection of CO_2 was justified for the chosen field as condensate recovery was enhanced after the injection phase.

Khan, et al., (2013) performed a simulation study applying experimental data and considering different injection scenarios to demonstrate the potential of enhanced gas condensate recovery during CO_2 injection in gas condensate reservoirs outlining two favourable factors that influence both the recovery and CO_2 storage, which are injection time and injection rate.

Similar to Nasiri et al., (2015), (Mithani & Jamiolahmady, 2018) conducted a simulation study to evaluate the injection of methane, lean gas, and CO_2 for condensate treatment. Their results show that the injection of CO_2 yielded the highest gas and condensate recovery. They also recommended that appropriate phase behaviour and experimental core flood analysis should be performed to generalise the results obtained from a series of simulation studies.

Kumar et al., (2015) and Vo & Horne (2016) evaluated the efficiency of different gas injection strategies to alleviate condensate banking and improve gas and condensate recovery. They injected (N_2), (CH_4), (CO_2), and Lean natural gas into a fractured core and concluded that CO_2 injection had the highest condensate re-vaporisation potential but would require a higher molar volume for pressure maintenance.

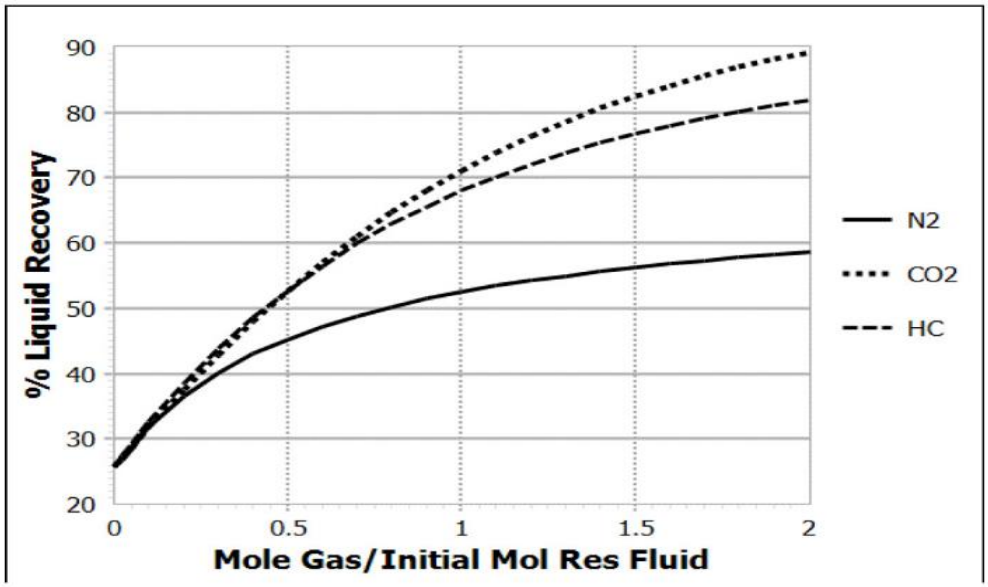

Figure 2.2: Percent liquid recovery with each of the three injection gases. (Kumar et al., 2015)

Husiyandi Husni & Jamiolahmady (2017) performed a numerical simulation study on the H-n-P injection of a remedial fluid with varying compositions of CO_2 and a wettability alteration chemical for ECGR in a carbonate reservoir. Their result shows that the rate and duration of injection highly influence the effect of CO_2 while the wettability modifier chemical is dependent on the treatment radius, but the combined injection of both fluids yielded better performance than an injection of CO_2 or chemical only. It was also reported that the reservoir fluid composition plays a vital role in determining the effectiveness of simultaneous injection of the remedial fluid.

Mithani & Jamiolahmady, (2018) performed a simulation study to investigate the problems of the early breakthrough of injected gases and their adverse effects on condensate production, considering a high permeability reservoir affected by the impact of inertia and coupling. Their result shows that during the injection of three different fluids (CH_4, CO_2, and lean gas), breakthrough time and condensate yield vary significantly while considering the velocity effects. However, one major issue identified during this study was estimating the gas and condensate yield post breakthrough of injected gas, indicating the injection of CO_2 could be better than CH_4 and lean gas. They recommended that experimental studies need to be done to validate their results.

Odi (2012a); Su et al., (2017); Ayub & Ramadan (2019) investigated the injection of CO_2 in gas condensate reservoirs considering several condensate accumulation scenarios and the corresponding treatment methods, all concluding that the injection of CO_2 is relatively the most efficient condensate prevention or alleviation technique and have suggested that further studies need to be done to analyse viable methods for CO_2 injection

in gas condensate reservoirs. Figure 2.3 shows that during the process of CO2 flooding, condensate oil saturation gradually decreased. The injected CO2 not only supported the reservoir pressure, but also increased the saturation pressure (to lower liquid dropout) by re-vaporisation.

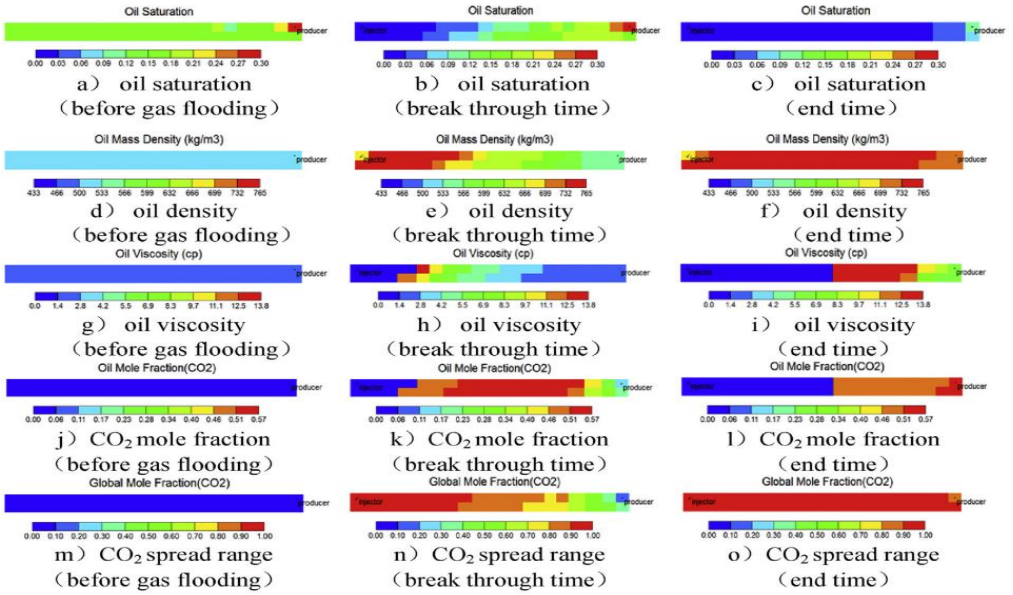

Figure 2.3: Core cross sectional view of condensate seepage flow characteristics variation. (Su et al., 2017)

Ding et al., (2019) conducted an experimental study on improving hydrocarbon recovery from tight gas reservoirs. Several factors influencing CO_2 injection in tight cores, including permeability, diffusion, and adsorption, were also studied. The results showed that the injection of supercritical CO_2 had enhanced the gas recovery by 18.9% relative to depletion. They also recommended further experimental tests to investigate the impact of phase behaviour changes and miscibility on the recovery factor.

Mohammed et al., (2020) conducted an experimental study investigating gas alternating gas (GAG) technique for enhanced gas recovery and CO_2 storage in sandstone rock cores. The tests were performed below the dew point at 40C and 1500psi which was below the minimum miscibility pressure by nitrogen as cushion gas following every stage of CO_2 injection. Their results indicated that methane recovery and CO_2 storage capacity improved significantly with lower N_2 volume in the injected gas stream. Although not mentioned in this work, it is assumed that improved methane recovery was because, with a lower volume of N_2 concentration, the system will quickly achieve multiple contact miscibility (Soltan Sleiman et al., 2021). It is important to mention that the N_2 and CO_2 were injected continuously with no shut-in period to enhance fluid interaction and mass transfer between the injected and resident fluid. This experiment was aimed at

investigating the condensate recovery efficiency by multiple contact miscibility mechanism during continuous gas alternating gas (GAG) injection.

Mohsin et al., (2021) performed a simulation study on the injection of CO_2 into depleted gas condensate reservoirs as an enhanced recovery method to investigate the potential of achieving improved gas and condensate recovery while reducing associated CO_2 production linked to natural gas production. Their results show that the injection of CO_2 improved the productivity of both gas and condensate by approximately 35% by delaying the production plateau by 1.5 years.

2.6 H-n-P CO_2 Injection

The cyclic injection of CO_2 where only one well is used as an injector for treatment purposes and then converted to the producer for hydrocarbon recovery is referred to as the H-n-P injection technique. This section discusses the H-n-P CO_2 injection as a condensate treatment technique. Due to limited information on the field-scale implementation and applicability of the H-n-P CO_2 injection method, most of the reports presented in literature are either experimental or simulation-based.

Teresa & Coma, (1988) conducted a laboratory study to investigate the H-n-P CO_2 injection for improved recovery of light oil with 32° API in a Berea core. From their results, incremental oil recovery was observed after every H-n-P injection circle. They compared the recovery efficiency from the cyclic CO_2 flooding to that observed during a corresponding CO_2 continuous flood. The volume of CO_2 injected during the Cyclic flood was lesser with higher oil recovery observed. This higher recovery was because of the presence of the multiple-contact miscibility mechanism in the CO_2 cyclic flood. They concluded that soaking time is required to maximise the fluid interaction which leads to swelling and extraction of hydrocarbon into the CO_2-rich phase. They suggested that further studies be conducted to investigate the influence of oil swelling, relative permeability effects, and reservoir pressure, especially when working below or near the minimum miscibility pressure (MMP).

Zhang et al., (2004) performed experimental and simulated cyclic CO_2 flooding to enhance light oil recovery from a waterflood reservoir. Appropriate phase behaviour and fluid modelling of the oil/CO_2 mixture were done to aid the simulation. The results indicated a 10% increment in condensate recovery during the depletion phase. CO_2 was dissolved in the oil phase preferential to methane over a period of pressure decline after which further CO_2 dissolution was no longer observed. They suggested that the effect of

pressure on oil/CO_2 mixture should be further investigated and optimised for maximum benefits during enhanced oil recovery.

Einstein et al., (2007) conducted H-n-P injection tests to investigate the re-vaporisation capability and condensate recovery efficiency when CO_2 is injected into a depleted gas condensate reservoir, considering specific reservoir conditions to optimise the interaction between the in-situ liquid condensate and the injected fluid as a function of temperature. Parameters like the soaking time were analysed, while residual condensate saturation and sweep efficiency were determined from experimental core displacement data. The recovery efficiency of just over 65% indicated that H-n-P CO_2 injection was effective.

Odi (2012) performed laboratory tests to evaluate the potential of applying H-n-P CO_2 injection for the removal of near-wellbore condensate. They observed that liquid dropout can be delayed as the injected CO_2 can considerably reduce the dew point pressure of the in-situ fluid and hence maintain the high gas-effective permeability of the system. They also observed that the re-vaporising effect of CO_2 on the accumulated condensate can be significantly affected by time, so it is best to optimise CO_2 injection and contact time.

Eshkalak et al., (2014) performed a comparative simulation study on CO_2 H-n-P and re-fracturing treatments for gas and condensate production by implementing a non-linear pressure drop in a dual-porosity and permeability model. According to their results presented in Figure 2.4, it was concluded that H-n-P CO_2 injection was not the best treatment option as 96% of the injected CO_2 was produced. They suggested the development of an optimum H-n-P CO_2 injection technique.

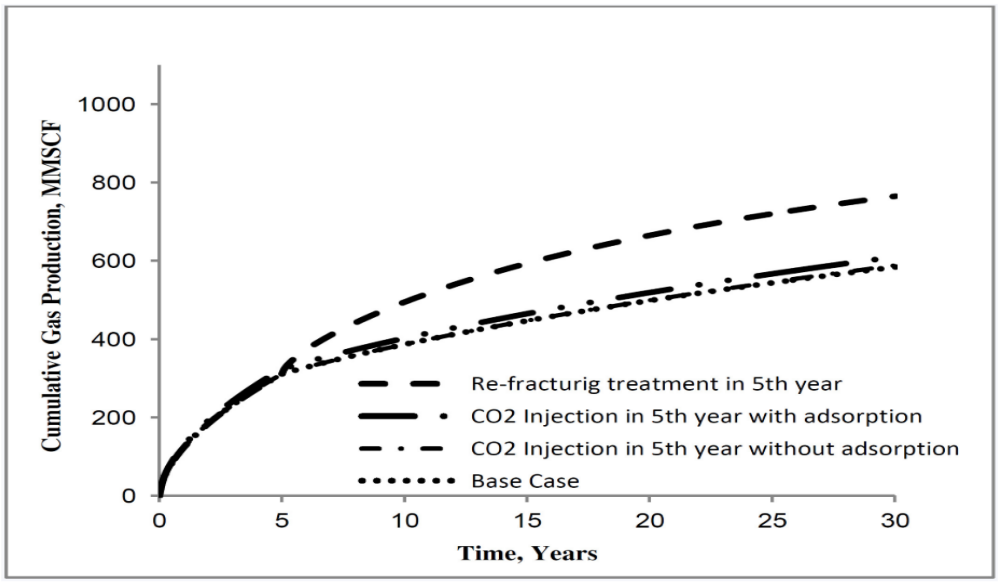

Figure 2.4: Cumulative gas production for all four scenarios. (Eshkalak et al., 2014)

Experimental studies conducted by (Meng et al., 2015) and (Meng & Sheng, 2016) indicate that the H-n-P CO_2 injection approach is more effective for EGR compared to the continuous CO_2 gas flooding method because the rapid pressure increase during the H-n-P process, which is absent during gas flooding method would enhance the re-vaporisation mechanism required for the transfer of heavier hydrocarbon components from the liquid phase to the gas phase, therefore improving the recovery efficiency to about 85%.

In literature, there are reports of chemical injection (relative permeability modifiers) for condensate-blocking removal. The results from the simulation studies done by (Sheng et al., 2016) report that the chemical injection method increases gas and condensate recovery by 1-3%, while the corresponding numbers are between 8-20% for the H-n-P CO_2 injection method when compared with the primary depletion scenario, their results were supported by reports from a simulation study performed by Husiyandi & Jamiolahmady, (2017).

Meng et al., (2019) conducted experimental and simulation studies on a binary gas condensate mixture to determine the enhanced gas condensate recovery performance of H-n-P CO_2 injection. They highlighted four mechanisms (pressure support, vaporisation, viscosity reduction, and oil swelling) that influence the recovery process but failed to quantify their effects and how they contribute to the process. The results obtained from the H-n-P CO_2 injection study demonstrated that condensate recovery was improved from 17% to 25% after four cycles of CO_2 injection. For the experimental case, the initial condensate saturation after natural depletion was 10.8%, and after 5 cycles of CO_2, H-n-P this was reduced to 7.5%, approximately 30% condensate recovery. In other words, their simulation results did not satisfactorily match the experimental results, that is, condensate recovery was underpredicted relative to the experimental results. They suggested that this poor match can be attributed to CO_2 injection period and injection pressure and further studies on developing injection techniques that focus on optimizing these parameters should be considered.

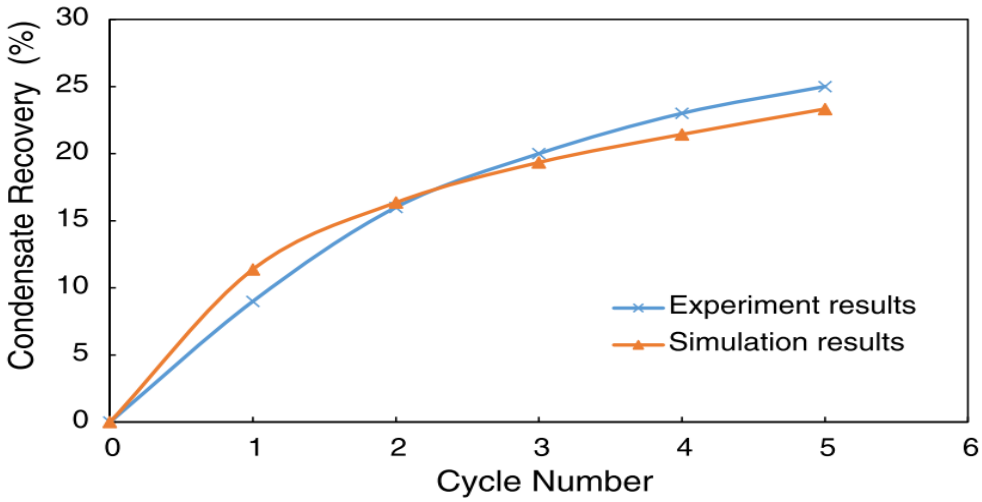

Figure 2.5: Condensate recovery comparison of simulation results with experimental data for H-n-P CO_2 injection. (Meng et al., 2019)

Todd Hoffman & Reichhardt (2020) conducted a simulation study to investigate the relative effects and significance of four mechanisms (pressure support, vaporisation, viscosity reduction, and oil swelling) that influence condensate recovery during H-n-P CO_2 injection. During the simulation study, a model was built to allow all four mechanisms to contribute to the recovery which was referred to as the base case. The influence of individual mechanisms was then evaluated by turning off and on (one at a time) each mechanism to determine the relative contribution of each mechanism. They reported that a variation in the gas-oil-ratio (GOR) will significantly alter the influence of each of these mechanisms. With vaporisation being the most significant for reservoirs with high GOR contributing up to 87.5% of the recovery due to CO_2 injection, oil swelling for low GOR reservoirs with a contribution up to 65.8%, pressure support only plays a minor role by contributing only about 21.9% and 6.3% for high and low GOR reservoirs respectively and viscosity reduction with the least impact of 9.8% and 0% in low and high GOR systems. They recommended that other mechanisms including interfacial tension, rock-fluid interaction, and fluid-fluid interaction should be further investigated.

A thorough review of the Injection of CO_2 for EGCR was reported by Iddphonce et al. (2020). They presented reports spanning the last decade for two CO_2 injection methods: continuous and H-n-P CO_2 injection methods. For continuous CO_2 injection, gas and condensate recovery can be improved by up to 26% after the primary depletion process, and over 60% of the injection CO_2 is stored in the reservoir. While the amount of CO_2 produced during the H-n-P CO_2 injection technique is much higher, condensate recovery can be improved by over 35% after primary depletion. They concluded that further studies

should be conducted to optimise the interaction between injected fluid and resident fluid, hence addressing the challenge of high CO_2 production during H-n-P injection. It is important to mention that as part of this research the conventional H-n-P CO_2 injection technique was conducted and the results support the findings reported by Iddphonce et al. (2020). This further justifies the development of a more effective H-n-P CO_2 injection technique to improve condensate recovery and also CO_2 storage.

2.7 CO_2-Gas Condensate Interactions

The pressure maintenance of a gas condensate reservoir is vital for optimum gas and condensate recovery. In the case of H-n-P CO_2 injection, the interaction between the resident fluid and injected CO_2 is dependent on the dispersion mechanism, CO_2 solubility into condensate by diffusion, condensate swelling, re-vaporisation, and extraction of intermediate/heavy components. According to Monger et al. (1988) and Monger & Coma (1988), H-n-P CO_2 injection for gas and condensate recovery is mainly described as a miscible process where the coherent forces of capillarity are eliminated as the interfacial tension decreases. It is important to note that the process of CO_2-Gas condensate miscibility is highly dependent on the reservoir pressure and temperature.

Holm & Josendal (1982) stated that the condensing/vaporising mechanisms govern the recovery process from a gas condensate reservoir. Still, in most cases, both mechanisms might be simultaneous, making it very complex to quantify their individual effects on the system. Whitson & Brulé (2000) and Luo et al. (2001) confirmed the possible interaction between injected gas and retrograde condensate when injected below or above its dew point could be governed by vaporisation or condensation mechanisms, respectively. These findings are generally valid for gas injection exercises performed for condensate alleviation. The results of experiments performed during this study also confirm the vaporising mechanism to be the dominant recovery mechanism when implementing the H-n-P injection of single component gases into depleted gas condensate reservoirs. As pressure decreases significantly in a gas condensate reservoir, the composition of the retrograde condensate can influence the governing mechanism and the miscibility of both injected and resident fluid. The condensate becomes heavier, resulting in higher interfacial tension between injected fluid and resident gas condensate.

Høier & Whitson (1998a, 1998b), Jessen & Orr (2004) conducted experiments to obtain the minimum miscibility pressure between CO_2 and gas condensate mixtures. They stated that contrary to previous knowledge, miscible displacement can be accomplished at pressures well below the dew point pressure of a hydrocarbon mixture. The dynamic

miscibility between injected CO_2 and resident condensate is best quantified by unique laboratory experiments such as first-contact miscibility (FCM), multiple-contact miscibility (MCM), and swelling test. This study has adopted the proposed approach and quantified the miscibility of CO_2 and resident fluid at a pressure below the dew point for binary and multi-component gas condensate fluid, by performing the FCM, MCM, and swelling tests.

Shtepani (2006) and Hou et al. (2016) performed experimental and simulation studies on gas-condensate and CO_2 phase behaviour for four different CO_2-Gas/Condensate mixtures with 20, 40, 60, and 80 mole % CO_2 addition, respectively. The constant composition expansion test results indicated that CO_2 was completely soluble in the gas condensate fluid, and the liquid dropout decreased after each step of CO_2 mole percent addition. At 80 mole percent injected CO_2, the gas condensate fluid was a single-phase gas with no retrograde condensate formed. Confirming total CO_2 and resident fluid miscibility. See Figure 2.6 below for graphical illustration.

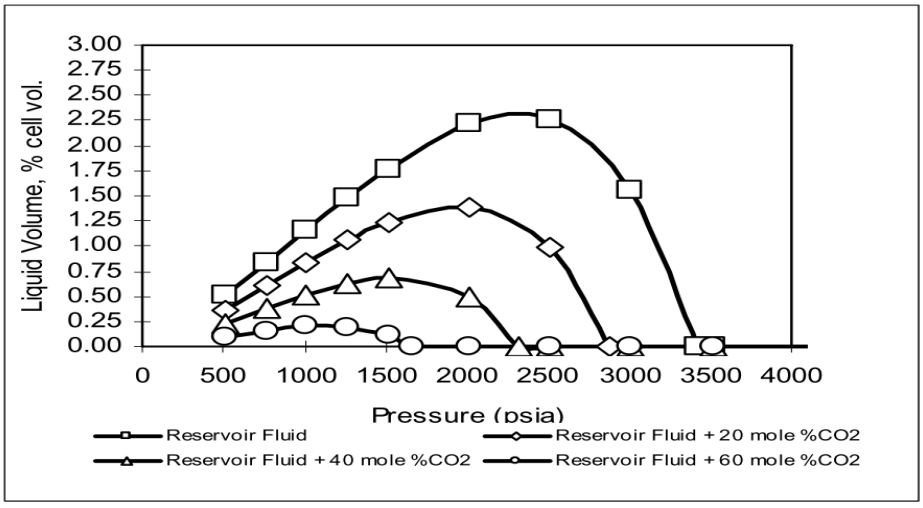

Figure 2.6: Constant composition expansion at 212 F – Liquid dropout with CO_2 addition. (Shtepani, 2006)

Shtepani et al., (2006) described an approach that relates primarily to the laboratory and modelling studies that precede compositional simulations and field pilot tests of CO_2 storage in gas condensate reservoirs. It is known that CO_2 injection in depleted gas condensate reservoirs may allow enhanced gas recovery by reservoir re-pressurization or pressure maintenance. They conducted a swelling test considering the FCM and MCM to determine the level of interaction during CO_2 injection for EGCR in a depleted reservoir. They stated that pressure diffusivity is typically several orders of magnitude larger than molecular diffusivity, where a larger volume of CO_2 was dissolved in the condensate at a

pressure above the MMP relative to the volume dissolved at lower pressure (below MMP) even with a higher concentration of CO_2 in the system.

Khan et al., (2013) performed a comparative simulation study on a gas condensate reservoir to evaluate the effect of CO_2 solubility on gas and condensate recovery. They performed two sets of simulations, firstly considering CO_2 solubility and secondly, without CO_2 solubility. Higher condensate recovery was recorded when the effect of CO_2 solubility was considered.

Nasriani et al., (2014) also conducted a comparative simulation study on the effect of different injection gases for condensate recovery using a PVT cell and a synthetic reservoir model produced from a single well. They evaluated the swelling and vaporisation abilities of various gases on condensate and concluded that CO_2 yielded the best recovery when solely injected for condensate re-vaporisation in the PVT cell. They stated that the injected CO_2 would affect the reservoir fluid by favourably altering its composition. The high level of CO_2 solubility/mixing in condensate liquid enhances its potential to swell and re-vaporise the condensate when contacted at pressures way below the dew point pressure.

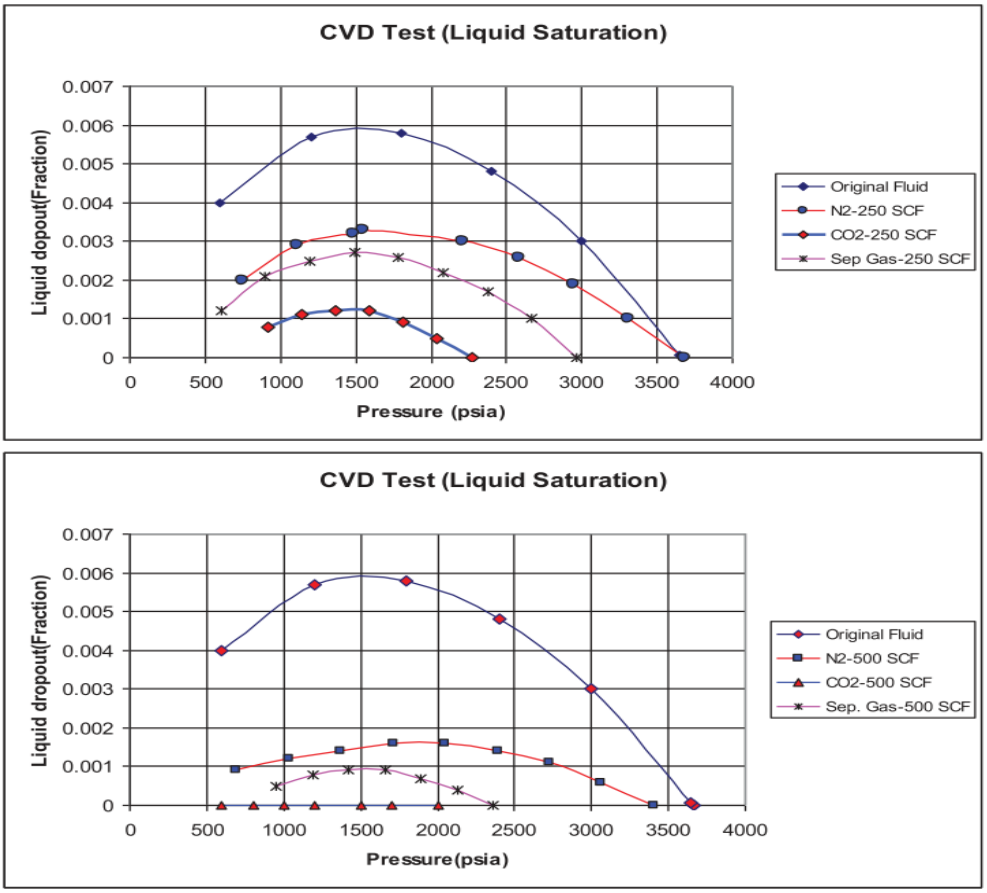

Figure 2.7: The effects of N_2, CO_2, and separator gas injections on the decrease of liquid formation at injection volume 250 SCF and 500 SCF. (Nasriani et al., 2014)

Liu et al., (2015) conducted a molecular dynamics simulation study on the microscopic mechanism that influences the volume swelling of CO_2 hydrocarbon system. They stated that pressure is an important factor to consider during the volume swelling of CO_2 hydrocarbon systems because pressure variation significantly affects swelling factor/Coefficient. They also observed that the level of interaction between CO_2 and hydrocarbon molecules is primarily responsible for swelling and vaporisation mechanisms.

Al-Abri & Amin, (2010) and Honari, (2016) identified pressure, temperature, phase behaviour, and fluid properties of the mixture as important factors that govern the mixing/interaction between injected CO_2 and resident fluid during CO_2 flooding for EGCR purposes. These factors were comprehensively explained by elucidating the physics governing the mixing between supercritical CO_2 and methane using a consolidated porous media. The obtained dispersion data was applied to quantify the effect of fluid composition, system pressure, and temperature on multiple contact phenomena occurring during the mixing process. The results from these studies state that the displacement pressure is a key factor that influences the recovery efficiency. Al-Abri & Amin, (2010) observed that condensate recovery increased by three folds when CO_2 was injected at near miscible conditions which was 23.4% when injected at 1100 psi compared to 69.7% at 3000 psi and an additional 9% for miscible conditions.

Vo & Horne, (2016) and Seteyeobot, et al., (2017) investigated the effect of reservoir fluid composition change on gas condensate reservoir productivity and concluded that the system composition and condensate accumulation depend highly on the production sequence or strategy that has been implemented, and recommended further studies to obtain a clear understanding of how these compositional variations and liquid dropout can be controlled.

Mohamadi-Baghmolaei et al., (2019) performed a series of experimental gas injections to investigate the effects of steady-state mass transfer between three different injection gases (CO_2, N_2, and CH_4) and condensate fluids represented by (C5, C6, and C7) in a porous system. Data from this study was applied in developing a new model for calculating the diffusion rate between injected gas and reservoir fluid as a function of certain factors like injection rate, type of condensate, and injection gas. Their results show that the injection rate and concentration change have significant effects on the estimation of the diffusion coefficient. These results were based on the continuous gas injection which may not be truly representative when developing a simulation model for a H-n-P

type injection scenario which is not dependent on the injection rate to improve the diffusion of injection gas into resident fluid but dependent on the miscibility mechanism and total shut-in period.

Nekoeian et al., (2019) emphasized that the non-equilibrium status neglected by compositional simulators assuming a local equilibrium may misinterpret the interaction process in a gas condensate system. Reservoirs with lower temperatures experience a higher mass transfer coefficient, hence exhibiting a more significant deviation from the local assumption on equilibrium in a gas condensate reservoir.

Most recently, Dindoruk et al., (2021) reviewed the miscibility-measurement techniques applied in most experimental tests published in open literature. A more significant number of these research outputs have failed to consider the inherent assumptions of MCM while solely relying on FCM for describing flow in porous media. They evaluated several methods of estimating the MMP and MCM and discovered a significant inconsistency in data obtained for particular fluid mixtures when using different techniques. Based on experimentally obtained data, they concluded that only methods like slim tube experiments, detailed slim tube simulations, and multiple-mixing-cell calculation methods that consider the effects of MCM should be used to evaluate the MMP of fluid systems. They recommended that the evaluation of the MMP for any hydrocarbon mixture and injected gas should follow a step-by-step process, especially those applied during the multiple contact test.

Results from the presented literature indicate that depending on the condensate alleviation technique implemented, the parameters that may influence its efficiency solely depends on the fluid interaction level and recovery mechanisms in play.

2.8 CO_2 Storage in Gas Condensate Reservoirs

With the increasing concerns and desires to decrease the amount of CO_2 emitted into the atmosphere, gas condensate reservoirs have been identified as potential storage sites for CO_2, which can also have the added benefit of enhancing the productivity of such reservoirs. Mogbo (2011) performed a simulation study on a gas condensate field to determine the potential of injecting CO_2 for EGCR and CO_2 storage. He concluded that to maximise the CO_2 storage capacity of the reservoir, it is essential to maintain the reservoir pressure below the caprock fracture pressure. In this case, CO_2 injection continued until pressure approached 90% of the initial reservoir pressure, and then injection was paused, resulting in the storage of an appreciable amount of CO_2. He

suggested further studies need to be done on validating reservoir integrity to improve and facilitate the storage potential of gas condensate reservoirs.

Leeuwenburgh et al., (2014) considered the injection of CO_2 and nitrogen in gas condensate reservoirs for enhanced gas recovery. They reported that a larger volume of CO_2 was stored relative to nitrogen when both gases were injected individually for enhanced condensate recovery at the end of the conventional production cycle. The density difference between injected CO_2 and liquid condensate favoured the piston-like displacement of accumulated condensate and delayed CO_2 breakthrough time during continuous CO_2 injection. The breakthrough time was much quicker for the injection of N_2, compared to CO_2, due to the poor miscibility between N_2 and condensate when both gases were injected separately at similarly high injection rates. However, it was concluded that to maximise the CO_2 tolerance of the system, CO_2 was best injected gradually rather than quickly over short durations.

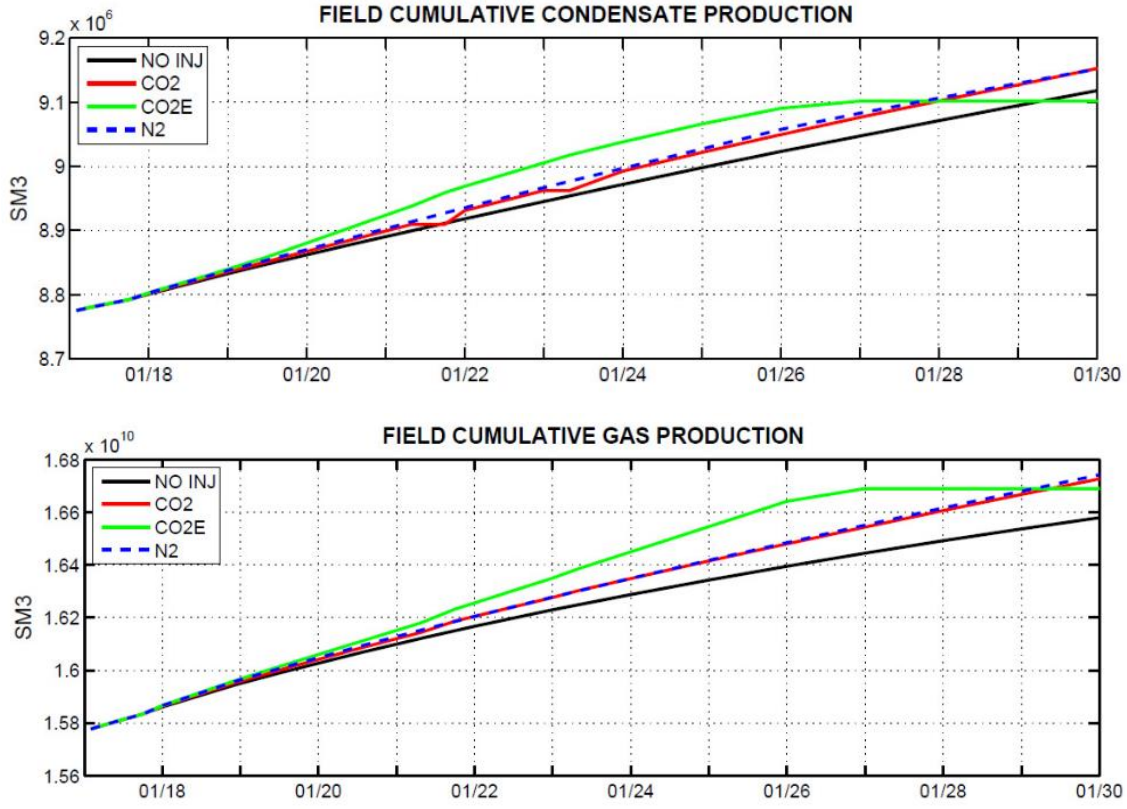

Figure 2.8: Field cumulative gas and condensate production for the four scenarios. (Leeuwenburgh et al., 2014)

Narinesingh & Alexander (2014) conducted a simulation study on CO_2 injection in gas condensate reservoirs to investigate the effect of the injection gas pressure on condensate recovery and CO_2 storage. It was observed that CO_2 considerably enhanced condensate

production to as high as 16%. Approximately 90% of the injected CO_2 was left in the reservoir, trapped as a supercritical fluid. Pressure increase was directly proportional to the volume of CO_2 trapped but had little effect on CO_2 solubility in the formation water.

Cui et al., (2015) conducted a simulation study on the injection of CO_2 for geothermal energy exploitation in depleted gas reservoirs at high temperatures. They evaluated different CO_2 storage forms like CO_2 mineral storage, dissolved storage, and supercritical storage in sandstone and carbonate reservoirs. They concluded that the storage capacity of both reservoirs is maximised when CO_2 is stored in its supercritical state rather than by CO_2 mineralization or dissolution.

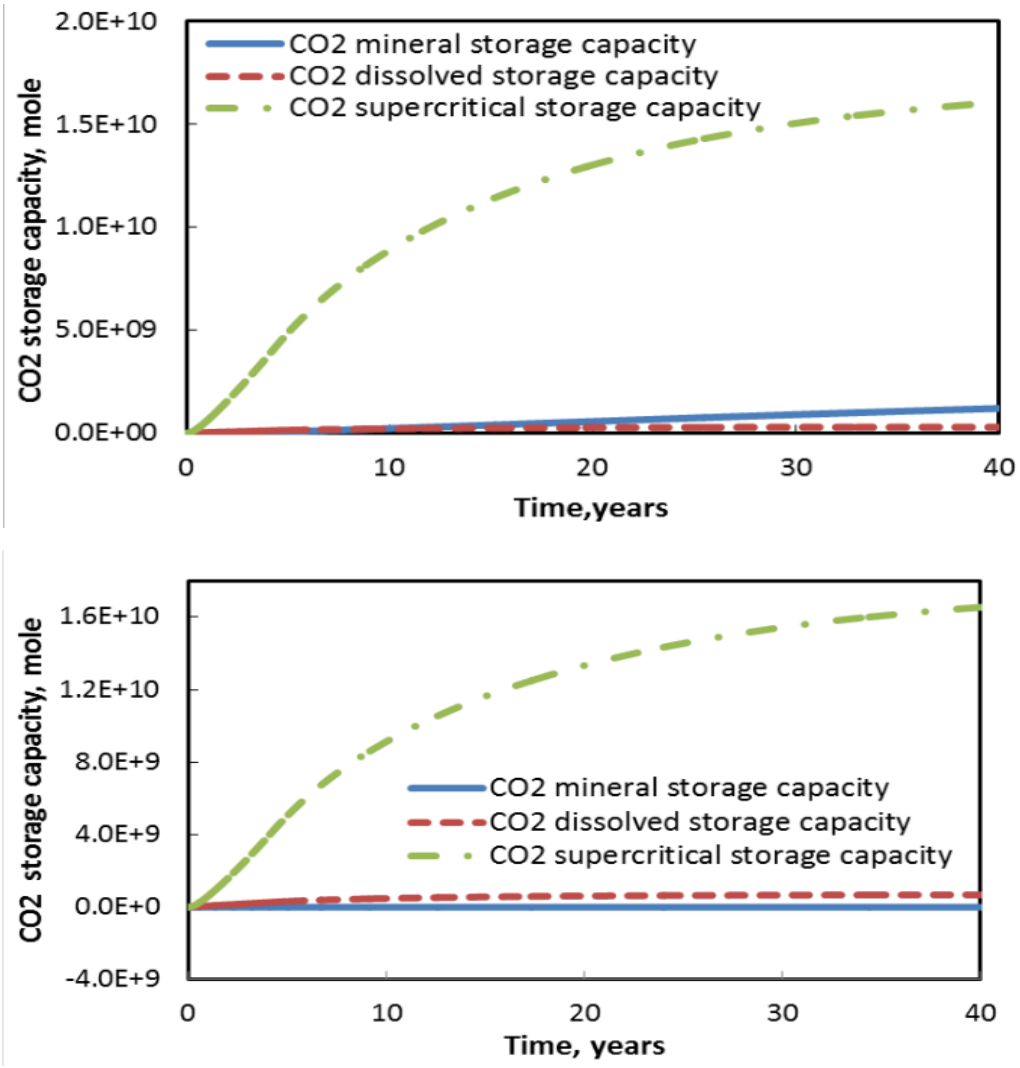

Figure 2.9: CO2 storage capacity in sandstone reservoir (Top) and carbonate reservoir (bottom). (Cui et al., 2 015)

Complementing the results from this study, Jia et al., (2019) performed both experimental and simulation studies to investigate the possibility of achieving CO_2 EGR

and ultimately CO_2 storage in depleted gas condensate reservoirs. They performed sensitivity analysis on CO_2 injection rate, composition, and time to optimise the CO_2 breakthrough. Results from this study show that total CO_2 storage of about 30-40% of the initial hydrocarbon pore volume is achievable and hence lesser presence of greenhouse gas in the production stream.

The results obtained from CO_2 injection studies are mostly limited to generic analytical and numerical models due to a lack of CO_2 injection and storage experimental data. Relative permeability or residual saturation is amongst the most uncertain model parameters that must be tested against observed data to achieve generally applicable conclusions that can be implemented beyond generic studies.

2.9 Review Summary

It is hard to justify that there are significant contributions from previous studies on the fundamental mechanisms of CO_2 flooding in depleted gas condensate reservoirs. This is primarily because there are varying often conflicting reports on the recovery efficiency of injected gases (CO_2, N_2, CH_4, or Lean gas), considering different injection scenarios and reservoir conditions that have been employed. These gases have been injected at different reservoir conditions, flow rates, and volumes during the gas cycling process. Results from Siregar et al. (1992); Subero (2009); Hassanzadeh et al. (2013); and El Gohary et al. (2014) suggested that N_2 injection at pressures above P_{Dew} will reduce the recovery of condensate by stripping the produced gas stream of heavier hydrocarbon components, but will improve condensate recovery if injected at pressures below P_{Dew}. However, (Sadooni & Zonnouri, 2015) performed an experimental swelling test by injecting an estimated volume of N_2 into a rich gas condensate system and reported that nitrogen had a favourable effect on liquid dropout but increased the P_{Dew} of the system. Most recently, Soltan et al. (2021) conducted a series of simulated gas-condensate PVT and swelling tests to analyze the level of interaction when CO_2, N_2, and CO_2/N_2 combination are injected into a gas condensate (synthetic binary and multi-component) system. Results from this study show similar trends to those obtained by (Nasriani et al. 2014) and (Sadooni & Zonnouri, 2015). They reported that N_2 interaction with a gas condensate fluid would decrease condensate accumulation (i.e., heavier components) by enriching the produced gas stream through re-vaporisation. These results conflict with those from the aforementioned studies by (Siregar et al., 1992); (Subero, 2009); (Hassanzadeh et al., 2013); and (El Gohary et al., 2014) that stated the N_2 interaction with

the gas-condensate fluid would strip the fluid of its heavier components hence making the produced gas stream lighter and discounting re-vaporisation.

At the same time, Gachuz-Muro et al., (2011) evaluated the efficiency of different gas injections to alleviate condensate banking and improve gas and condensate recovery. They injected N_2, CH_4, CO_2, and lean natural gas into a fractured core. Their experimental results concluded that the injection of CH_4 was a better option when compared to N_2 and CO_2, with recoveries of 51.70%, 18.70%, and 34.78%, respectively. They did not verify and quantify the mechanism responsible for the outcome of these findings.

Al. Abri, Sidiq, & Amin (2012) performed an experimental study to determine the recovery efficiency of condensate following injection of CO_2, CH_4, and a mixture of both gases. Their findings noted that maximum condensate recovery was obtained during the injection of pure CO_2 with a recovery of 80% of the condensate in place. They also monitored the relative permeability of the condensate and injection gas as a function of liquid saturation. They concluded that a small amount of injection gas inside the core drastically reduced the relative permeability of the condensate. However, there was consideration of the level of interaction between the resident fluid and injected gas.

Kumar et al., (2015) performed a core flood experimental study similar to (Gachuz-Muro et al., 2011) using real reservoir fluids. They evaluated the miscibility and condensate re-vaporisation potential of C_1, CH_4, and N_2 when injected into a depleted gas condensate system. They concluded that CO_2 showed the highest capability to vaporise the already condensed liquid. This was contrary to the reports from (Gachuz-Muro et al., 2011) who had shown that the injection of methane (CH_4) yielded better condensate recovery compared to the recovery observed during the CO_2 injection. However, due to a lack of appropriate identification of the interaction mechanism between injected gases and the resident fluid, it is difficult to determine the reason for these inconsistencies from these reports.

Nasriani et al., (2015) distinctly pointed out the lack of adequate experimental data on the CO_2/gas condensate fluid interactions and the inaccuracy of the untuned equation of state to adequately capture such effects.

Zhengyuan et al., (2017) reported a combined experimental and modelling study on CO_2 injection, concluding that CO_2 significantly improved condensate recovery. However, their work lacked sufficient data on the interaction between injected CO_2 and resident fluid.

Nasriani et al., (2019) reported a simulation study on the injection of the same gases used by (Gachuz-Muro et al. 2011 and Kumar et al. 2015). They presented simulation data for the swelling tests conducted on an original fluid sample from a gas condensate reservoir during N_2, separator gas, and CO_2 injection. They concluded that CO_2 was the most efficient gas for pressure maintenance and decreasing condensate dropout, thereby enhancing recovery. The results presented were based on the study of the reservoir fluid composition, which was a lean gas. No studies and data were reported for other categories of gas condensate (intermediate and rich) fluids and the mechanisms governing fluid interactions in such systems. Additionally, there are no experimental data to verify these simulated swelling data.

Therefore, adequate phase behaviour experimental studies are required to clarify the level of interaction and recovery mechanisms in play between CO_2 and gas condensate systems when CO_2 is injected for EGCR and CO_2 storage purposes. Although numerous studies of CO_2 injection into conventional crude oil reservoirs have been developed and implemented in practice, very little work has been done on EGCR by CO_2 injection.

In other words, it is important to state that the application of non-hydrocarbon gas injection for enhanced gas condensate recovery (EGCR) is still in the developmental stage. The mixing/interaction between the injected gas and resident reservoir fluid is yet to be extensively understood. Particularly when considering the impact of fluid interaction, the effects of reservoir fluid composition, reservoir conditions, injection pressure, miscibility, and re-vaporisation capability of the injected fluid on hydrocarbon recovery during continuous or H-n-P condensate treatment methods. Hence, the inability to optimise the recovery process during the injection of non-hydrocarbon gases has led to limited pilot trials. In this study, we have been able to investigate the effects of all the above-mentioned parameters on the recovery of condensate during H-n-P CO_2 injection.

This chapter presents the literature review conducted to place the current experimental and simulation study within the context of previous simulation-based studies. These earlier studies relied solely on EOS predictions, which may not have accurately captured the interactions between fluid phases and flow behaviour for EGCR and CO_2 storage processes due to the absence of supporting experimental data. The main objective of this study is to develop a practical framework that combines experimental and simulation studies to identify and quantify the contributing mechanisms that govern the interaction between CO_2 and gas-condensate fluids during CO_2 injection for EGCR and CO_2 storage purposes.

The effectiveness of the Injection scenario under Investigation Is supported by comprehensive experimental phase behaviour tests and well-calibrated EOS models, which have been adjusted using experimental data.

Chapter 3 - Phase Behaviour Measurements

In the summary of the literature review presented in Chapter 2, it was highlighted that there are misconceptions or issues related to CO_2-hydrocarbon mixing and the level of interactions required for hydrocarbon swelling and extraction, that needs to be further analysed. The study presented by Liu et al., (2015) attempts to proffer a solution to this problem by investigating the microscopic mechanism of swelling in binary mixtures of CO_2-alkane systems. This was a welcomed approach, but their method lacked applicability as they only considered CO_2 interaction with dead oil represented by single components like hexane, cyclohexane, octane, and decane. It has already been established that CO_2 is readily soluble in the listed components when contacted individually or as part of the composition of the reservoir fluid. Another shortcoming is that the effects of heavier components like tetradecane, pentadecane, hexadecane, and eicosane on volume swelling and extraction during CO_2-gas condensate mixing/interaction have not been investigated. Understanding this phenomenon is vital when designing a condensate alleviation technique because the accumulated condensate may be composed of fractions of heavier components.

However, a more applicable approach would be to perform appropriate phase behaviour analysis to investigate the level of CO_2-hydrocarbon mixing/interaction using live oil samples at reservoir conditions, such as real fluid or recombined samples. The experimental analysis performed in this study considers this missing link identified by (Liu et al., 2015), which could provide a better understanding of the mechanism of hydrocarbon volume swelling when contacted with supercritical CO_2. Hence, bridging the gap by generating useful data applicable for designing efficient CO_2 injection methods for enhanced gas condensate recovery and other reservoir engineering applications.

For the CO_2 injection part of this study, two gas condensate fluid samples were designed to exhibit similar dew point and liquid dropout properties of a real-rich gas condensate fluid. It was appropriate to perform these proposed tests with a rich gas condensate fluid as the high liquid dropout would enhance the efficient description and characterization of the volume swelling, component extraction, and the mechanism in play during CO_2-GC interaction. Fluid-1 is a binary gas condensate fluid composed of methane and octane only and Fluid-2, a ternary gas condensate mixture composed of methane, octane, and hexadecane, to present the properties of a rich gas condensate fluid with a heavier component. Working with such fluids with well-defined properties helps

to reduce the uncertainty of fluid description and better understand the dominant mechanisms.

3.1 Fluid Design and Recombination

Prior to fluid recombination, the required volume of Fluids -1 and -2 was estimated considering the capacity of all the equipment to be utilised during the experimental analysis, the volume of fluid required for displacing, conditioning, and pressurizing the fluid chamber before each test. A 2-litre rocking cell and a 300 cubic centimetre cell were used for component conditioning and recombination. Each cell is thoroughly cleaned with cleaning agents including toluene, methanol, and acetone before vacuuming. A pre-estimated volume of the lightest component (based on its molar density) is injected into the rocking cell, and pressurised to the desired combination pressure which is usually above the simulated dew point pressure of the system and allowed to stabilise. Then the required volume of the heavier components is added one after another while maintaining a constant system pressure at each stage. After all the components have been added, the cell is shut and allowed to stabilise and reach equilibrium pressure. The cell is shaken at intervals to facilitate the effective mixing of the components. All pre-estimated working volumes for phase behaviour and injection studies were obtained from the PVTi module of Schlumberger Eclipse 300 simulation software. While the component properties were sourced from the National Institute of Standards and Technology (NIST) data bank. The Methane, Octane, and Carbon dioxide were about 99.9% pure.

Fluid-1: A simple binary gas-condensate fluid model with well-defined properties is used to reduce uncertainty and better identify the contributing mechanisms. This binary mixture consists of Methane (CH_4) and Octane (C8H18), which were combined at 5500 psi and 20^{o} C with a ratio of 90:10, respectively, to exhibit similar compositional characteristics of a rich gas-condensate fluid with dew point pressure of 4115 psi and liquid drop of 29.17%. Combining at an atmospheric temperature significantly facilitated the recombination procedure, eliminated the complexities of working at an elevated temperature, including safety considerations, and ensured that the desired quantity and compositional integrity of the mixture were achieved. It has to be added that later the fluid temperature was raised to 60C as it was impossible to determine the miscibility/interaction between injected CO_2 and resident fluid at 20C because CO_2 would exist as a liquid and not as a supercritical fluid, which is the more realistic state for CO_2 injection purposes and hence the desired state for this study.

Fluid 2 – A ternary mixture of Methane (CH_4), Octane (C_8H_{18}), and n-Hexadecane ($C_{16}H_{34}$) with a ratio of 90:8:2, respectively, was prepared. The same procedure implemented for Fluid-1 was adopted. However, due to the physicochemical properties of hexadecane that make it a solid and not transferable at 5500psi and temperatures below 38^oC, pressure was kept constant at 5500psi while the temperature was increased to 60^oC before injecting hexadecane into the equilibrated Methane-Octane mixture. Preliminary phase behaviour tests were conducted at these conditions to confirm the integrity of the fluid.

Phase behaviour tests were performed on both fluids 1 and 2 and with and without CO_2 addition to determine the impact of CO_2. Particular attention was paid to fluid 2 to evaluate if the presence of a heavier component that is less soluble with CO_2 at the test conditions would significantly affect the condensate recovery potential of the identified recovery mechanism. The main parameters obtained from the constant composition expansion test are dew point pressure, liquid dropout, and pressure at the maximum liquid dropout.

3.2 Apparatus and Precautions

In this study, the multifunctional Phase equilibria (PVT) cell equipped with a 100cc high-pressure high-temperature (HPHT) fluid compression chambers, high-resolution digital imaging camera, heating jacket, pressure transducers, data acquisition system, and high-pressure pumps were used to conduct a series of experiments to evaluate the level of phase behaviour changes that occur during CO_2-GC mixing. The operating temperature and pressure range from 0 – 200C and 0 – 10,000 psi respectively. Considering these pressure and temperature ranges, the instrument is well adapted for studying the pressure, volume, and temperature relationship for various reservoir fluid and CO_2 mixtures. Prior to operating and conducting any experimental procedure, appropriate training on equipment operation, gas bottle usage, pressure boosting, and fluid recombination was undertaken and completed. All the general laboratory safety and control measures were strictly adhered to during these experiments. A schematic diagram of the phase equilibria cell is presented in Figure 3.1

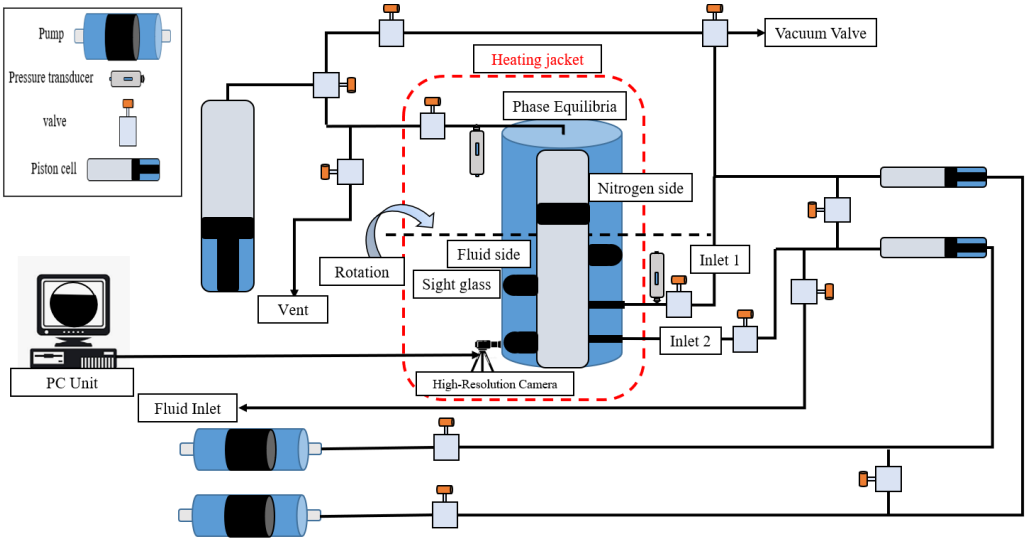

Figure 3.1: A Schematic Diagram of the HPHT Phase Equilibria (PVT) Cell at Heriot-Watt Gas condensate Laboratory.

3.3 Experimental Phase Behaviour Analysis (Fluid-1&-2)

With the fluid sample stabilised and ready to use, the PVT cell and all connected cells are cleaned and vacuumed. Nitrogen is injected and pressurised to 5500psi, the pumps are used to maintain the pressure while making sure the system is leak-tight before increasing the temperature to 60°C and allowed to stabilise. About 2.5 pore volumes (PV) of single-phase fluid which is already stabilised at the test conditions is injected into a PVT Cell to displace nitrogen and void the system of unwanted components which could act as a contaminant. The constant composition expansion (CCE) phase behaviour analysis is conducted initially without CO_2 to obtain dew point pressure (P_{Dew}) and liquid dropout (LDO) profile of the original fluid and then repeated with the incremental addition of CO_2 to observe the resultant changes in P_{Dew}, LDO profile, and shrinkage factor. For each of the two fluids, six PVT experiments (i.e., (0) without CO_2 at 20C, (1) without CO_2 at 60C and (2) with 20% CO_2 at 60C, (3) with 40% CO_2 at 60C, (4) with 60% CO_2 at 60C, and (5) with 80% CO_2 at 60C) were carried out for CASE-1 (CO_2 injection above P_{Dew}) and three PVT experiments which are (6) with 20% CO_2 at 60C, (7) with 40% CO_2 at 60C, (8) with 60% CO_2 at 60C) for CASE-2 (CO_2 injection below P_{Dew}). In these experiments, CO_2/Gas condensate interactions were analyzed for these two cases, which are described below.

3.3.1 CASE-1: CO_2 injection above dew point: ($P>P_{Dew}$)

CO_2, equivalent to 20% of the original fluid volume, was injected at 5500 psi. The pressure was then dropped gradually while maintaining a constant temperature of 60 °C to obtain the dew point, maximum liquid dropout, and liquid volume. The LDO shrinkage potential of CO_2 on the resident fluid was determined considering the maximum liquid dropout volume with the addition of CO_2 relative to that without CO_2. Data obtained include Liquid Shrinkage (which refers to the change in the percentage of liquid dropout (LDO) for cases with and without CO_2 present in the original fluid). These steps were followed for any of the three CO_2 compositions, each one by increasing the pressure back to 5500 psi before a new batch of CO_2, equivalent to 20% of the original fluid volume, was incrementally added.

3.3.2 CASE-2: CO_2 injection below dew point: ($P<P_{Dew}$)

In this case, the pressure of the single-phase fluid without CO_2 above its P_{Dew} was dropped to achieve the system conditions at Maximum LDO (3000 psi and 60 C) before CO_2 was injected to determine the swelling potential and ultimately estimate how much condensate was re-vaporised/extracted. CO_2 was injected incrementally, each time equivalent to 20% of the original fluid volume, while the liquid/condensate volume was monitored over time (24 hrs), then the swell factor was determined.

It should be noted for CASE-1, liquid dropout (LDO) is measured at different pressure, whereas in CASE-2, liquid saturation (LSAT) is measured at different times and fixed pressure of 3000 psi which is the system pressure at the maximum liquid dropout (LDO_{Max}) of the original fluid without CO_2.

The simulation of the phase behaviour experiments (CCE, Swelling, and vaporisation) was done using the PVTi module of the ECLIPSE300 simulator. Several equations of state (EOS) models were considered, all based on Peng Robinson's (1978) EOS. These EOS models were tuned to match the experimental data of the original fluid and also those with an added volume of CO_2. In this process, the binary interaction coefficient (BIC) was the primary tuning parameter.

3.4 IFT and MMP Measurements

In this study, the pendant drop method was used for interfacial tension (IFT) measurements. A regular IFT test was conducted between the equilibrated condensate and CO_2 at 3000psi and 60°C using the DSA100 KRUSS-RIG setup consisting of an

HPHT windowed cell, capillary needle, high-resolution camera, light source HPHT cells, temperature control system, and HPHT transducers. This pressure condition was earlier determined from the PVT analysis to be the system pressure at LDO_{Max} of the original fluid without CO_2 at the test temperature of 60C and was the starting point for Case-2 phase behaviour tests. Considering that CO_2-condensate was first contact miscible at these conditions, a vanishing interfacial tension (VIT) test was performed to determine the minimum miscibility pressure (MMP). The first contact miscibility (FCM) occurs in cases when the environment phase (CO_2) and the droplet phase (Condensate) exhibit total miscibility in all proportions on contacting each other. This phenomenon is observed to happen at pressures above the MMP for CO_2-condensate systems. While the multiple-contact miscibility (MCM) occurs below the MMP when complete mixing between CO_2 and condensate is not instantaneous but may be achieved over time if both fluids remain in contact. The MMP is a physical parameter closely related to the local displacement efficiency, hence is an important design parameter for optimizing gas flood recovery as well as recovery by re-vaporisation. These tests were performed following the appropriate experimental and safety procedures to preserve the integrity of generated data.

3.5 Determining Miscibility Mechanism (FCM or MCM)

The equilibrated condensate was injected into the HTHP viewing cell of the DSA 100-KRUSS-RIG already conditioned with CO_2 initially at test conditions of 3000psi and then at lower pressure values, all at a temperature of 60C. The system was monitored to evaluate if the condensate evaporated into the CO_2 phase on first contact without forming a droplet. The CO_2-condensate VIFT experiment was performed to determine the MMP between the injected condensate and resident CO_2. The MMP was obtained from a VIFT plot and at the pressure point where both fluids were no longer first contact miscible. However, due to its importance on the level of condensing/vaporising mechanisms, multiple-contact miscibility (MCM) tests were also performed using the PVT cell method. During the VIFT test, condensate was injected into the CO_2 environment, and at the estimated MMP, a condensate droplet is expected to be formed. While during the PVT cell tests, CO_2 was injected into the cell containing condensate, and at MMP, a visible contact boundary between both fluids was present. Both tests were monitored at equal time intervals for 48 hours.

3.6 Data Analysis and Results Discussion

3.6.1 Experimental Phase Behaviour Analysis

3.6.1.1 Case-1: CO_2 Injection above P_{Dew} (Fluid-1)

Phase Behaviour Analysis – Constant composition expansion (CCE) tests were performed to estimate the dew point pressure (P_{Dew}) and liquid saturation profile of the original fluid without adding CO_2. This test was initially carried out at a temperature of 20°C and then at 60° C, and the results are shown in Tables 3.1 and 3.2, respectively.

Table 3.1. Experimental PVT test data with 0% CO_2 at 20 °C, binary fluid-1.

Condensate Type	Test	P_{Dew}(psi)	P@ LDO_{Max} (psi)	LDO_{Max} (%) wrt Cell Vol @ P_{Dew}
Rich Gas Condensate (0% CO_2)	Experimental	4115	3300	33.32

Table 3.2. Experimental PVT test data with 0% CO_2 at 60 °C, binary fluid-1.

Condensate Type	Test	P_{Dew}(psi)	P@ LDO_{Max} (psi)	LDO_{Max} (%) wrt Cell Vol @ P_{Dew}
Rich Gas Condensate (0% CO_2)	Experimental	4029	3300	29.17

At 60°C, the phase behaviour changes of the original fluid when contacted with increasing volumes of CO_2 were investigated. In addition to the data of the CCE tests reported in Tables 3.1 and 3.2, referred to as set-0 and set-1, four more PVT experiments were carried out. These were sets -2, -3, -4, and -5 corresponding to the cases with the addition of -20%, -40%, -60%, and -80% of CO_2, respectively, to the original fluid at 5500 psi, which is above P_{Dew} of the original fluid. It is observed that the CO_2/gas condensate interaction results in a decrease in the P_{Dew} and LDO at each stage of CO_2 addition, as shown in Table 3.3.

Table 3.3. Experimental CCE test data with the incremental addition of CO_2 at 60 °C, binary fluid-1.

Condensate Type	Sets	P_{Dew}(psi)	P@ LDO_{Max} (psi)	LDO_{Max} (%) wrt Cell Vol @ P_{Dew}
Rich Gas (0% CO_2)	Set-1	4029	3300	29.17
Rich Gas (20% CO_2)	Set-2	3910	2800	26.70
Rich Gas (40% CO_2)	Set-3	3379	2500	19.81
Rich Gas (60% CO_2)	Set-4	2872	1800	11.13
Rich Gas (80% CO_2)	Set-5	2053	1000	5.12

It is noted that the LDO volume after the original fluid contacted with varying volumes of CO_2 has significantly decreased. Hence, the shrinkage potential of CO_2 can be determined using these measured experimental data. The obtained volume data were used to calculate the shrinkage factor based on the following equation (equations 1 & 2). The main outcome of the corresponding LDO shrinkage due to CO_2 addition is presented in Table 3.4.

Some investigators use swelling factor even though the LDO volume is reduced. In this study, the shrinkage factor calculated using the correlation proposed by (Maneeintr, K. et al., 2014) is reported in Table 3.4.

$$Shrinkage\ Factor\ (S.F) = \left({}^{LSAT_{ref}}\Big/_{LSAT_{x\%CO2}}\right) \quad (1)$$

$$LDO\ Shrinkage\ (\%) = \left({}^{(LDO_{ref}\ -\ LDO_{x\%CO2})}\Big/_{LDO_{ref}} * 100\right) \quad (2)$$

Where, $LSAT_{x\%CO2} = Maximum\ Liquid\ Saturation\ @\ x\%\ of\ SCCO2\ Injected$

$LSAT_{ref} = Maximum\ Liquid\ Saturation\ @\ 0\% SCCO2\ Injection$

Table 3.4. Shrinkage factor and liquid shrinkage data, based on max-liquid dropout (in %) data, before and after CO_2 addition at $P>P_{Dew}$ and 60°C, binary fluid-1.

	CO_2 (%)	Sets	LDO_{Max} (%)	Shrinkage Factor	LDO Shrinkage (%)
Experimental CCE Swell Tests Main Results	0	Set-1	29.17	1.00	0.00
	20	Set-2	26.70	1.09	8.47
	40	Set-3	19.81	1.47	32.09
	60	Set-4	11.14	2.62	61.81
	80	Set-5	5.12	5.61	82.44

The shrinkage factor at 20% and 80% CO_2 additions are 1.1 and 5.6, respectively. This means that the LDO volume is 1.1 and 5.6 times less than that obtained for the original fluid. It is also noted that LDO_{Max} decreased by 8.5% when the first batch of CO_2 was added; the corresponding number when 80% CO_2 was added is 82.4%.

3.6.1.2 Case-2: CO_2 Injection below P_{Dew}

Swelling and Vaporisation Tests – Three more tests were performed when CO_2 was injected at a pressure of 3000 psi, which is the pressure corresponding to the LDO_{Max} of the original fluid without CO_2. These were referred to as sets -6, -7, and -8, corresponding to the cases with the addition of -20%, -40%, -60% of CO_2, respectively. Data obtained

during these tests clearly show the swelling effect of CO_2 on condensate. The obtained volume data were used to calculate the swelling factor based on the following equation (equations 3 & 4).

$$Swelling\ Factor\ (S.F) = \left({MAX\_LSAT_{x\%CO2}} \Big/ {MAX\_LSAT_{ref}} \right) \quad (3)$$

$$Vapourized\ Volume\ (\%) = \left({LSAT_{initial} - LSAT_{final}} \Big/ {LSAT_{initial}} \right) * 100 \quad (4)$$

The liquid saturation tends to increase from its initial volume ($\boldsymbol{LSAT_{Ini}}$) to a certain maximum volume ($\boldsymbol{Max\_LSAT_{x\%CO2}}$) due to the dissolution of CO_2 in the condensate before vaporisation begins and the final liquid saturation ($\boldsymbol{F\_LSAT_{x\%CO2}}$) recorded after 24 hrs. See Table 3.5.

Table 3.5. Swell factor and vaporised condensate volume data, based on the max-liquid dropout (in %), before and after CO_2 addition at $P<P_{Dew}$ and 60°C, binary fluid-1.

	Sets	CO_2 **(%)**	**Initial LSAT (%)**	$\boldsymbol{Max\_LSAT_{x\%CO2}}$ **(%)**	$\boldsymbol{Final\_LSAT_{x\%CO2}}$ **(%)**	**Swell Factor**	**Vapourised Volume (%)**
Experimental CCE Swell Tests Main Results		0	28.73	28.73	28.73	1.00	0.00
	Set 6	20	28.73	34.43	24.83	1.20	13.57
	Set 7	40	28.73	43.65	14.90	1.41	39.71
	Set 8	60	28.73	57.18	0.00	1.99	100.00

At the end of 80% CO_2 injection in CASE-1, the system still exhibited a liquid saturation value of approximately 5.12%, while for CASE-2, the system exhibited 0% liquid saturation at the end of 60% CO_2 injection. It is observed that with equal volumes of CO_2 injected at each stage, condensate was extracted more efficiently by swelling and vaporisation in CASE-2 relative to shrinkage in CASE-1. It is acceptable to conclude that injecting below the P_{Dew} is more optimal for condensate banking alleviation.

3.6.2 Simulation and Equation of State (EOS) Tuning

3.6.2.1 Fluid-1 EOS Tuning/Modelling at 5000psi, 20°C and 60°C

EOS-1.1 was generated using the PVTi module and component properties obtained from NIST without tuning to any experimental data. An initial comparison of the measured P_{Dew} and LDO data obtained at 20C without CO_2 added and that predicted by EOS-1.1 at similar conditions showed a significant deviation, Figure 3.2. EOS-1.1 was tuned to match the measured data by applying a multiplier to the BIC of the light and

heavy components to obtain EOS-1.2. At this stage, EOS-1.2 predictions adequately matched the experimental data. This is clearly demonstrated in the data presented in Figure 3.3.

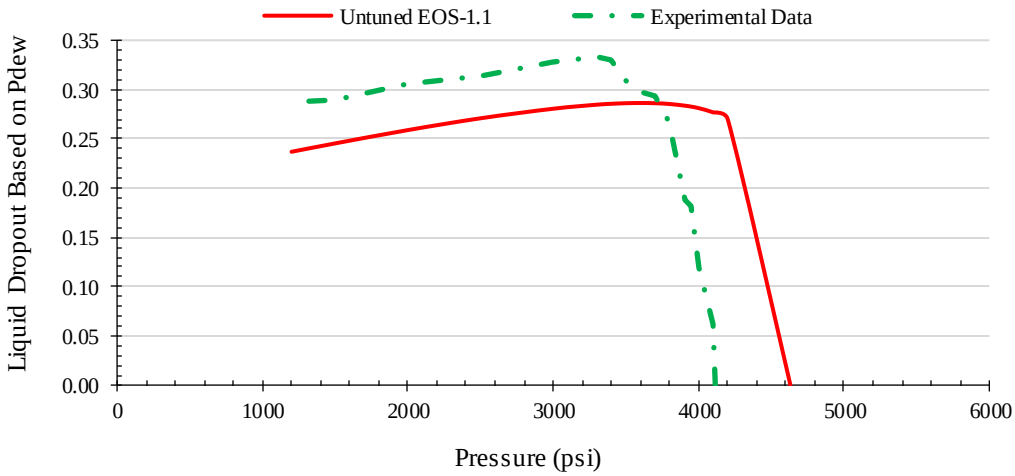

Figure 3.2: Untuned EOS-1.1 versus experimental data without CO2 at 20C, Set 0.

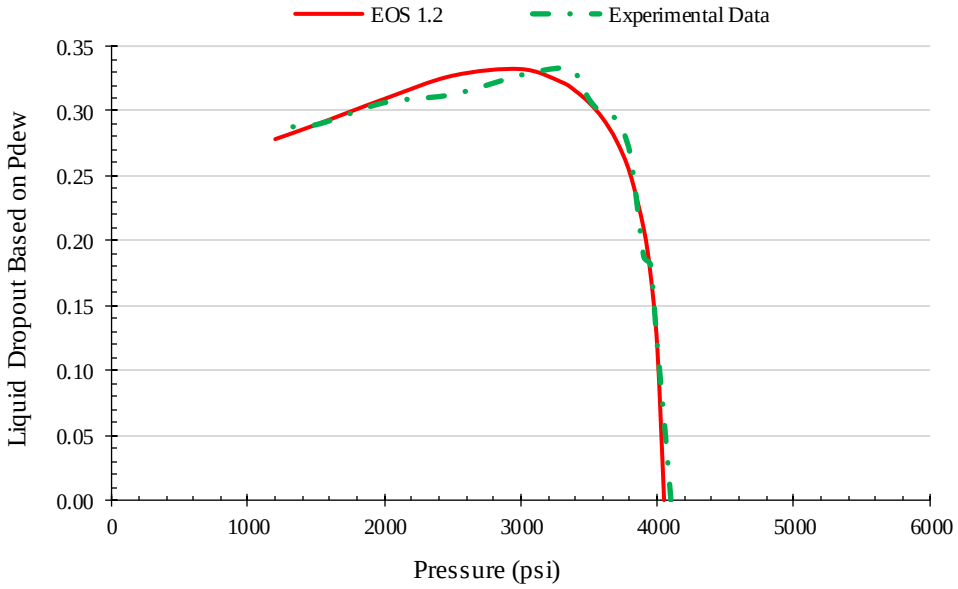

Figure 3.3: EOS-1.2 predictions versus experimental data without CO_2 at 20C, Set 0.

EOS-1.2 was applied to predict the phase behaviour of the original fluid, initially for set-1 (the case without CO_2 at 60C) and then set-2 (the case with 20% CO_2 at 60C) of CASE-1. The results show a good match for set-1, but a significant deviation was observed for set-2. This poor match of set-2 data corresponding to the addition of CO_2 to the original fluid depicted the inability of EOS-1.2 to adequately capture any phase change due to CO_2 gas condensate interactions. Hence, it will also be inadequate for predicting any phase changes that may occur in CASE-2. Figures 3.4 and 3.5 show the results for EOS-1.2 predictions.

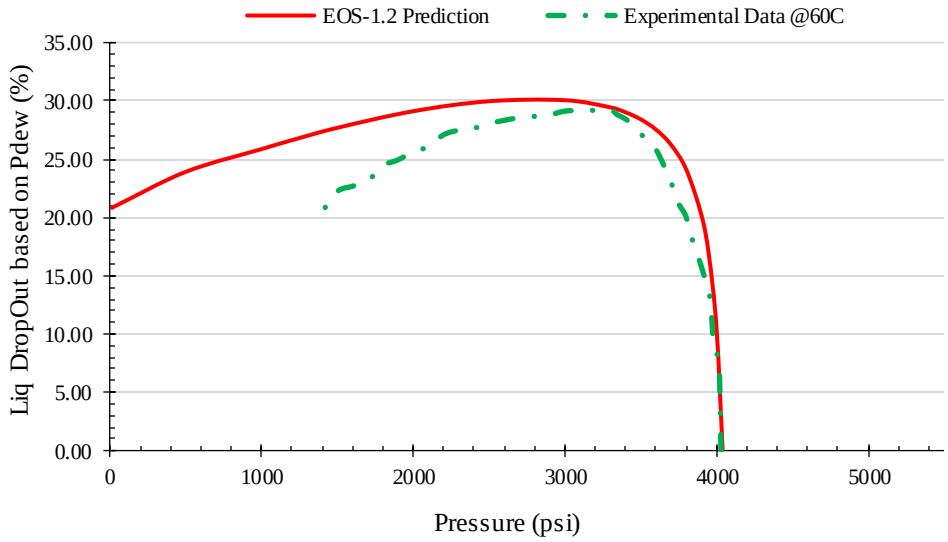

Figure 3.4: EOS-1.2 Prediction versus experimental data at 60C without CO_2, Set 1.

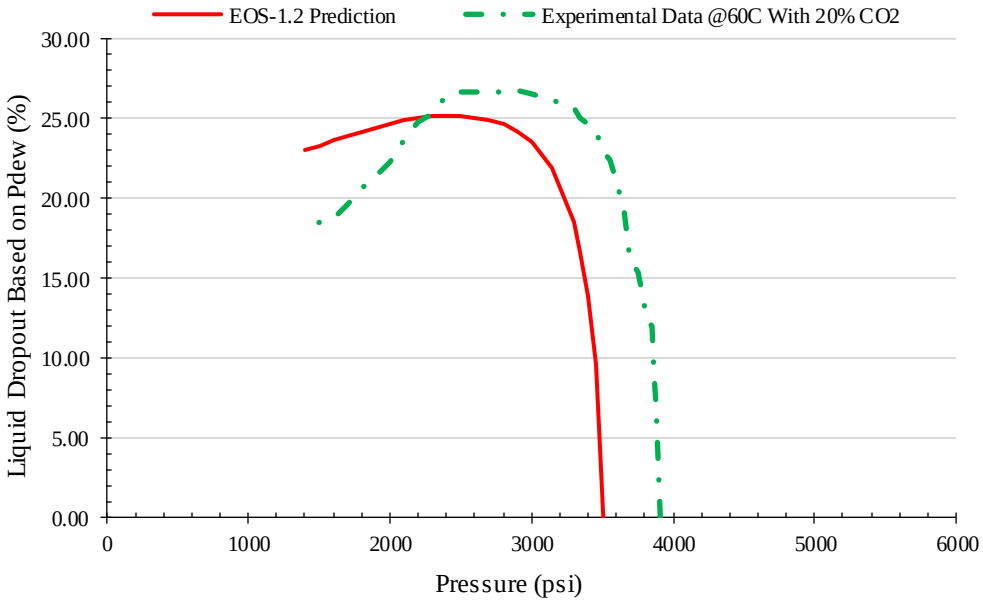

Figure 3.5: EOS-1.2 Predictions versus experimental data with 20% CO_2 at 60C, Set 2.

EOS-1.2 was then tuned further to match set-2 data and is referred to as EOS-1.3, now having a good match with set-2 experimental data shown in Figure 3.6 below.

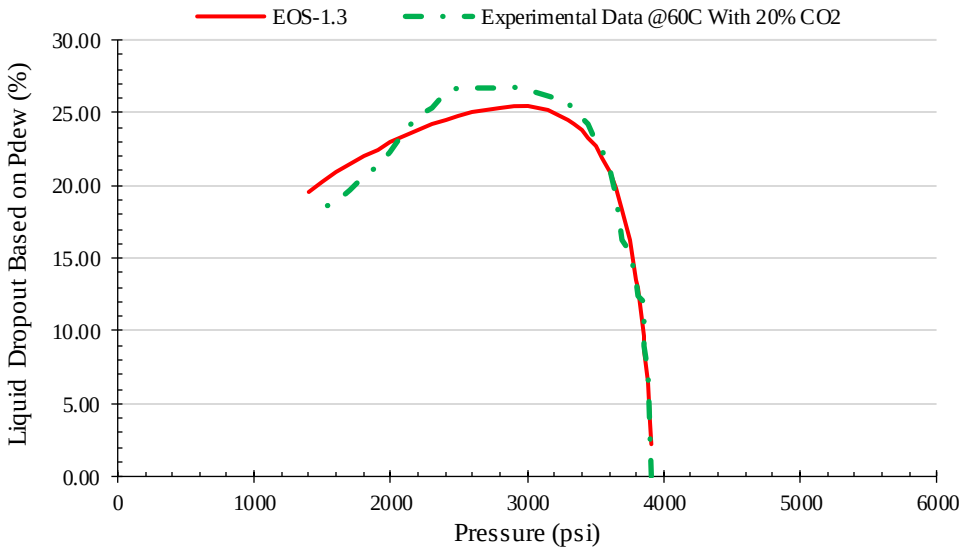

Figure 3.6: EOS-1.3 Predictions versus experimental data with 20% CO_2 at 60C, Set 2.

EOS-1.3 was checked and noted that it is also able to capture the effects of the presence of higher amounts of CO_2 reasonably predicting experimentally measured sets-3 and -4 data, with 40% and 60% added CO_2, respectively, as shown in Figures 3.7 and 3.8. The EOS predictions of set-5 experimental data with 80% CO_2, not shown here, were also close to the measured data.

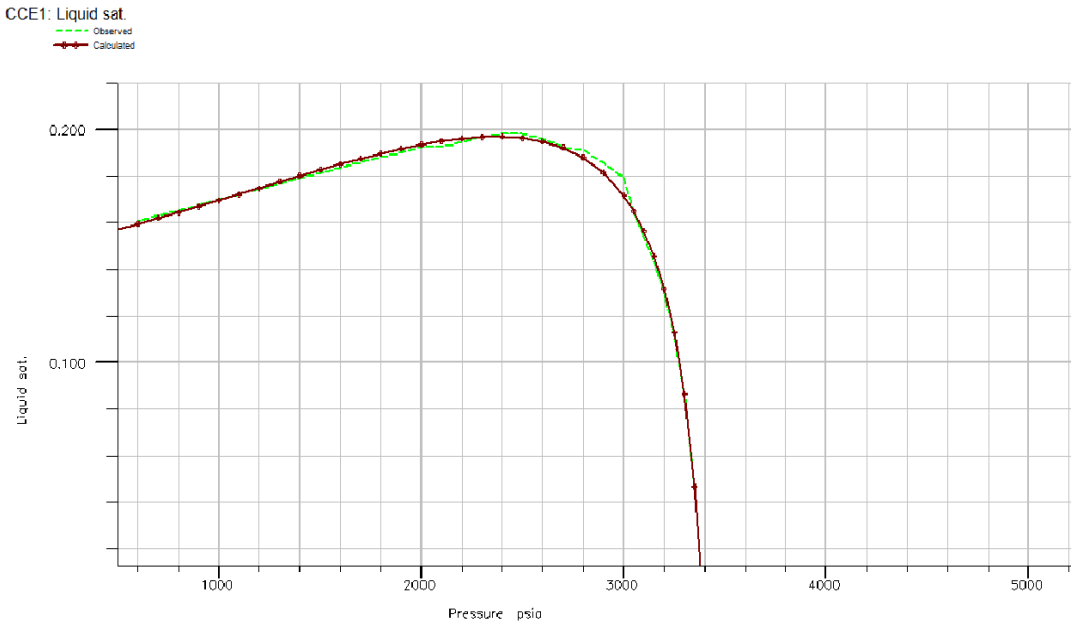

Figure 3.7: EOS-1.3 Predictions versus experimental data with 40% CO_2 at 60C, Set 3.

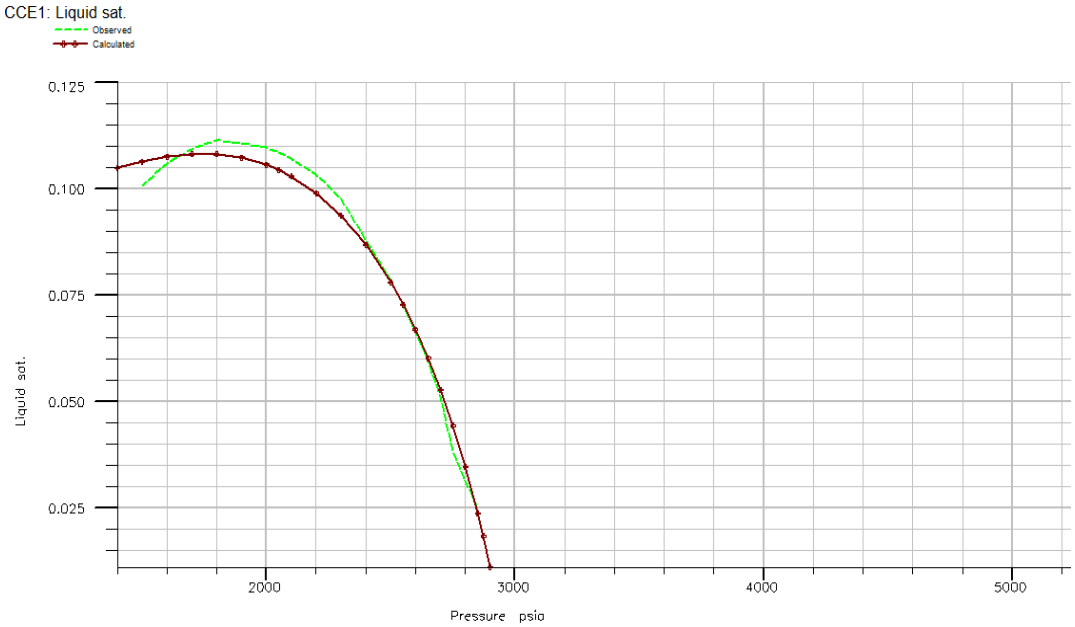

Figure 3.8: EOS-1.3 Predictions versus experimental data with 60% CO_2 at 60C, Set 4.

EOS-1.3 was now applied in predicting the corresponding phase behaviour (LDO shrinkage and swelling factors) during CASE-1 (Sets 3-5) and CASE-2 (Sets 6-8), respectively. The results presented in Figure 3.9 show a good match for both cases, even if these data were not used in the tuning process.

CASE-1

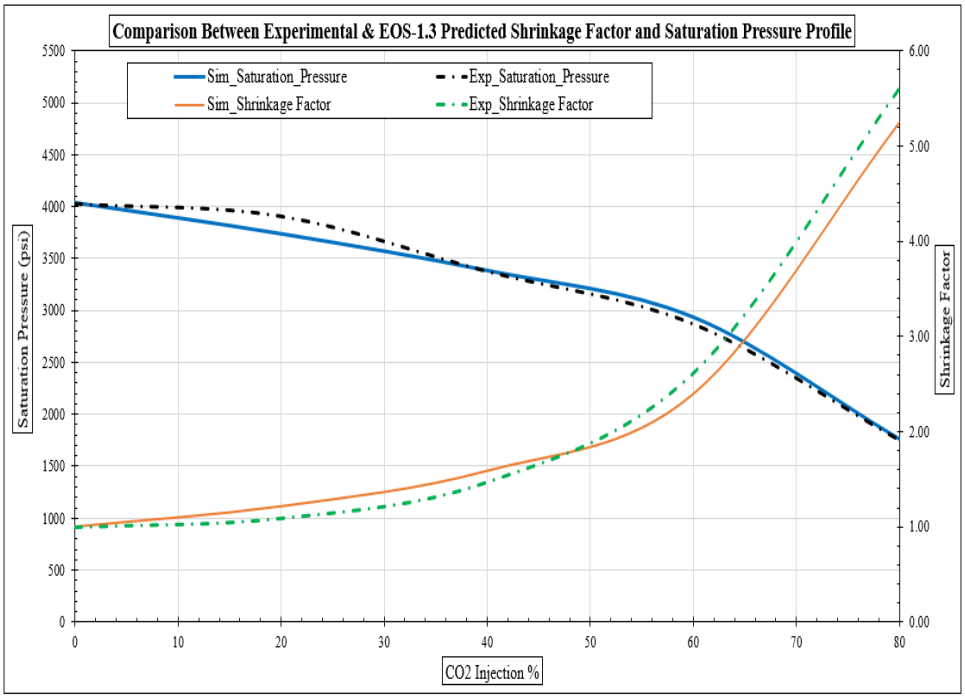

CASE-2

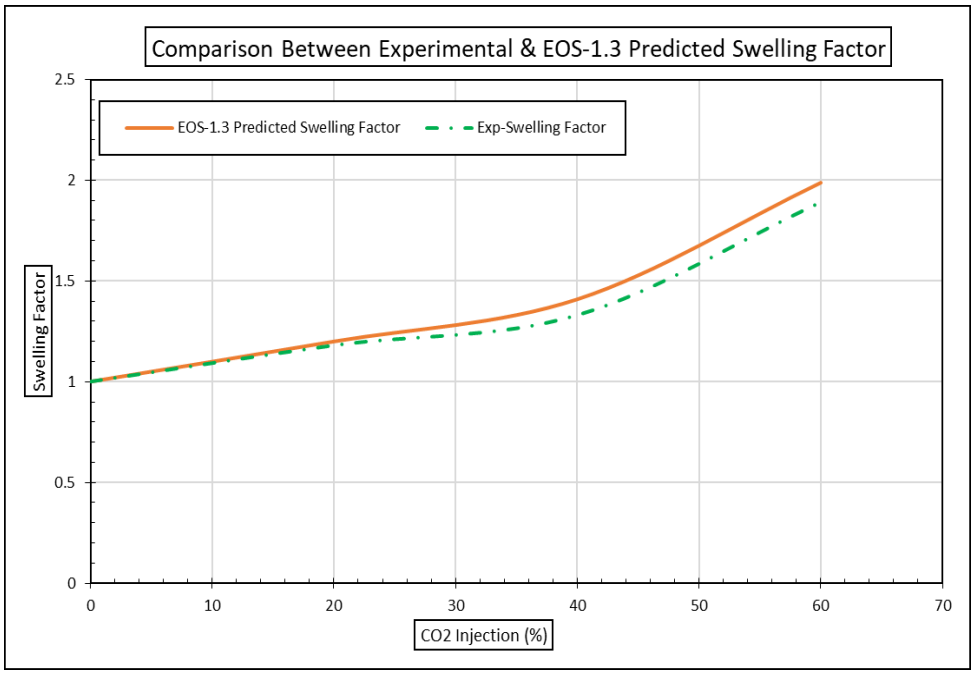

Figure 3.9: EOS-1.3 Predictions compared to experimental pressure profile and shrinkage (Primary and Secondary vertical axis respectively) for CASE-1 and swelling (CASE-2) data with CO_2 at 60C, Sets 1 to 8.

A summary of the predictive capability of all these three EOS models considering three sets of experimental data for P_{Dew} and LDO of the selected fluid either without or with CO_2, is shown in Table 3.6.

Table 3.6: Quality of prediction of three EOS for experimental data sets 1 to 8.

EOS	EXPERIMENTS	RESULTS	COMMENTS
EOS-1.1	SET 0:20C without CO_2	Poor Match	Mismatch after several tuning attempts
	SET 1: 60C without CO_2	Poor Match	
	SET 2: 60C with 20%CO_2 above P_{Dew}	n/a	CO_2 exists in liquid phase
EOS-1.2	SET 0: 20C without CO_2	Good Match	Good match
	SET 1: 60C without CO_2	Good Match	Good match for P_{Dew} & LDO
	SET 2: 60C with 20%CO_2 above P_{Dew}	Poor Match	Good match for LDO only
EOS-1.3	SET 0: 20C without CO_2	Good Match	Good match for P_{Dew} & LDO
	SET 1: 60C without CO_2	Good Match	
	SETs 2, 3, and 4 5: 60C with CO_2 above P_{Dew}	Good Match	
	SETs 6, 7, and 8 LDO Shrinkage: 60C with CO_2 below P_{Dew}	Good Match	Good match for Shrinkage Factor & Liquid Saturation

3.6.2.2 Fluid-2 EOS Modelling

3.6.2.2.1 Case-1: CO_2 Injection above P_{Dew}

Before performing the phase behaviour study on the identified composition for the ternary fluid mixture, it was appropriate to design the mixture to exhibit liquid dropout (LDO) similar to Fluid-1 and having the same amount of C_1 but with some C8 replaced by C_{16}. A range of fluid compositions was tested using EOS-1.3. Table 3.7 shows the predicted LDO for six variations of compositions of C_1, C_8, and C_{16}.

Table 3.7: Phase behaviour data predicted by EOS-1.3 for a ternary-rich gas condensate mixture with different compositions, all at 60C.

	FLUID 1	FLUID 2					
Components	*EOS-1.3*	*Comp-a*	*Comp-b*	*Comp-c*	*Comp-d*	*Comp-e*	*Comp-f*
CO_2 (%)	N/A	N/A	N/A	N/A	N/A	N/A	N/A
CH_4 (%)	90	90	90	90	90	90	88
C8-H18 (%)	10	8	6.5	7.5	7	6	10
C16-H34 (%)	0	2	3.5	2.5	3	4	2
LDO_{Max} (%)	29.1	29.35	36.4	30.2	32.5	40.8	38.5

'*Comp-a'* was considered the most suitable target because the liquid dropout for this mixture is very similar/comparable to that of Fluid-1 with less than 1% variation.

Phase behaviour analysis – A CCE test was performed using the '*Comp-a' composition* to measure the P_{Dew} and LDO of the recombined fluid without the addition of CO_2 to the original fluid. The measured data were not similar to those predicted by EOS-1.3 for this fluid composition. EOS-1.3 overpredicted P_{Dew} by approximately 400 psi and underpredicted LDO by 4%. Table 3.8 shows the experimental and predicted data, respectively.

Table 3.8: CCE experimental data measured and predicted by EOS-1.3, at 60C, fluid-2.

Test Type	Condensate Type	P_{Dew}(psi)	P@ LDO_{Max} (psi)	LDO_{Max} (%) wrt Cell Vol @ P_{Dew}
Experimental	Rich Gas (0% CO_2)	5860	3700	33.44
EOS-1.3	Rich Gas (0% CO_2)	6201	4400	29.35

The observed LDO of this ternary fluid is close enough to that of binary fluid-1 (less than 5% deviation). Hence, no further attempts were made towards adjusting the LDO for Fluid-2 to be closer to that of fluid-1, which possibly could have been achieved by adding more gas to make it lighter. This was avoided because it would have created more uncertainty on the composition of the fluid as the aim was to maintain a similar C1 Mol fraction of 90% for both fluids and investigate any changes in phase behaviour after replacing some C8 with C16.

Therefore, additional CCE tests, similar to those done on Fluid-1, were performed with incremental volumes of CO_2 added to the original Fluid-2. The results are presented in Table 3.9.

Table 3.9: Experimental CCE and shrinkage data with the addition of various amounts of CO2 at 60 °C, fluid-2.

Condensate Type	Sets	P_{Dew}(psi)	P@ LDO_{Max} (psi)	LDO_{Max} (%)	Shrinkage Factor
Rich Gas (0% CO_2)	Set 9	5860	3900	33.44	1
Rich Gas (20% CO_2)	Set 10	4630	3100	25.62	1.30
Rich Gas (40% CO_2)	Set 11	3698	2300	19.59	1.71
Rich Gas (60% CO_2)	Set 12	2741	1530	12.11	2.76

Data Comparison – The phase behaviour and LDO shrinkage data for Fluids 1 and 2 are compared in Table 3.10, to evaluate and quantify the level of interactions between the injected and resident fluids. The results show that the level of interactions is somewhat similar for both fluids. There are variations ranging from 2% to 7% in the swell factor of FLUID-2 at each stage relative to FLUID-1. However, at the end of 60% CO_2 addition, both fluids exhibit similar $P_{Dew,}$ LDO, and their LDO_{Max} are approximately 2.8 times smaller.

Table 3.10: CCE and LDO shrinkage data for FLUID-1 and FLUID-2.

EXPERIMENTAL DATA FLUID -1				**EXPERIMENTAL DATA FLUID -2**		
Condensate Type	**P_{Dew}(psi)**	**LDO_{Max} (%)**	**Shrinkage Factor**	**P_{Dew}(psi)**	**LDO_{Max} (%)**	**Shrinkage Factor**
Rich Gas (0% CO_2)	4029	29.17	1.00	5860	33.44	1
Rich Gas (20% CO_2)	3910	26.7	1.09	4630	25.62	1.30
Rich Gas (40% CO_2)	3379	19.81	1.47	3698	19.59	1.71
Rich Gas (60% CO_2)	2872	11.13	2.62	2741	12.11	2.76
Rich Gas (80% CO_2)	2053	5.2	5.61	P_B	n/a	n/a
LDO Change (%)		61.84			63.78	

The predictive capacity of EOS-1.3 was tested for ternary fluid test data with and without CO_2 added to the original mixture with a summary of main observations shown in Table 3.11. For sets -9 and -10, the predicted values were not close to the corresponding measured data. Hence, EOS-1.3 was tuned using PVT experimental data of Set -9 without CO_2. This exercise was completed by adjusting the Acentric factors, Omega A & B, and the binary interaction Coefficient (BIC) variables of the light hydrocarbons (C1) by a multiplier value of one (1), and Omega A of the heavy components (C8, C16) by a multiplier of 2 and 3, respectively. The predictions of this new EOS-1.4 were close to P_{Dew} and LDO of set-9 experimental data at 60C. When EOS-1.4 was applied for predicting the P_{Dew} and LDO of set-10 (with 20% mol frac of CO_2 added to the original fluid), there was an acceptable match with maximum LDO for experimental, i.e., the predicted and measured values were 25.6% and 25.9%, respectively, but P_{Dew} was significantly underestimated by about 230psi. Hence, EOS-1.4 was further tuned to set-10 experimental data by keeping parameters and multipliers constant for the light hydrocarbon but increasing the multiplier for the BIC between CO_2 and the heavy

components to 2 and 3, respectively. This new EOS, EOS-1.5, was applied for predicting P_{Dew} and LDO values for sets -11 & -12, which showed a good match. A close agreement was also observed for the swelling data that have not been used for tuning this EOS, confirming the reliability of the tuning process.

Figure 3.10 is a graphical representation of the predicted and measured LDO shrinkage data by EOS-1.5.

Table 3.11: Quality of prediction by three EOS, for sets 9 to 12, Fluid-2.

EOS	EXPERIMENTS	RESULTS	COMMENTS
EOS-1.3	SET 9: 60C without CO_2	Poor Match	Mismatch for P_{Dew}, but acceptable LDO
	SET 10: 60C with 20%CO_2	Poor Match	
EOS-1.4	SET 9: 60C without CO_2	Good Match	Good match for P_{Dew} & LDO
	SET 10: 60C with 20%CO_2	Poor Match	Good LDO match, Poor P_{Dew}
EOS-1.5	SET 9: 60C without CO_2	Good Match	Good match for P_{Dew} & LDO
	SET 10: 60C with CO_2	Good Match	
	SET 11 & 12: 60C with CO_2	Good Match	

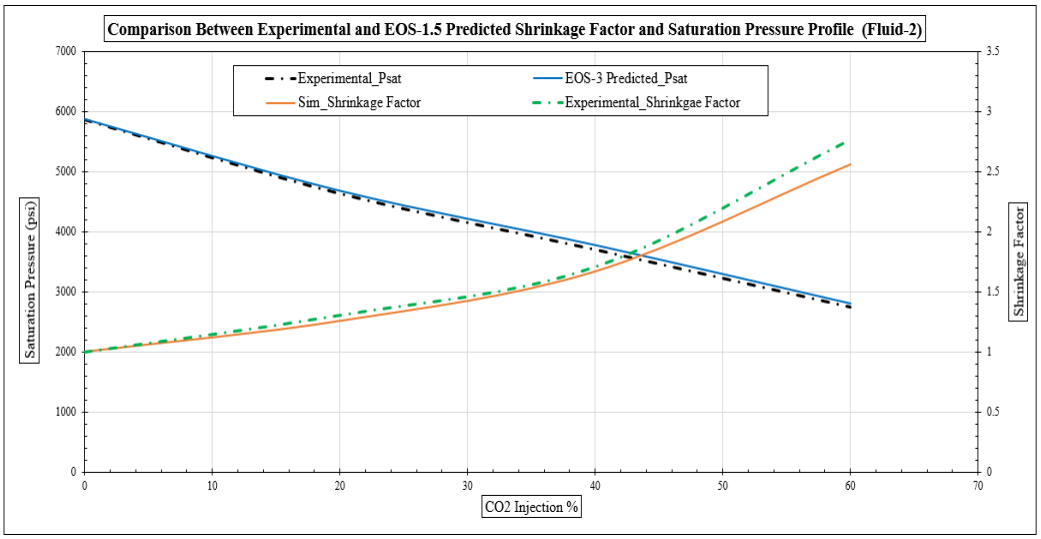

Figure 3.10: EOS-1.5 Predictions versus experimental saturation pressure (Primary horizontal axis) and shrinkage factor data (secondary horizontal axis) at 60C.

3.7 Experimental Interfacial Tension and Miscibility Analysis

The results of IFT measurements using pendant drop and PVT cell tests showed that at a constant temperature of 60°C, IFT is inversely proportional to pressure until it is zero when both phases attain complete miscibility either by FCM or MCM. For this study, it was safe to conclude that at the test conditions of 3000psi and 60°C, there was complete dynamic miscibility between the condensate and injected CO_2. The MMP pressure was measured to be 1500 psi. During this test, no droplet was formed on contacting equilibrated condensate with the CO_2 environment phase at any pressure above this value. Results from the VIT test confirms that at pressures below the MMP, CO_2-condensate interaction/mixing exhibited a multiple-contact miscibility process where complete miscibility is highly influenced by the contact time, which was evident in both the VIT and PVT cell MCM tests. For the VIT test, the droplet size reduced by about 90% of its original size after 48 hrs of contact time. For the PVT cell test, the contact boundary between CO_2 and condensate gradually disappeared over the same 48 hrs period. These results are presented in Table 3.12 and Figure 3.11, respectively.

Table 3.12: Measured IFT data for CO2-condensate system at a constant temperature of 60C.

Pressure (psi)	IFT (mN/m)
3000	0
2500	0
2000	0
1500	2.58
1400	5.06
1300	8.11
1200	12.08
1000	19.50
500	38.01

VIFT

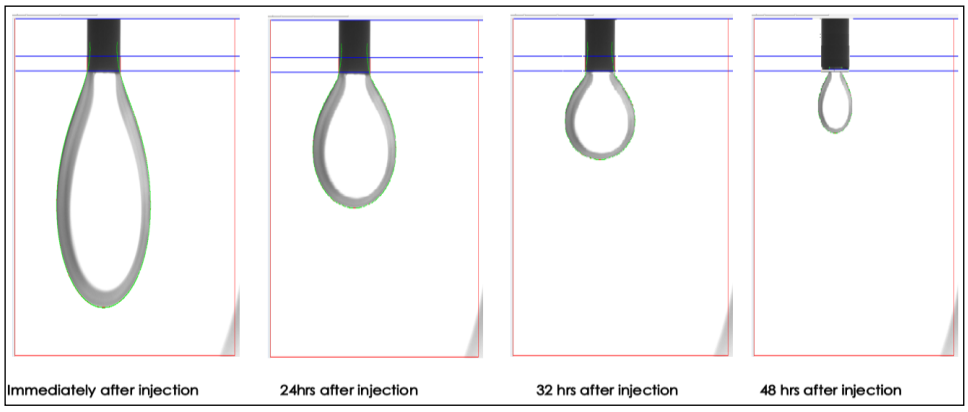

Figure 3.11a: Images from the CO2-condensate VIFT test conducted at 1500 psi and 60C From left to right, showing the gradual dissolution of CO2 into injected Equilibrated Condensate.

PVT

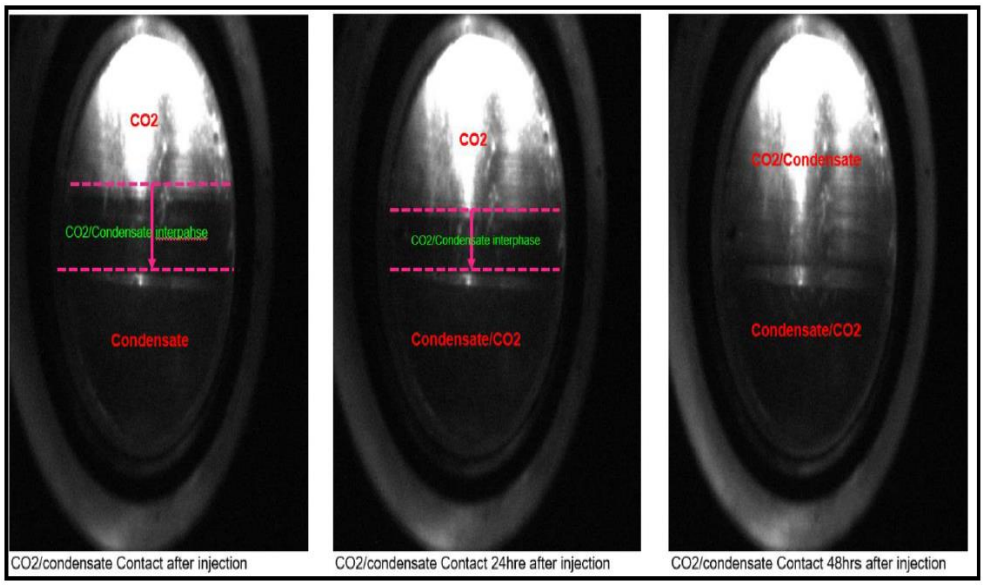

Figure 3.11b: Images from the PVT Cell CO2-condensate miscibility (MCM) test conducted at 1500 psi and 60C, From left to right, showing the gradual dissolution of CO2 into injected Equilibrated Condensate.

3.8 Summary and Conclusions

Gas-condensate fluids behaviour especially when CO_2 is added is complex. Therefore, it is important to measure appropriate types and amounts of PVT experimental data that are used to tune the equation of state model that appropriately describe their behaviour.

In this chapter, the phase behaviour of supercritical carbon dioxide (CO_2) with a binary gas condensate mixture at two temperatures (20C and 60C) was investigated. Two types of experiments in terms of the pressure at which CO_2 is added to the GC mixture were performed. In the first kind, Case-1, various amounts of CO_2 were added to the original fluid at a pressure of 5500 psi which is above the dew point pressure of the mixture before performing the constant composition expansion and shrinkage tests. In the second type, Case-2, various amount of CO_2 was added at 3000 psi which was the pressure corresponding to the LDO_{Max} of the original fluid without CO_2. The swelling factor and corresponding liquid volume were determined and measured respectively after each phase of CO_2 addition.

Thirdly, to better understand and quantify the level of interaction and also determine the mechanism that governs the mixing between the injected CO_2 and resident fluid, a series of interfacial tension and vanishing interfacial tests were conducted. The results obtained from these measurements include the minimum miscibility pressure (MMP) estimated to be 1500 psi, above which the CO_2/resident fluid interaction was primarily

governed by a first contact miscible mechanism while the MCM mechanism governed the interaction below the MMP. The CO_2-condensate miscibility for fluid-1 was measured by using a PVT cell, observation shows that complete miscibility is achievable below MMP only by multiple contacts over a period of 48 hrs.

The condensate shrinkage and vaporising tests were repeated for a ternary gas condensate mixture at the same conditions to investigate the effect of the presence of heavier hydrocarbon composition on the level of CO_2 and resident fluid interaction. After analyzing and comparing the measured data for both cases, it was acceptable to conclude that based on the selected compositions of the reservoir fluid used in this study, the addition of the heavier hydrocarbon component (hexadecane) to the original fluid had no significant effect on the mixing/interaction with the injected CO_2. Considering this result, it was assumed that a similar miscibility mechanism could govern the fluid interaction for the system above and below the MMP. Therefore, no miscibility tests including the vanishing interfacial tension and PVT cell MCM test were conducted for the ternary gas condensate mixture.

Some of the data obtained from the first and second tests of each set of experiments performed on the two binary and tertiary fluids were used for tuning the equation of state (EOS) whilst other tests results were applied to determine the predictive capability of the tuned EOS.

By identifying the binary interaction parameter of light and heavy components as an important tuning parameter, the effective tuning of EOS parameters for these fluid systems was demonstrated.

Considering the presented results in this study, the following conclusions can be made for both the binary and ternary gas condensate fluid models with and without CO_2 added:

1. Data obtained clearly shows the shrinkage and swelling effect of CO_2 on condensate, In Case-1, the liquid dropout is observed to shrink with increased concentration of CO_2, and in Case-2, the Liquid saturation tends to increase (Swelling) from its initial value on contact with CO_2 to a certain maximum swelling point before vaporisation begins.
2. In Case 1 where the pressure of CO_2 injection exceeded the dew point pressure ($P>P_{Dew}$) there was a reduction (shrinkage), in the amount of liquid dropout. This decrease went from 29% to 3% after increasing the CO_2 saturation to 80%. Conversely in Case 2 where CO_2 injection pressure was lower than the dew point pressure ($P<P_{Dew}$) the liquid saturation was completely vapourised when the

system was saturated with 60% CO_2. These findings indicate that condensate vaporisation proves to be a more effective method for removing condensate accumulation relative to shrinkage. Thus, it is advisable to employ CO_2 injection for condensate swelling and vaporisation than, for pressure maintenance.

3. Appropriate EOS tuning is required to achieve an accurate description of gas condensate fluid behaviour with and without CO_2 in the original fluid sample.
4. Appropriate tuning of BICs between light and heavier components significantly improves EOS's ability to match measured experimental data and future predictive capability of an EOS.
5. To improve the predictive capability of EOS when CO_2 is added to the system, only some of the measured CO_2-resident fluid PVT data are required.

These results help to identify the levels of interaction between CO_2 and gas-condensate fluid systems which is beneficial for subsequent studies on efficient EOS tuning and designing the systematic H-n-P CO_2 injection for gas condensate recovery and CO_2 storage purposes.

Chapter 4 - H-n-P CO_2 Core Flood Experiments

4.1 Theory/Methodology Development.

The injection of supercritical CO_2 into depleting gas condensate reservoirs has been identified as a viable option for enhanced gas condensate recovery. The injectivity of CO_2 and its interaction with the reservoir fluid need to be clearly understood to optimise the recovery process. As previous established from literature, supercritical CO_2 injection into hydrocarbon-bearing rock formations with high permeability has been found to be less effective than in low-permeability formations. This is because, in high permeability rocks, CO_2 tends to flow through the larger pores and bypass the smaller pores where it could interact with hydrocarbons. As a result, the contact area between CO_2 and the hydrocarbons is reduced, leading to lower recovery efficiency and early breakthrough of CO_2. This research aims to verify if such a hypothesis is applicable for the H-n-P injection method proposed here. In this chapter series of core flood experiments are performed to help aching this objective.

The procedures followed during the implementation of a H-n-P injection, include the Huffing phase, soaking phase, and Puffing phase. The soaking period could play a significant role in enhancing the CO_2-Resident fluid interaction as the well is shut in for a prolonged period. The H-n-P CO_2 injection method would most probably be preferred to continuous CO_2 injection. This is because, it is assumed that by implementing the H-n-P CO_2 injection method, a limited volume of CO_2 would be injected relative to the volume required during the continuous injection method. Both methods are usually aimed at enhancing the recovery of heavy components, which have been left behind as condensate during the production phase. Several conventional field H-n-P CO_2 injection pilot tests have been performed. However, due to the high volume of CO_2 injection required to repressurise the reservoir to the above dew point in the H-n-P conventional method and the corresponding volume of CO_2 produced during the back flow process, the viability of the method has also been questioned. Also, the cost of setting up surface production and separation facilities capable of handling high volumes of CO_2 production is a significant disadvantage.

Therefore, there is a need to develop a modified or systematic injection scenario where the amount of CO_2 injected and its interaction with the resident fluid is optimised while achieving significant condensate recovery and CO_2 storage.

In this study, series of H-n-P CO_2 core flood injection experiments, related to the appropriate phase behaviour study outlined in Cases -1 and -2 in chapter three, were performed using a synthetic binary gas condensate mixture on selected core samples. During Case-1 phase behaviour study, various amount of CO_2 was injected at pressure above Pdew and its impact on liquid drop out behaviour was studied. Whilst in Case-2 CO_2 was injected at a pressure of 3000 psi corresponding to the maximum liquid drop-out (LDO_{Max}) of the resident fluid without CO_2.

The three sets of core flood experiments were designed considering all observed data from both sets of PVT tests. One of these two sets, which is the main focus of this study, represent a new H-n-P method proposed here whereby CO_2 is injected at the pressure corresponding to LDO_{Max} of the resident fluid which after first CO_2 injection cycle includes CO_2. In this method the system pressure remains below Pdew. The second set of experiments is a pure natural depletion without CO_2 injection. The third set of experiments resembles the conventional H-n-P method whereby the system is pressurised by CO_2 injection to a pressure above Pdew.

These tests were performed on cores with different permeability to evaluate the impact of reservoir permeability on CO_2 injectivity and interaction with reservoir fluid at different injection pressures above and below the dew point. The liquid saturation profile, condensate recovery, CO_2 production profiles, and corresponding pressure data were recorded.

Results from Case-1 PVT tests for any of the CO_2 injection amount were used to identify the corresponding LDO_{Max} and the pressure range over which only a small variation in the LDO_{Max} is observed. The latter data serve as the pressure region suitable for the individual H-n-P CO_2 injection cycle during the core flood test resembling the H-n-P method proposed here. This pressure range ensures that whilst injecting CO_2 into the core which results in increased pressure the phase behaviour does not change, and the corresponding PVT data of Case-1 PVT tests are directly applicable. Figure 4.1 illustrates these pressure points and the corresponding variation in the LDO.

On the other hand, Case-2 results were used to design the injection pattern including the injection rate and soaking time with consideration given to the total time required to maximise the level of CO_2 and resident condensate interaction which enhances the swelling and vaporising mechanism. Figure 4.2 illustrates the relationship between CO_2-condensate interaction over a specific contact time.

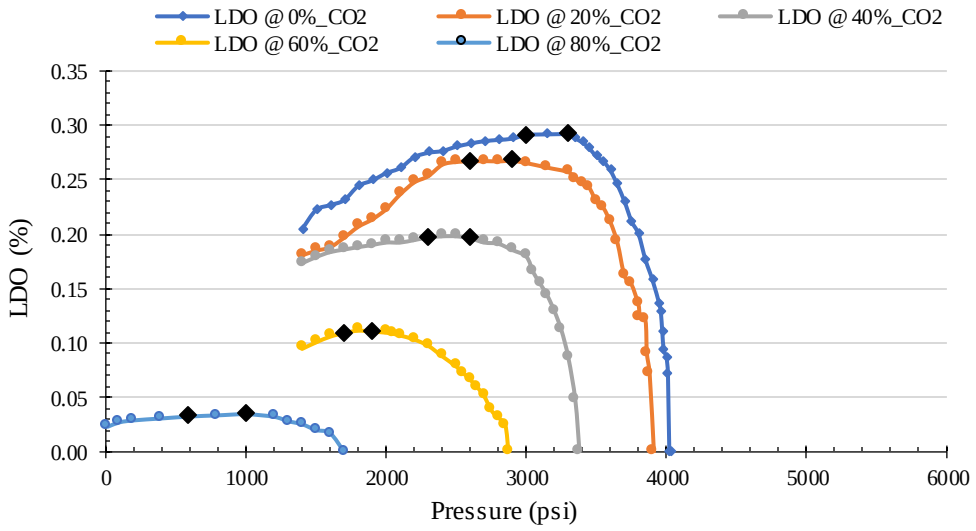

Figure 4.1: Liquid drop-out versus pressure behaviour for fluids with five different added CO_2 volumes and the corresponding pressure limits over which CO_2 injection occurred and variation of LDO is small. (Black dots indicate pressure boundary to achieve LDO max during incremental CO_2 injection)

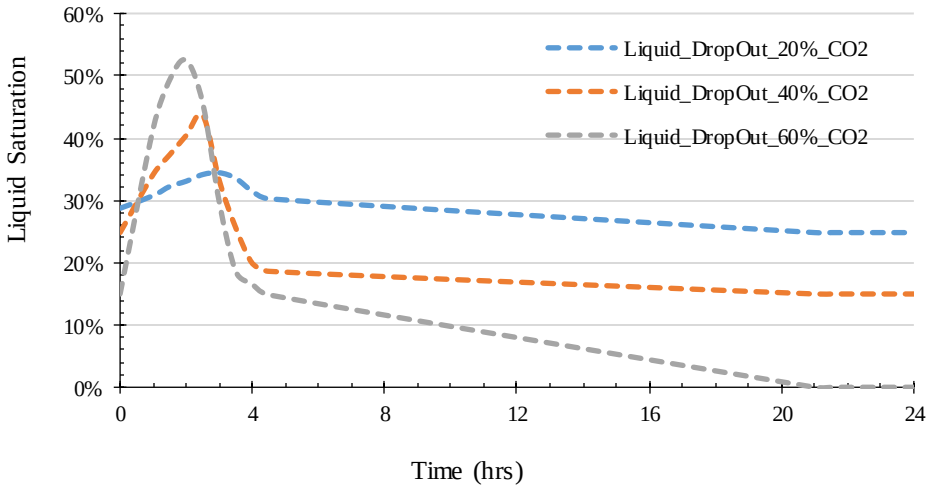

Figure 4.2: Liquid saturation versus soaking time when resident condensate was contacted with an incremental volume of CO_2.

For the first set of core flood tests, calculations were required to estimate the volume of CO_2 relative to the amount of initial fluid in the core to be injected at measured pressure points (corresponding to pressure points at LDO_{Max} for varying CO_2 composition in the resident fluid) that are equivalent to the same volume ratio used during the PVT tests. The volume of CO_2 corresponding to 20, 40, 60, and 80 % of the resident fluid was calculated considering the initial molar volume and percentage composition of the resident fluid at each stage of injection using the following steps.

Step 1 – Obtain the molar volume of C1-C8 at the observed identified injection pressure from EOS and convert from $cf/lb{-}mol$ to $cc/gmol$.

Step 2 – Calculate the total volume of single phase C1C8 injected.

Step 3 – Calculate the number of moles of C1C8 injected.

Step 4 – Calculate the number of moles of CO_2 to be injected equivalent to 20% of the total volume obtained from step 2.

Step 5 – Using the density of CO_2 at the specific pressure and temperature obtained from 'NIST', Calculate the volume of CO_2 to be injected in cubic centimeters (cc)

Step 6 – Applying the real gas equation $PV{=}ZnRT$, estimate the final pressure of the system after injecting CO_2.

Step 7 – Repeat Steps 1 – 6 for each cycle which corresponds to 40, 60, and 80 % respectively while also considering the changing injection pressure at each injection stage.

It is important to mention that Step 6 is required to determine the pressure range for the injection of CO_2, soak pressure, and production pressure constraints, respectively. As this boundary would enable a more accurate analysis of the interaction between the injected fluid and resident fluid at pressures not exceeding or dropping below the pressure range for maximum liquid saturation as identified and presented in Figure 3.12

4.2 Experimental Setup and Data Acquisition System

All H-n-P CO_2 injection tests were performed using an HPHT Binder oven consisting of a core holder, HPHT fluid cells, flow control valves, pressure transducers, temperature control system, and lines connected in series to a back pressure regulator, gasometer, CO_2 analyser, and a vent valve. Figure 4.3 shows the schematic of the experimental setup used in this study. Prior to the commencement of any core flood experiment, all fluid-containing cell and flow lines are taken out, and cleaned with appropriate cleaning solutions including toluene, methanol, and finally acetone. All cells and lines are left to dry out properly then put back in the oven and vacuumed. Nitrogen is injected to pressurise the system (all lines and cells) and the setup is tested for leaks using snoops and an electronic leak-testing device. Once the system is certified leak-tight and pressure is stable, the pumps and transducers are recalibrated to reduce errors on the electronic displays.

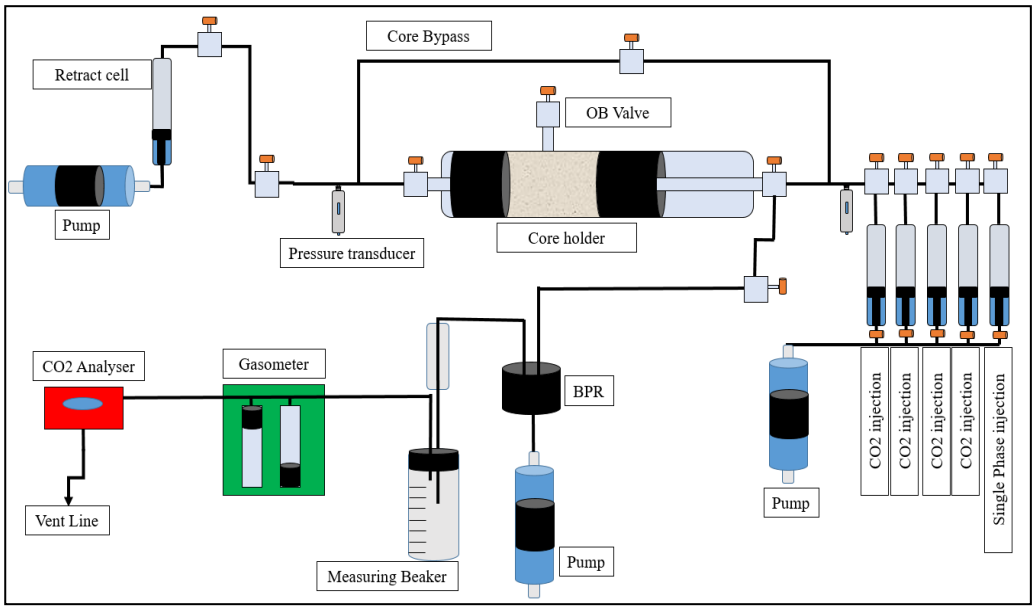

Figure 4.3: Schematic diagram of the HPHT set-up used in core flood setup for the H-n-P CO_2 injection.

4.3 Core Selection, Properties Determination, and Preparation

Considering that a new systematic H-n-P CO_2 injection method was to be tested, it would be appropriate to investigate the efficiency of condensate recovery and CO_2 storage when implementing the proposed method on a variety of known reservoir rock types. Three (3) different rock types including Berea sandstone, Carbonate, and Indiana Limestone core samples were used. It is important to mention that these core samples have permeability values ranging from high (336 mD), low (3.23 mD), and ultra-low (0.03 mD) permeability. It has been previously established in literature that the injectivity of supercritical CO_2 into any hydrocarbon-bearing rock bed is inversely proportional to its permeability. Hence, the injectivity of CO_2 was an important factor to consider when designing this systematic injection method targeted at improving condensate recovery while achieving CO_2 storage. These variations in the rock permeability provide the opportunity to evaluate the effects of permeability alteration on the injectivity of supercritical CO_2, the level of interaction between CO_2 and resident fluid, mobility of CO_2-GC phase, and the storage efficiency of this proposed method.

Prior to conducting any core flood experiments on any core sample, the core was cleaned, dried, wrapped and put into a core holder, and flushed through initially with several pore volumes of methanol and then nitrogen put through at varying flow rates and a pressure of 2000 psi to extract any residual volume of methanol. The core was then taken out of the core holder and weighed before it was placed in an oven which had been

pre-heated to 100 ^{o}C to dry over 48 hours. The core was then weighed again to obtain its dry weight and other rock properties including length, diameter, permeability, porosity, bulk, and pore volumes were measured in the laboratory.

The steady-state method was used to measure the absolute permeability of all three core samples. Dry core samples were rewrapped using aluminium foil and rubber sleeves before being put into the core holder and the core holder put into the rig. Each core was cleaned by injecting approximately 12 pore volumes of methane through at low pressure before connecting to a vacuum pump for 2 hours which ensured that the rig was totally voided of any unwanted component. Two sets of steady-state absolute permeability measurements were conducted on each core sample. The liquid and gas absolute permeability measurements were conducted using methanol and nitrogen at a pressure of 2500 psi while maintaining a core overburden pressure of 3000 psi.

Boyle's Two-Cell Helium Gas method was used to measure the porosity of all core samples. Each porosity measurement was conducted at a pressure of 100 psi with core overburden set to 500 psi. Multiple measurements were completed on each core to obtain stable and reliable porosity values. These measured values were used in estimating the pore volume of each core respectively. The measured properties of all three core samples are presented in Table 4.1.

Table 4.1: Measured physical properties of the core samples used for the systematic H-n-P CO_2 method.

Core Sample	Length (cm)	Diameter (cm2)	Permeability (mD)	Porosity (%)	Pore Volume (cc)
Berea Sandstone	18.95	5.08	336.00	18.99	67.97
Indiana Limestone	20.10	5.04	3.23	15.30	59.80
Carbonate Rock	18.80	5.11	0.03	4.66	17.98

At the end of the permeability and porosity measurements, the entire rig is flush with nitrogen and the core is removed, stripped, dried, rewrapped, and placed back into the rig and prepared for further experimental procedures.

4.4 High Permeability Berea Sandstone Core

4.4.1 Systematic H-n-P CO_2 Injection (TEST-1)

As mentioned previously, series of core flood experiments were conducted with CO_2 injected incrementally (20% at each stage) over four cycles with intermediate soaking and production time. These first set of tests were conducted with steps closely following

the corresponding PVT tests described in the previous chapter. These experiments are replicated in the new H-n-P CO_2 injection method proposed here whereby CO_2 is injected at the LDO_{Max} of the resident fluid prior to any new CO_2 injection step. The injection occurs over a pressure range close to the LDO_{Max} pressure over which the variation of liquid drop is minimal. Prior to CO_2 injection, the entire rig was conditioned by injecting methane and pressurizing to 5500 psi at 20°C, which is above the dew point pressure of the synthetic binary gas condensate mixture.

The following steps were followed during the CO_2 injection stages.

- Step 1 – A total of 2.2 pore volumes of already pressurised single-phase gas condensate fluid was slowly injected at a rate of 7 cc/hr into the core displacing methane while maintaining the system pressure at 5500 psi.
- Step 2 – CO_2 was also charged into the injection cells at 3000psi and atmospheric conditions.
- Step 3 – Then oven temperature was increased stepwise and in 10C increments until 60C while monitoring the cells and overburden pressure, then the system is left to stabilize.
- Step 4 – Depletion from the initial pressure of 5500psi to the test pressure of 2400psi was established. Then, the system was allowed to stabilize at test conditions @ 60C during which the resultant gas and condensate produced were monitored and recorded.
- Step 5 – Injection of CO_2 at a predetermined rate began until a 20% saturation ratio which was based on the initial volume of fluid injected into the core at single phase, was achieved.
- Step 6 – Soaking time was established by shutting both inlet and outlet over the same period (36hrs) as that during the PVT analysis.
- Step 7 – The system was then opened to production with pressure reducing slowly and constrained at the lower pressure boundary. Gas, condensate, and CO_2 production were monitored and recorded until pressure reached the set boundary.
- Step 8 – The test was stopped, and an incremental volume of CO_2 was injected into the core to increase the saturation to 40% and then 60%. Here and at the end of each CO_2 injection ration steps 5, 6 & 7 were repeated.
- Step 9 – The effluent gas was passed through a gas meter and then a CO_2 gas analyzer to determine the volume of gas produced and the amount of CO_2 (determined Volumetrically) in the produced gas, respectively.

The CO_2 injection core flood experiment was divided into two depletion sessions namely, pre- and post- CO_2 injection phases. The pre-treatment session is characterised by primary depletion from the initial pressure of 5500 psi to 2400 psi. Constraining the bottom hole pressure to 2400 psi ensured the accumulation of condensate at the maximum condensate dropout point.

The post-treatment session began with the injection of CO_2 at pre-determined rates and volumes that corresponds to 20% of the initial volume of gas condensate fluid in the core. The CO_2 injection pressure was constrained by pre-determined lower and upper-pressure limits obtained from the PVT test (CASE-1), while the injected volume was calculated based on the gas condensate saturation in the core prior to injection. For each cycle, production lasted eleven hours, CO_2 was injected for two hours, and the core was shut for thirty-four hours to allow adequate soaking and CO_2-resident fluid interaction time before production commenced. The injection pressure values for cycles 1 to 3 were above MMP of approximately 1500 psi obtained from the VIT test for the CO_2-GC mixture used in this study, while that for cycle 4 was below MMP.

It was observed that condensate production improved significantly from an initial value of 20.2% obtained post-primary depletion to approximately 66.4% after three of the four cycles of CO_2 injection, while an estimated 63.9% of the total injected CO_2 was stored at the end of cycle 3. In other words, the positive effect of the applied EGR method in the re-vaporisation of condensate and CO_2 storage was considerable for injection cycles 1, 2, and 3 recovering an additional 46.4% of the accumulated condensate after H-n-P CO_2 cycles 1, 2, and 3. This improved recovery was achievable as the CO_2-GC interaction occurred mostly above the MMP, significantly minimizing the negative effects of the MCM process on the vaporising mechanism. However, it is important to highlight that for cycle 1, the injected volume of CO_2 was small compared to the volume of condensate in the system, and only a negligible volume of condensate recovery was observed. In line with this and during this cycle, dissolution of CO_2 was high hence low CO_2 production. When the volume of injected CO_2 increased by 20% and 40% to 40 and 60% for cycles 2 and 3, respectively, significant condensate recovery and CO_2 storage were recorded for both these cycles. In fact, cycle 3 yielded the highest condensate recovery of around 29.3%, indicating an elevated level of CO_2-condensate interactions.

For injection cycle 4, despite the highest CO_2 to resident condensate volume ratio, re-vaporisation was small, resulting in around 3.3% additional recovery from 66.4% to 69.7 at the end of the fourth cycle. During this cycle, CO_2 production increased significantly,

storing only about 14.9% by volume, which is equivalent to 43.2 Mol% of injected CO_2 as the system pressure was 1100 psi, which is significantly below the measured dew-point pressure (P_{Dew}) of 4029 psi and also 400 psi below the MMP. In other words, during cycle 4, both condensate recovery and CO_2 storage were small while CO_2 production increased significantly relative to cycles 2 and 3.

The volume of produced gas and the percentage of CO_2 present In It was measured volumetrically bypassing the production stream through a gas meter and CO_2 analyser connected in series and applying a gas material balance and mass conservation equation. Figures 4.4, 4.5, and 4.6 show the production pressure profile, corresponding condensate recovery (both in cc and as % of the initial condensate saturation of 29%) for the system, and volume of CO_2 injected, produced, and stored, and total Mol% stored.

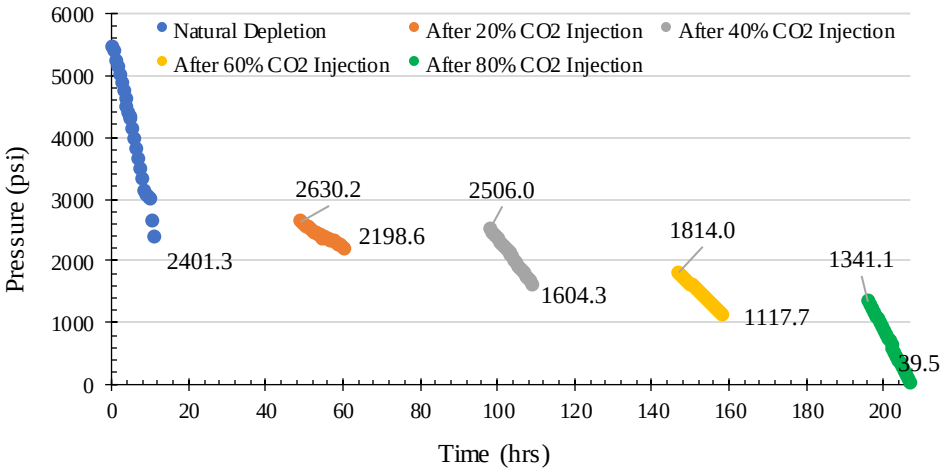

Figure 4.4: Pressure profile for primary depletion phase and H-n-P CO_2 depletion cases on Berea Sandstone (TEST-1).

(a)

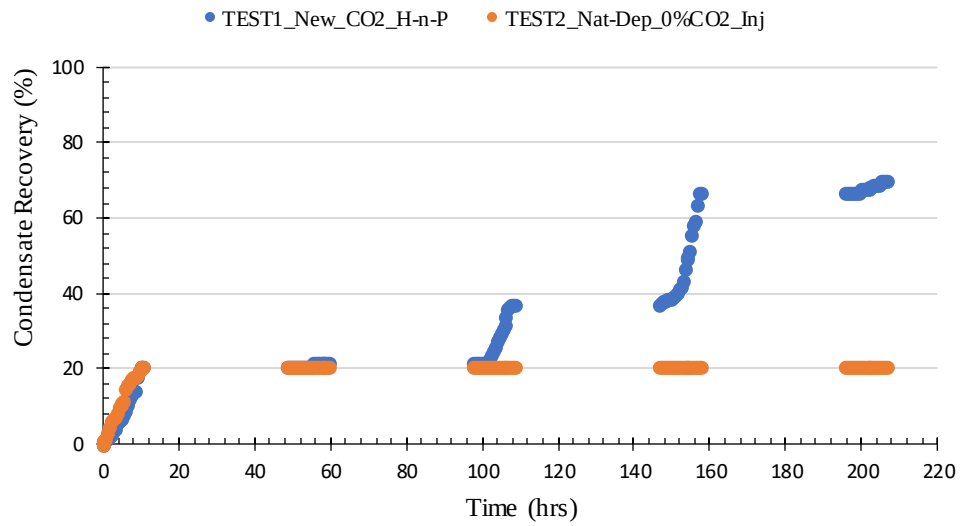

(b)

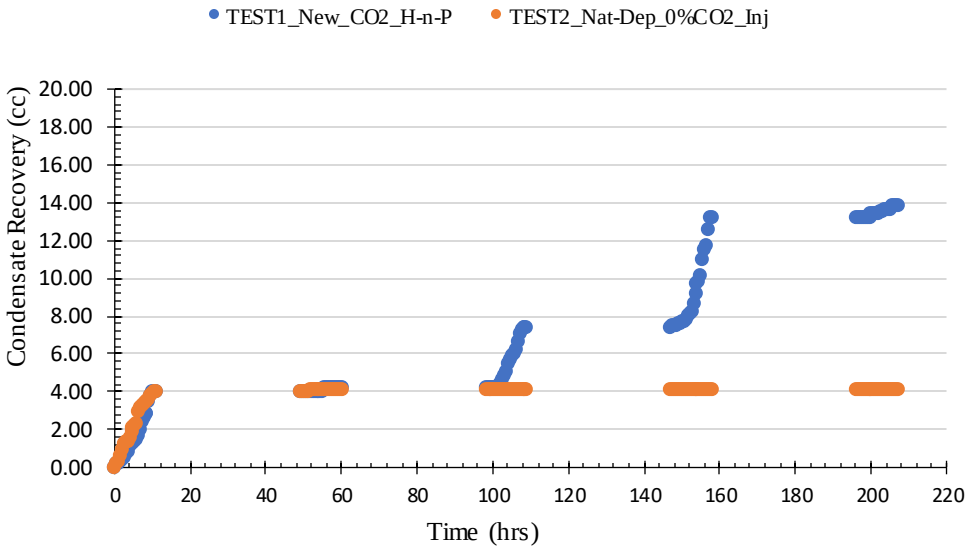

Figure 4.5: Condensate recovery in (a) cc and (b) percentage of S_{ci}=29% for primary depletion and H-n-P CO_2 injection cases on Berea Sandstone (TEST-1).

(a)

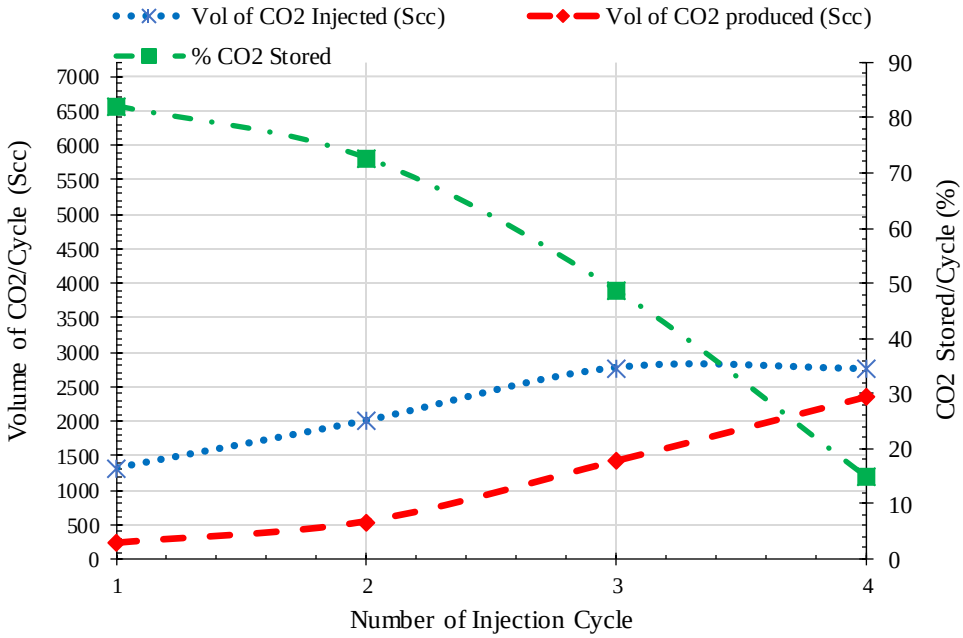

(b)

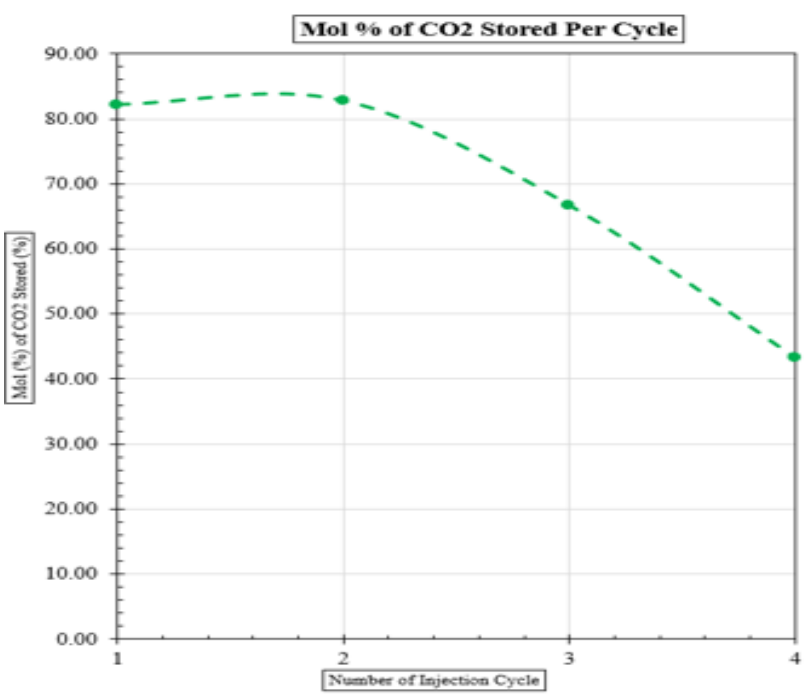

Figure 4.6: (a) Volume of CO_2 injected, produced (primary vertical axis) along with percent stored per cycle (secondary vertical axis), (b) Mol percentage of CO_2 stored per cycle for Berea Sandstone (TEST-1).

4.4.2 Natural/Primary Depletion to Abandonment Pressure (TEST-2)

To adequately evaluate the benefits of the proposed H-n-P CO_2 injection technique, a natural depletion test was performed at similar test conditions using the same binary gas-

condensate mixture and production scenario applied during the H-n-P CO_2 enhanced recovery process. That is, similar steps as those of test 1 were followed but no CO_2 was injected at reservoir conditions after any depletion stage. Figure 4.7 presents the pressure profile implemented during Test-2. The following steps were followed during Test 2.

- STEP 1 – Single phase fluid was injected into the core (7cc/hr. for 21hrs = 2.2 Pore Volumes) to displace methane at 5500psi and atmospheric conditions.
- STEP 2 – Then oven temperature was increased stepwise until 60C while monitoring the cells and overburden pressure, then the system was left to stabilize.
- STEP 3 – 11 hrs of depletion from initial pressure to system pressure (upper limit) post CO_2 injection. Gas and condensate production were recorded simultaneously.
- STEP 4 – Then, system stabilization was achieved by allowing 36hrs shut-in time to replicate 36 hrs of soaking period similar to Test 1.
- STEP 5 – Step 3 was repeated in five stages of production to have the same pressure limits as Test 1.
- STEP 6 – The test was stopped when there was no more visible condensate production.

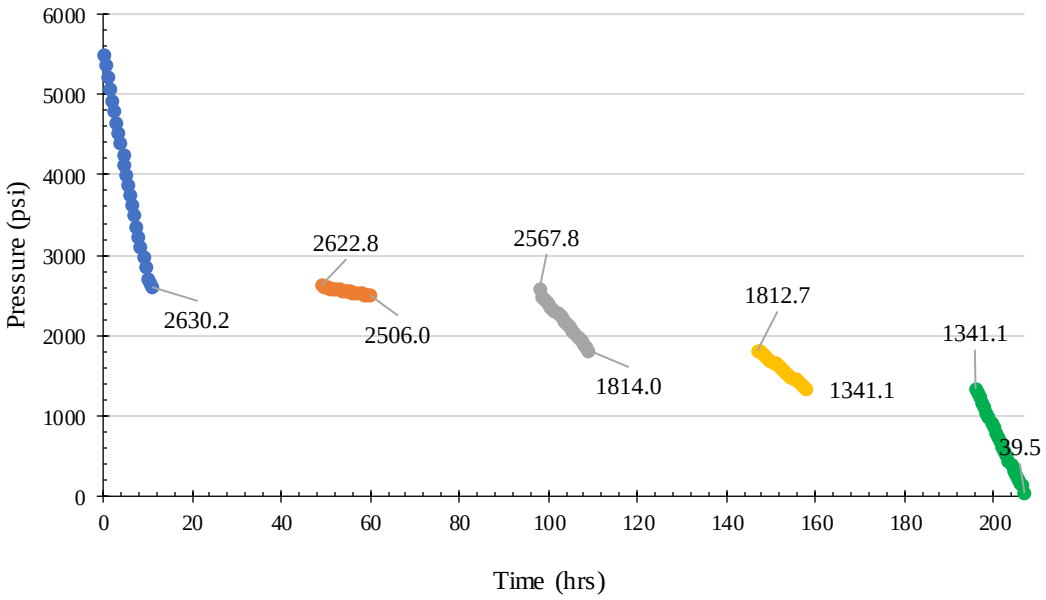

Figure 4.7: Pressure profile for primary and H-n-P CO_2 depletion cases on Berea sandstone (Test-2, No CO_2 injection).

The comparison between the condensate recovery (in cc of the initial condensate saturation of 19.77cc) during Tests 1 and 2 is presented in Figure 4.8. At the end of production, condensate recovery was 20.74% of the initial Condensate saturation of

19.77cc, which is a total of 4.1cc in Test-2. These results clearly indicate that the proposed H-n-P CO_2 injection significantly enhanced condensate recovery while achieving considerable CO_2 storage as long as the injection pressure is above MMP.

(a)

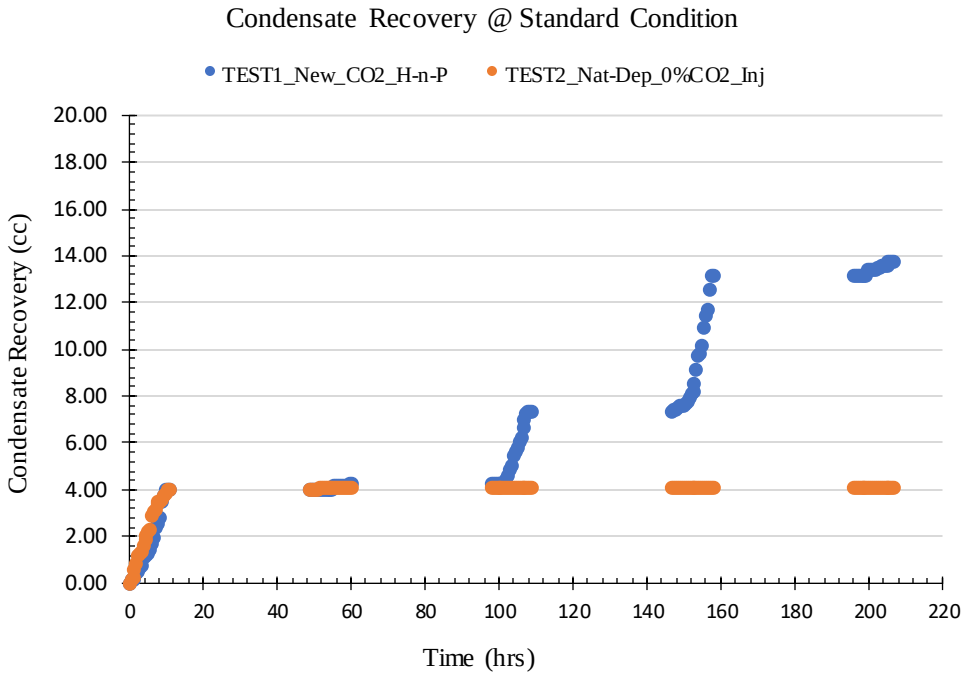

(b)

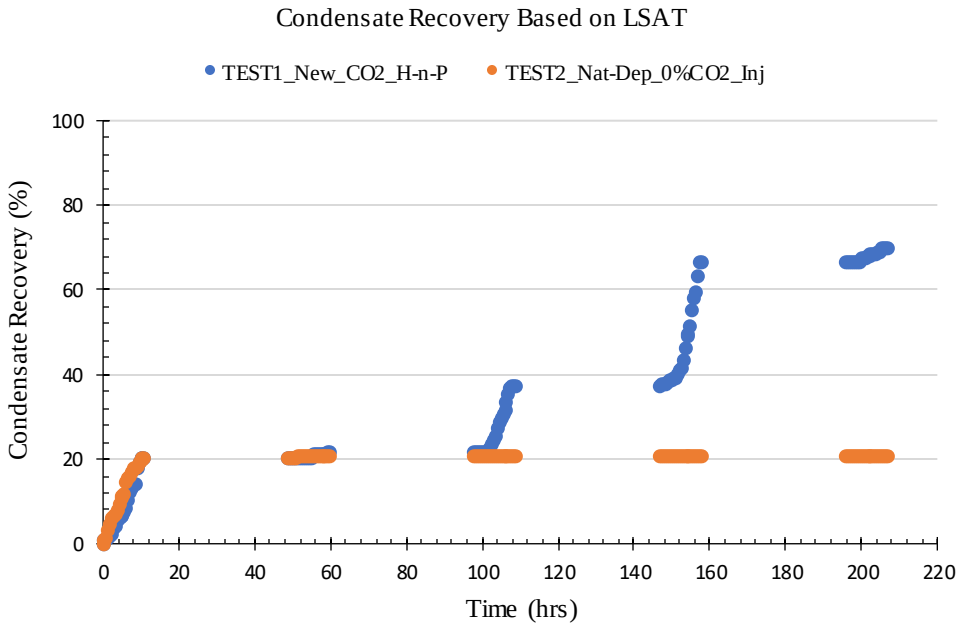

Figure 4.8: Condensate recovery (LDO) in (a) cc and (b) percentage of S_{ci}=29% for primary depletion and H-n-P CO_2 injection cases on Berea sandstone (TEST-1 & TEST-2).

4.4.3 Conventional H-n-P CO_2 Injection (TEST-3)

In TEST 3, the volume of injected CO_2 is not constrained, by pressure limits over which the variation in LDO but rather by the depleted and target reservoir pressures. That is, Test-3 followed a similar production profile to Tests -1 & -2, but CO_2 was injected solely to repressurise the system back to the initial pressure which is above the initial P_{Dew} of the original fluid. This test aimed to replicate a conventional H-n-P method. A soaking time of thirty-four hours was also allowed before the next stage of production began. This process was repeated for all four H-n-P injection cycles.

In this test, condensate recovery was improved from an initial 21.2% after depleting the system naturally (from 5500 to 2380 psi) to about 80.3% at the end of four H-n-P CO_2 injection cycles. 54.1% out of this additional 59.1% recovery was achieved during the first three cycles, where both the CO_2 injection pressure and depletion pressure range remained above the MMP.

Recovery from cycle 1 was higher than cycles 2 & 3 even with similar volumes of CO_2 injected, recovering 24.7% out of the cumulative condensate recovery of 59.1% after CO_2 injection.

Similar to TEST 1, recovery at the end of cycle 4 was also very small, recovering only 17.6% of resident condensate (0.9cc out of 5.1cc) prior to this cycle and 5% out of the additional cumulative condensate recovery of 59.1%. It should be noted that in this cycle, CO_2 was injected at a pressure of 1103psi, which is below the measured MMP of 1500psi. At the end of CO_2 injection for cycle 4, the system pressure was 1732psi and dropped to 40psi over eleven hours of production. The system pressure quickly dropped below the MMP, where the effects of multi-contact miscibility (MCM) are present. However, due to the large volume of CO_2 injected at this stage, the effects of MCM on condensate production would be negligible. At the end of TEST 3, the total produced gas was 32.1% and 67.9% of hydrocarbon and CO_2 content, respectively. 59.1% additional condensate recovery was recorded after H-n-P CO_2 treatment with cumulative CO_2 storage of 51.6 mol% which is equivalent to 27.3% of the total volume of CO_2 injected.

At this stage, a detailed comparison of the cumulative condensate recovery profiles for all three tests and the CO_2 storage profile for Tests 1 and 3 was done.

Figure 4.9 shows the condensate recovery profiles for all three tests reported as a percentage of the initial condensate saturation in place and in (cc)'s at surface conditions.

(a)

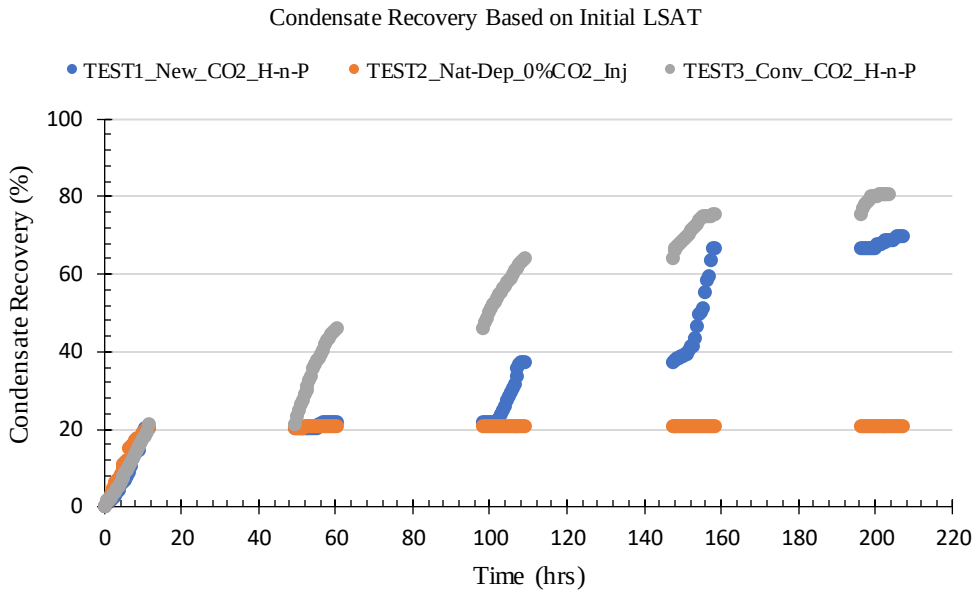

(b)

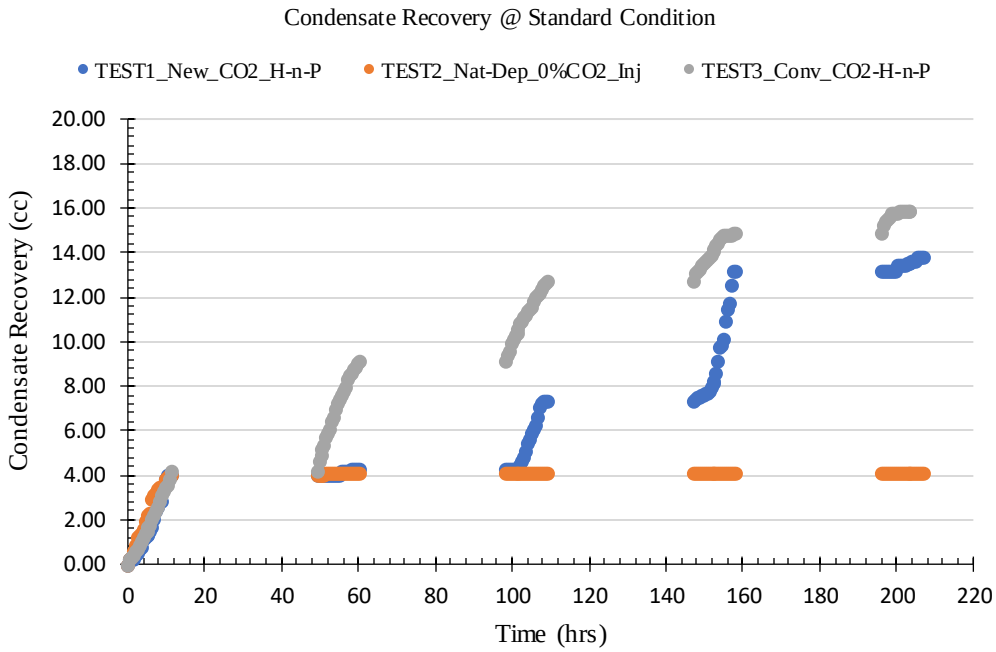

Figure 4.9: Comparison of condensate recovery recorded for three tests as (a) volume in cc, and (b) percentage of S_{ci} =29% for Berea sandstone.

Table 4.2 includes a summary of the condensate recovery and the CO_2 storage potential achievable when the systematic CO_2 injection method is implemented compared to the usual conventional CO_2 injection method.

Table 4.2: Comparison of cumulative condensate recovery and CO_2 storage profile for all injected CO_2 cycles on Berea sandstone (TEST-1 and TEST-3).

ROCK SAMPLE 1 – BEREA CORE	**Systematic H-n-P CO_2 Injection**		**Conventional H-n-P CO_2 Injection**	
Obtained Data		%		%
Total Volume of CO_2 Injected in Core from Cycles 1-4 (mol)	0.57		2.86	
Volume of CO_2 Stored relative to Total Volume of Injected CO_2 (mol)	0.37	64.59	1.47	51.55
Volume of Gas Produced from Cycles 1-4 only (L)	21.22		41.16	
Volume of CO_2 in Produced Gas Cycles 1-4 only (L)	4.53	21.36	31.04	75.42
Volume of Hydrocarbon in Produced Gas Cycles 1-4 only (L)	16.69	78.64	10.12	24.58
Cumulative Condensate recovery of Initial LDO (L)	13.80	69.70	15.90	80.30

The hydrocarbon recovery efficiency (in terms of volume of hydrocarbon in the total produced gas) for TEST 1 is 78.6%, which is higher than the 24.5% obtained during TEST 3. Condensate recovery is 10.6% higher in TEST 3, but this is at the cost of losing 54.1% of valuable hydrocarbon gas and injecting a significantly higher volume of CO_2 relative to TEST 1. That is, a total of 2.1PV and 5.1PV of CO_2 were injected at reservoir conditions during Tests 1 and 3 respectively. The absolute volume of CO_2 stored in TEST 3 is higher than that stored in TEST 1 but with five times more CO_2 in mol% injected in TEST 3. In other words, the net amount of CO_2 stored in TEST 3 is more, but the storage efficiency is poor compared to TEST 1. Figure 4.10 compares the amount of CO_2 injected and stored per cycle in Berea sandstone during Tests 1 and 3.

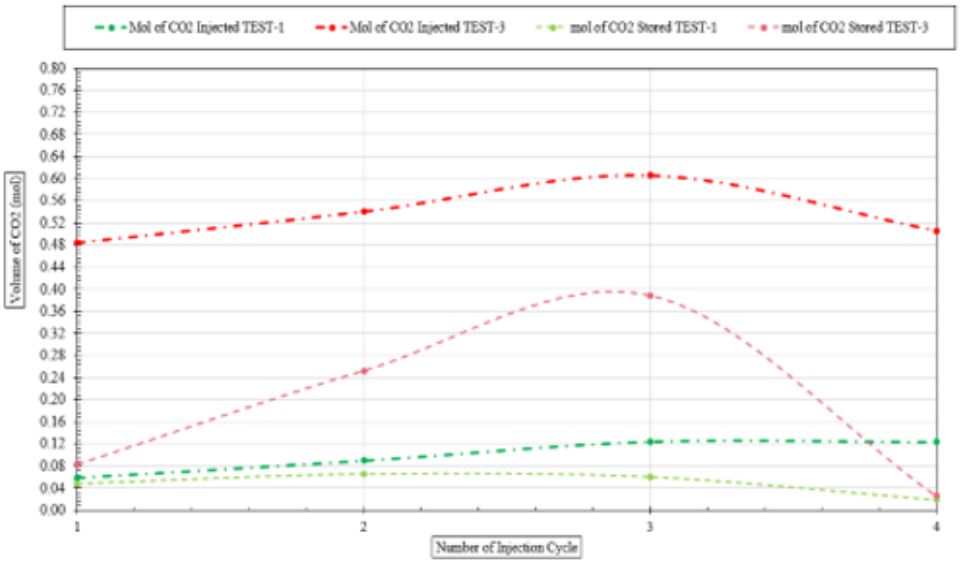

Figure 4.10: Comparison of CO_2 volume injected and stored per cycle for Berea sandstone (TEST-1 vs TEST-3).

Additionally, the production profile of individual components resulting from natural depletion and production cycles 1 to 4 of TEST-1 and TEST-3 was investigated. On the other hand, for TEST-2, we only examined the efficiency of condensate production considering the total produced gas. This analysis provided a comprehensive understanding of the production behaviour of these three tests. The individual component production profile from natural depletion & during cycles 1 – 4 for TEST-1 & TEST-3 and only condensate production efficiency for TEST-2 with respect to the total produced gas is presented in Figure 4.11

(a)

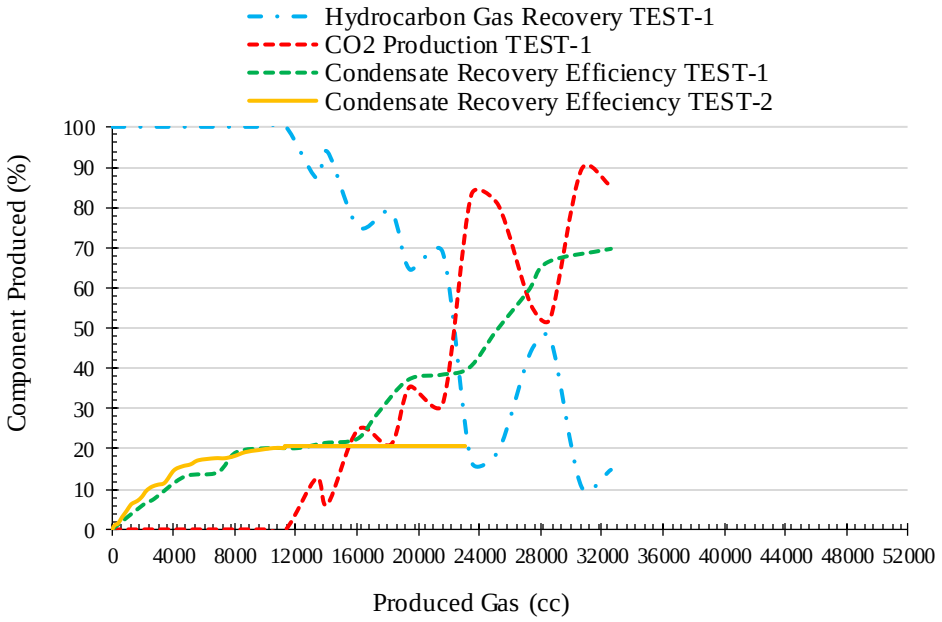

(b)

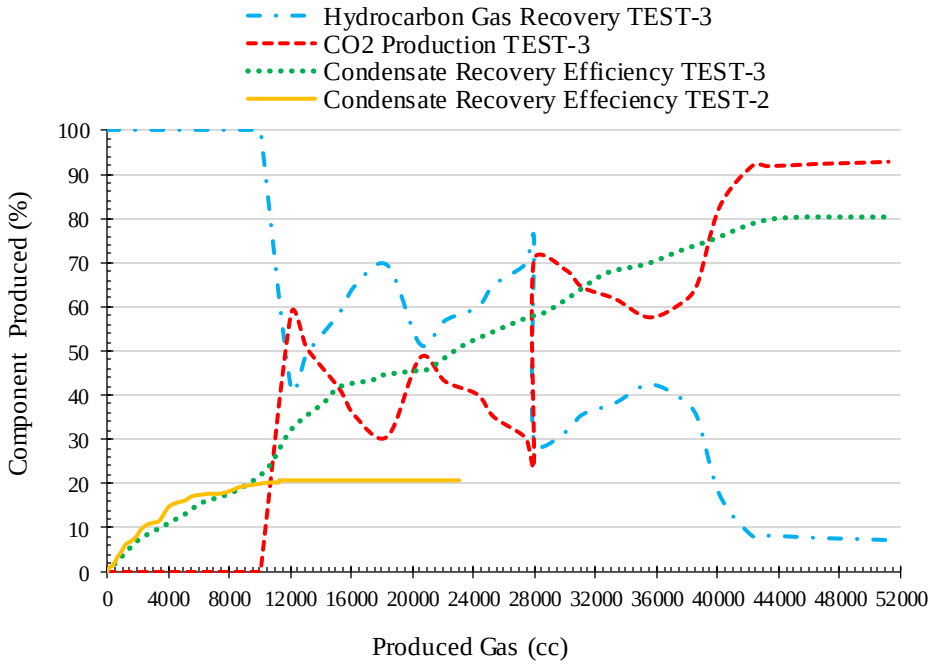

Figure 4.11: Comparison of production profile for primary depletion & various cycles of different tests wrt the total produced gas for Berea sandstone.

The general observations of the experiments performed on Berea sandstone can be categorised as:

i. Condensate recovery increased progressively from cycles 1 to cycle 3 in TESTs 1 and 3 with the corresponding incremental volume of CO_2 injection.

ii. Condensate recovery from TEST-3 was about 10.6% more when compared with recovery from TEST-1.

iii. The volume of CO_2 injected during TEST-3 was approximately 5.4 times more than that injected for TEST-1 when measured at reservoir conditions (Rcc).

iv. In TEST-3 the CO_2 storage efficiency and hydrocarbon recovery are lower, while the condensate recovery efficiency is higher relative to TEST-1, but this additional condensate recovery comes at the cost of injecting significantly higher volumes of CO_2.

v. H-n-P CO_2 injection treatment in depleting gas-condensate reservoirs significantly improved both gas and condensate recovery.

vi. CO_2 storage as mobile gas or by trapping is achievable.

vii. For best results in hydrocarbon gas and condensate recovery while achieving CO_2 storage, CO_2 injection pressure, volume, and level of interaction with resident fluid must be optimised.

viii. These results have shown that the H-n-P CO_2 injection treatment for depleting gas condensate reservoirs significantly improves condensate recovery efficiency but at the cost of injecting and producing very high volumes of CO_2 while the proposed method is able to match the recovery efficiency achieved but with lesser volumes of CO_2 injection and production.

4.5 Low Permeability Indiana Limestone Core

After performing the systematic H-n-P CO_2 injection on the high permeability Berea sandstone the results showed that the injection technique was efficient when implemented for enhanced condensate recovery and CO_2 storage. The efficiency of this injection technique was also evaluated by performing a replica CO_2 injection pattern as was done for the Berea sandstone on an Indiana limestone core. The Indiana limestone core is approximately 100 times less permeable relative to the Berea sandstone core. This test was performed to investigate the effects of the reservoir permeability variation on the fluid interaction, injection pressure, and the re-vaporisation of condensate on the results of the proposed H-n-P CO_2 injection technique. The measured properties of the Indiana limestone core sample are permeability of 3.23 mD, porosity of 0.153, and Pore volume of 59.79 cc. The same experimental procedure as that followed for the Berea was followed.

Similar to the high permeability test, this core flood experiment was also divided into two depletion phases namely, pre- and post-CO_2 injection phases.

The pre-treatment session is characterised by primary depletion from the initial pressure of 5500 psi to 2400 psi and the resultant gas and condensate that were produced, were monitored and recorded. Constraining the bottom hole pressure to 2400 psi ensured the accumulation of condensate and that the system was at maximum condensate dropout of about 29.12% which in this core would be equivalent to approximately 17.41 cc of condensate.

The post-treatment session constitutes of four cycles of incremental H-n-P CO_2 injection that began with the injection of CO_2 volume that corresponds to 20% of the initial volume of gas condensate fluid in the core for the first injection cycle. The test continued with volumes of 40, 60, and 80% for the second, third, and fourth cycles respectively.

The injection and production pressures were constrained by pre-determined lower and upper-pressure limits obtained from the PVT test (CASE-1) illustrated in Figure 4.12. The injected volume was calculated based on the initial gas condensate saturation in the core prior to injection. For each cycle, production lasted twenty-four hours, CO_2 was injected for two hours at 5.38 cc/hr, 12.59 cc/hr, 28.33 cc/hr, and 26.59 cc/hr followed by a shut-in period of 48 hrs for each cycle, respectively. Prior to the Huff phase, the core was shut-in for an additional twelve hours to allow adequate soaking and CO_2-resident fluid interaction time before production commenced and lasted for 24 hrs. These changes in the injection rate for CO_2 were based on the pore volume of the core and the calculated volume of CO_2 required to be injected for each cycle. The injection rates were varied to ensure that the appropriate volume of CO_2 was injected over a period of 2 hrs. In each core flood test, the required volume of CO_2 to be injected was precalculated and injected over 2 hrs similar to the PVT tests. During TEST-1 of the core flood on Berea core sample, the injection rates were 4.62 cc/hr. 7.82 cc/hr, 14.24 cc/hr, and 25.22 cc/hr corresponding to precalculated injection volumes of 9.24 cc, 7.82 cc, 14.24 cc, and 50.45 cc for cycles 1 - 4 respectively. Maintaining this slow injection rate ensured enhancing the CO_2–GC miscibility by multiple contacts over an extended period, as a result of gradual mass transfer in the system. While the change in shut-in and production time from 36 hrs to 48 hrs and 12 hrs to 24 hrs respectively, were implemented to compensate for the effect that permeability variation may have on the level of CO_2-resident fluid interaction and ultimately on the recovery mechanism which was already established from previous test to be swelling and vaporising mechanisms.

The injection pressure values for cycles 1 to 3 were above MMP of approximately 1500 psi obtained from the VIT test for the CO_2/gas-condensate mixture used in this study, while that for cycle 4 was below MMP.

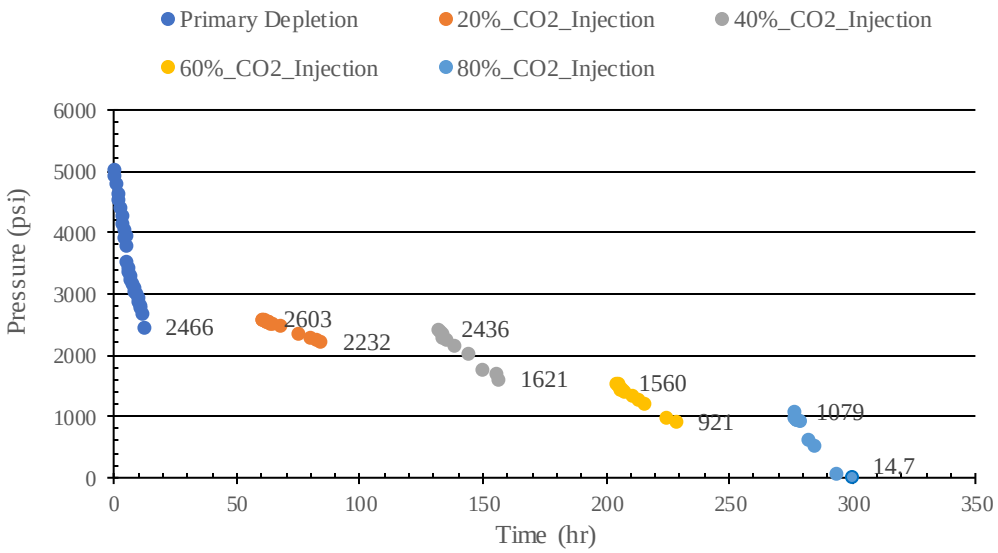

Figure 4.12: Pressure profile for primary depletion and H-n-P CO_2 injection cycles of Limestone core sample.

With an LDO of 29.12%, a total of 17.41 cc of condensate is expected to be present in the core at 2400 psi. The volume of gas condensate produced after 12 hours of primary depletion to reach this maximum condensate dropout pressure which is the first injection pressure for CO_2 was 2.6 cc. During the primary depletion stage, condensate production began after 1hr and increased slowly to about 2.6 cc (which is about 14.9% of the initial condensate volume) over 8.5 hrs, and then stopped. After this period, no condensate production was recorded for another 3.5 hrs see Figure 4.13. At this point, primary depletion was terminated, and CO_2 injection started as scheduled. It is important to note that after 7 hours of depletion, the system pressure had reached 3000 psi (P at LDO_{Max}) with only 2.0 cc of condensate produced.

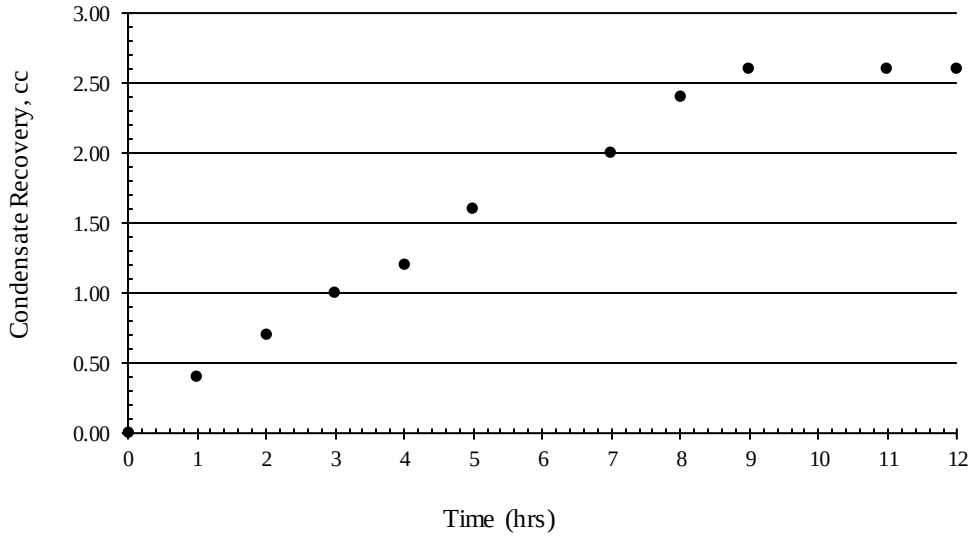

Figure 4.13: Condensate recovery profile during primary depletion phase of Limestone core sample.

Similar to the observations during the injection of CO_2 into the Berea high permeability core, condensate recovery after the first injection cycle was small, with significant condensate recovery observed during the second and third cycles. The fourth cycle is also characterised by negligible condensate production considering that it had the highest injected volume of CO_2. One observed difference during the pre-treatment depletion stage was that at 3000 psi (P at LDO_{Max}), 3.8 cc of condensate had been produced from the Berea core sample. Figures 4.14 and 4.15 shows the corresponding condensate recovery in (cc) and (%) after individual cycles of the systematic CO_2 injection method. There is a consistent increase in condensate production from cycles 1 to 4 as the volume of CO_2 injected increases for each cycle.

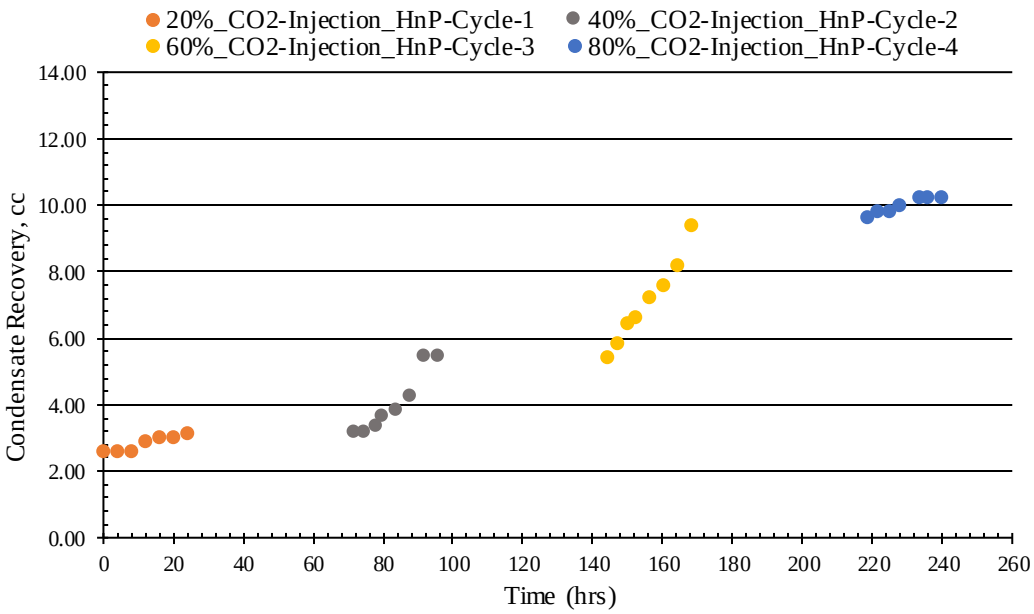

Figure 4.14: Cumulative condensate recovery (reported in volume) during H-n-P CO_2 injection cycles for Limestone core sample.

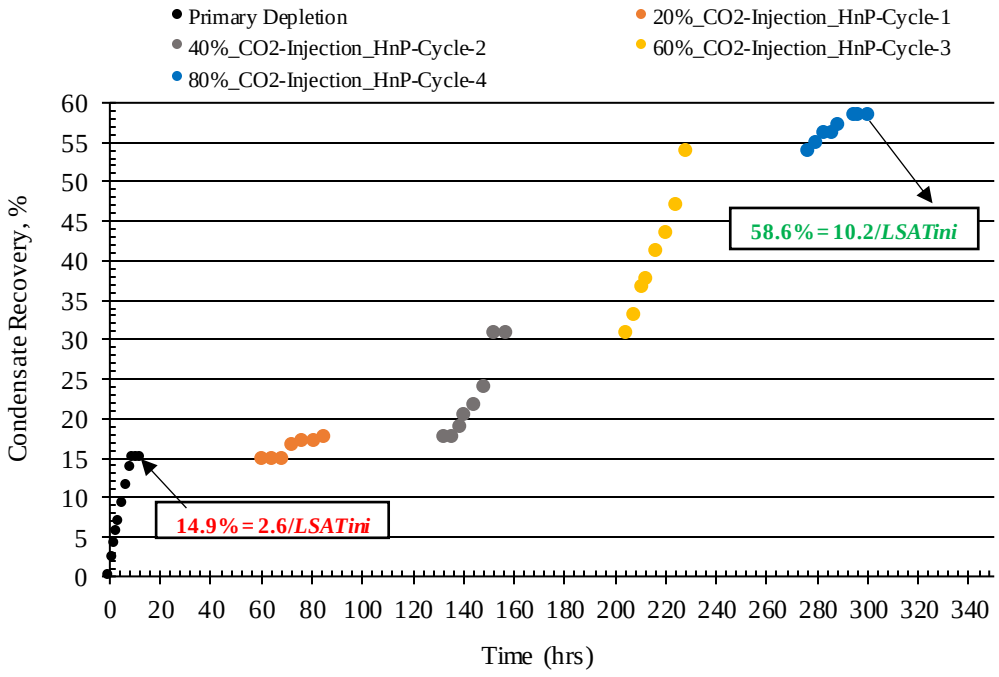

Figure 4.15: Cumulative condensate recovery during H-n-P CO_2 injection cycles (as percentage of S_{ci}=29.12%) for Limestone core sample.

At the end of the CO_2 cycles, an additional 40.9% condensate recovery was achieved taking the total condensate recovery to approximately 58.6% (which is 10.2cc out of the original condensate volume). A total of 2.5 PV of CO_2 was injected at test conditions, and a cumulative average of approximately 35.5% of the injected volume was stored at the

end of the CO_2 treatment. Cycle 1 had the lowest volume of produced CO_2 as only 10.76 cc of CO_2 was injected. CO_2 production maxed out at 24% within the first 8 hrs of production before declining gradually. CO_2 production increased during cycles 2, 3 exhibiting similar maximum points of approximately 35% before declining over a period. The highest recorded volume of produced CO_2 was observed during cycle 4. It was assumed that CO_2 dissolution in condensate was reduced because the CO_2/resident fluid interaction should happen at a pressure, which was below the MMP, hence CO_2/resident fluid mixing was governed by the multi-contact miscibility process which is not favourable for the swelling and vaporising mechanism. Figure 4.16 illustrates the CO_2 production profile during the proposed H-n-P injection into the Indiana limestone core.

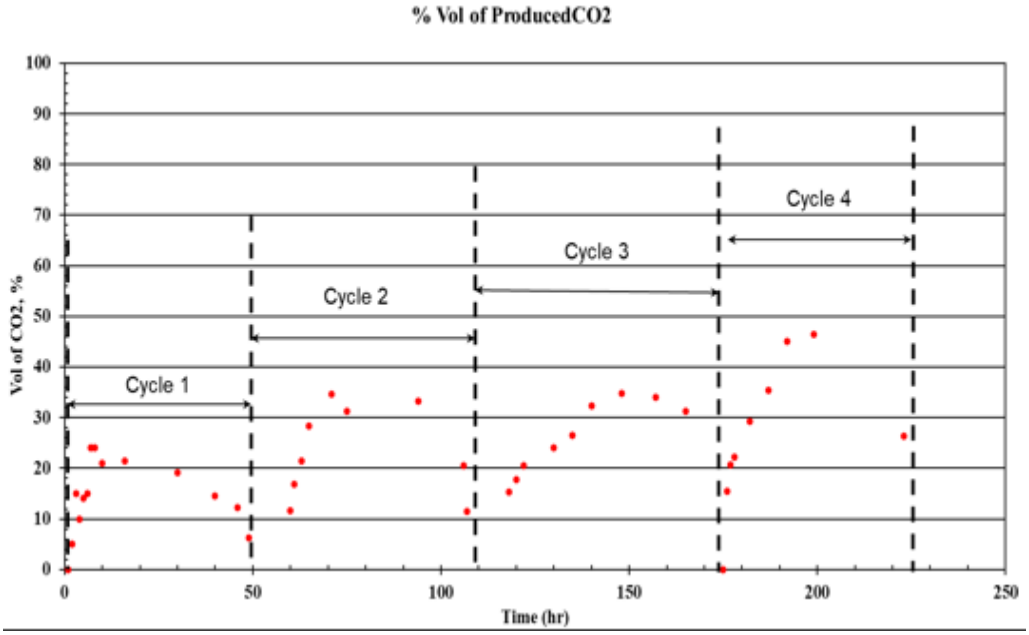

Figure 4.16: Volume of CO_2 produced in (%) of Total volume injected per cycle from Cycles 1 – 4 measured at reservoir condition for Limestone core sample.

4.6 Ultra-Low Permeability Carbonate Core

Ultra-low permeability carbonate rocks refer to geological formations composed primarily of carbonate minerals (such as limestone or dolomite) that exhibit very poor fluid flow properties. These rocks are commonly encountered in reservoir engineering and geology studies, particularly in the context of hydrocarbon exploration and production. The low permeability of these carbonate cores is due to several factors, including the fine-grained nature of the rock, the presence of micro-porosity, and the complex matrix and pore structure. The rock matrix consists of tightly packed carbonate

grains, and the pore spaces between these grains are often limited and interconnected through narrow channels, reducing the ability of fluids to flow through the rock.

Low injectivity for these types of formations is a common challenge especially when CO_2 is injected. It was considered valuable to perform the proposed CO_2 injection technique on this type of formation at the same reservoir conditions and using the same gas condensate fluid mixture to investigate the potential of improving condensate recovery and achieving CO_2 storage in these low k rocks. Therefore, an ultra-low permeability carbonate core sample was obtained, cleaned, and prepared. The properties of the core were measured in the laboratory to obtain an absolute permeability of 0.003 mD, porosity of 0.047, and pore volume of 18.0 cc.

The depletion process followed the same procedure as that described and performed for the Berea and limestone core samples. However, due to the challenges of injectivity of CO_2 into the ultra-low permeability cores, the soaking time and production time were increased to improve the CO_2-GC fluid interaction.

At the end of the primary depletion sequence, CO_2 was injected into the core for 2hrs but with varying slower rates relative to previous tests albeit to secure the required CO_2 injected volume beginning with 20% saturation of the original fluid volume in the core. Considering that the core permeability was much lower and impacts the injectivity of CO_2 into the core, this varying rates was implemented to maintain the system pressure and prevent the core from over pressuring and potential fracture. The soaking time was increased by 12hrs (from 36 hrs same as the soaking time for the tests conducted on the Berea and limestone core sample) to 48 hrs. This was followed by a production period of 24 hrs to reach the constrained lower pressure boundary. The 12 hrs increase in soaking time was based on the increased tightness of the core and to allow more time for injected CO_2 to reach and interact with the resident GC-fluid. Also, considering that the core was very tight, it was assumed that it should take longer more time to achieve sufficient CO_2-GC miscibility in this core due to the low permeability of the core. The produced gas, condensate, and CO_2 were monitored and recorded until the pressure reached the set boundary. After this step, the next cycle started by injecting an incremental volume of CO_2 following the sequence of 40, 60, and 80 % of the original injected single-phase fluid.

With the previously measured LDO of 29.12% and core pore volume of 18.0 cc, it was assumed that the condensate volume in the core after primary depletion was 5.24 cc. The primary depletion started when the system pressure was reduced from 5500 psi to 2400

psi corresponding to the lower pressure limit with LDO close to LDO_{Max} over a period of 12 hrs with a total condensate production of 0.25 cc. During the primary depletion stage, condensate production began after 2hrs and increased slowly over 8 hrs achieving 0.24 cc condensate production and then stopped with no condensate recovery observed over the last 2 hrs. It is important to note that after 9hrs of depletion, the system pressure was at 3000psi (P at LDO_{Max}), and only an additional 0.01cc of condensate production was observed for the next 600 psi drop in pressure, which corresponds to the last 2 hours of production resulting in only just 0.25cc of condensate recovery for the primary depletion phase. No condensate production was recorded for the last 2 hours. Figure 4.17 show a graphical representation of the condensate production profile during the primary depletion phase.

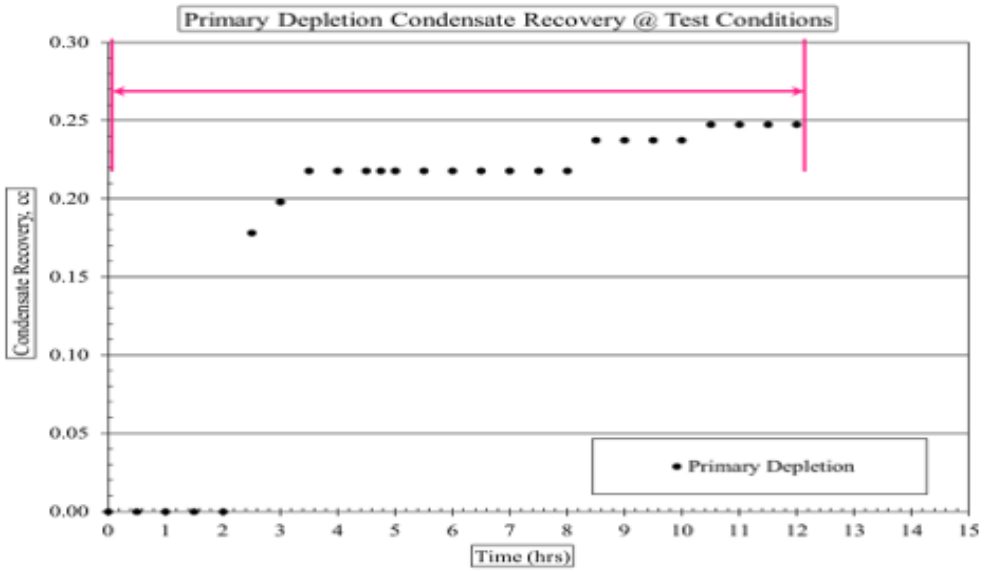

Figure 4.17: Condensate recovery profile during pre-treatment (primary depletion phase) for carbonate core sample.

Similar to the condensate production profile reported for the previous tests using the Berea and Indiana Limestone core samples, there is a consistent increase in condensate production from cycle 1 to 4 as the volume of CO_2 injected increased for each cycle as presented in Figure 4.18. and 4.19.

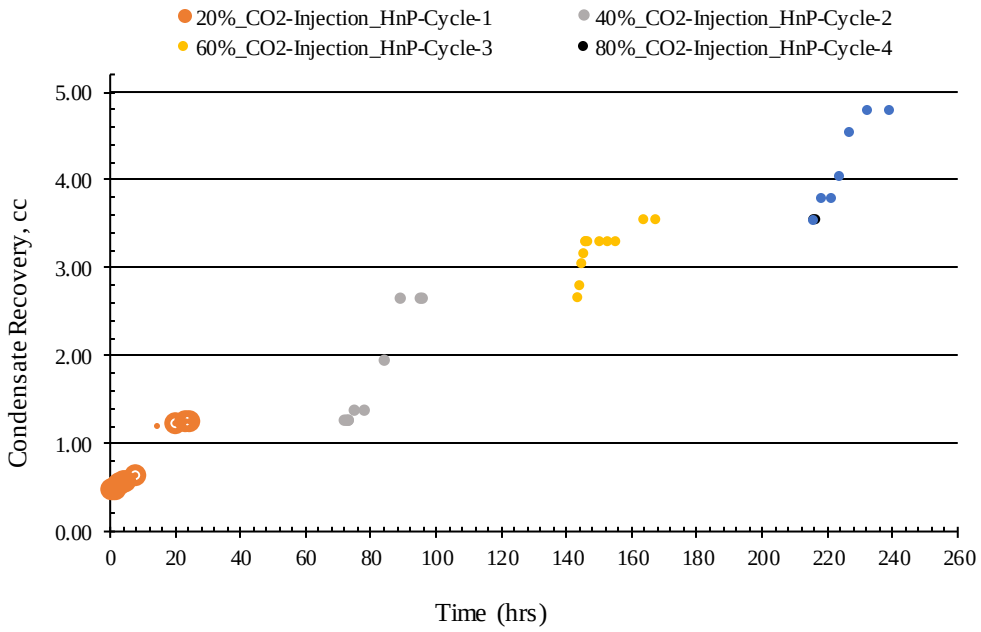

Figure 4.18: Cumulative condensate recovery profile (in cc) for cycles 1-4 (post-primary depletion phase) for carbonate core sample.

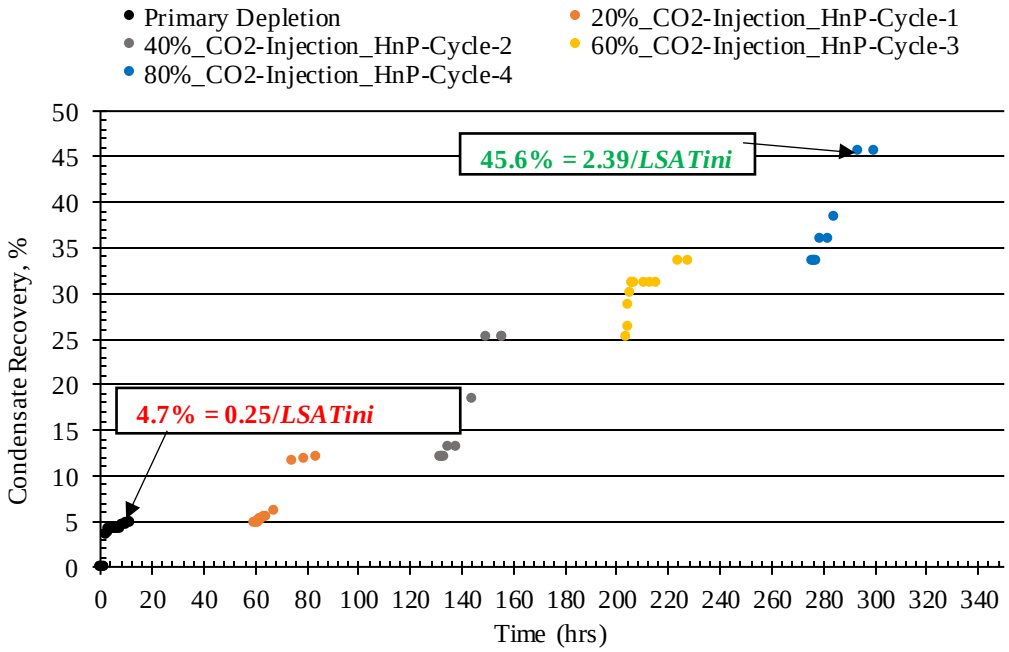

Figure 4.19: Cumulative condensate recovery profile (percentage of S_{ci}=29.12%) for primary depletion and cycles 1-4 (post-primary depletion phase) of carbonate core sample.

However, it was noted that the volume of condensate produced during H-n-P injection cycles 1 to 3 in this particular test was comparatively lower than that in previous tests. Cycles 1 – 3 exhibited reduced recovery efficiency, with only 1.8cc of the total 5.24cc or ~34% recovered while a substantial quantity of condensate (~ 64%) remained in the core. The highest volume of condensate recovery occurred during cycle 4, which involved the

highest volume of CO_2 injection. This was not the case in previous tests where cumulative condensate recovery of approximately 70% and 59% was achieved during cycles 1 to 3 and cycle 4 exhibited a relatively lower condensate recovery with the highest volume of CO_2 injected. Recall that total condensate recovery decreased by 11% when the rock permeability became 100 times tighter. The significant reduction in rock permeability is thought to have impacted the level of CO_2-GC interaction, leading to a decrease in the efficiency of the recovery process which is also the case in this ultra-low permeability core. At the end of the CO_2 injection, the volume of produced CO_2 was analysed, and the results indicate an increase of 15% between cycles 1 and 2, Cycles 2 and 3 had similar CO_2 production profiles, and cycle 4 had the highest CO_2 production with about 60% of the injected produced. These CO_2 production data are presented in Figure 4.20.

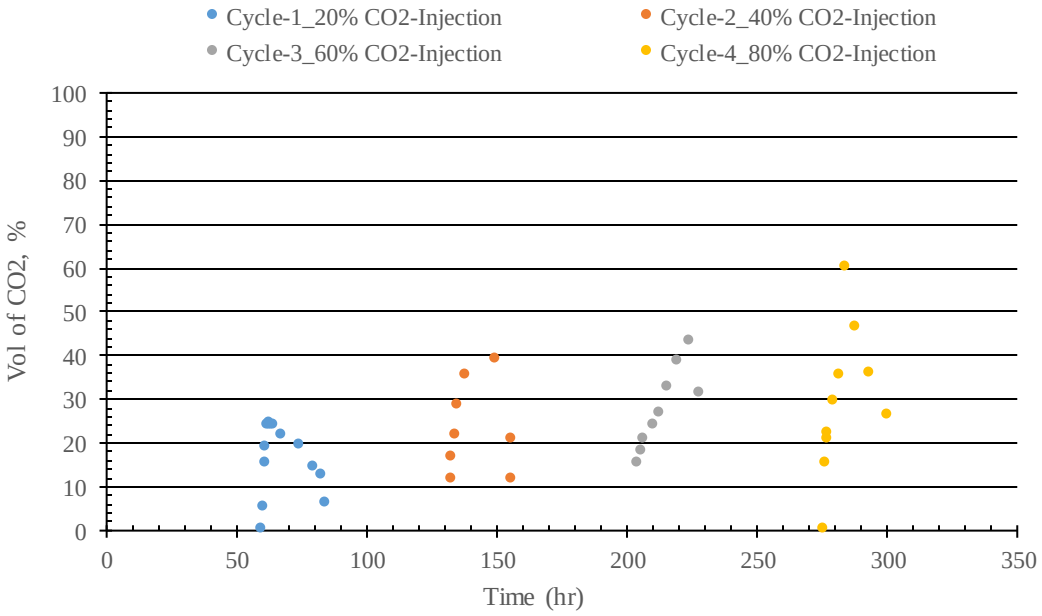

Figure 4.20: Volume of CO_2 produced as (%) of total injected volume of CO_2 per cycle measured at reservoir condition (post-primary depletion phase) for carbonate core sample.

4.7 Summary and Conclusions

In this study, a CO_2 injection technique was designed to optimise CO_2/Gas condensate interaction when the resident fluid is contacted with CO_2 at maximum liquid dropout. The total volume of CO_2 injected is optimised to ensure that at the end of each huff cycle, soaking period, and before puffing, the system pressure remains within the predetermined pressure boundary over where the change in LDO is small. This CO_2 injection technique is referred to as the systematic injection process.

The proposed H-n-P CO_2 injection technique was introduced aiming to optimise the interaction between the injected CO_2 and the reservoir fluid. The objective was to enhance the swelling and vaporising mechanisms, which play a crucial role in the recovery of condensate when implementing such a pressure maintenance technique. To evaluate the effectiveness of the proposed injection technique, experiments were conducted using three different rock samples. These samples had permeability values of 336 mD, 3.23 mD, and 0.03 mD respectively, representing a range of permeability conditions commonly encountered in reservoirs.

Throughout all three tests, a binary gas condensate fluid with properties resembling a rich gas condensate fluid (initial liquid dropout of 29.12%) was utilised. This choice of fluid with known fluid properties ensured consistency in the experimental conditions and allowed for a comparative analysis of the results. By implementing the proposed CO_2 H-n-P injection technique for these three cores and using the specified fluid, the potential for improving condensate recovery and CO_2 storage was investigated.

The results obtained from the pre- and post-CO_2 injection phase for these three cores, shown in Tables 4.3 and 4.4, clearly indicated a decline in condensate recovery as the cores became less permeable and porous. In other words, the core samples with lower permeability and porosity exhibited lower efficiency in terms of condensate recovery. In other words, among the three core samples, the Berea core sample, which had the highest permeability and porosity, demonstrated the most favourable condensate recovery efficiency. The Indiana limestone and Carbonate rocks are approximately 100 and 11,000 times less permeable, 1.2 and 4 times less porous relative to the Berea core. This finding suggests that the inherent characteristics of the Berea core sample, such as its higher permeability and porosity, facilitated a more effective interaction between the reservoir fluid and the injected CO_2, resulting in higher condensate recovery.

Table 4.3: Comparison of condensate recovery efficiency during primary depletion (pre-treatment) for all rock types.

Pre-Treatment			
Rock Type	**Permeability, mD**	**Porosity (%)**	**Condensate Recovery Efficiency**
Berea Core	336	18.44	20.2%
Indiana Limestone	3.23	15.3	14.9%
Columbia Carbonate Core	0.03	4.7	4.7%

Table 4.4: Comparison of condensate recovery efficiency after systematic H-n-P CO_2 injection (post-treatment) for all rock types.

Post-Treatment			
Rock Type	**Permeability, mD**	**Porosity (%)**	**Condensate Recovery Efficiency**
Berea Core	336	18.44	69.7%
Indiana Limestone	3.23	15.3	58.6%
Columbia Carbonate Core	0.03	4.7	45.6%

Although the LDO was similar for these core flood experiments, condensate recovery was observed to decrease by approximately 5.3% and 15.5% for the pre-CO_2 injection stages and by 11.1% and 24.1% for the post-CO_2 injection stages, when the core sample was changed from high to low and ultra-low permeability, respectively.

These results suggest that although the proposed CO_2 injection technique can alleviate condensate banking problems in Ultra-low and low permeability gas condensate reservoirs, it is more profitable when implemented on high permeable reservoirs.

Considering these results, permeability is most likely not the only rock property that may have negatively impacted the recovery efficiency of the proposed injection method across all three-core sample. Other rock properties including mineralogy, rock mechanics, heterogeneity, and fluid-rock interaction can also play significant roles during CO_2 injection for EGR and CO_2 storage.

It is important to state that during the primary depletion phase, the pressure was decreased gradually from the initial system pressure of 5500 psi to 2400 psi which was the lower pressure limit where only a small variation of ~2% in the maximum liquid dropout was observed. In each of the proposed H-n-P CO_2 injection/treatment cases, only about 2.2 PV of CO_2 injection was required to obtain approximately 40% additional recovery. When implementing the systematic CO_2 H-n-P injection technique on all three core samples, it was observed that for the Berea sandstone and Indiana limestone, condensate recovery across all four cycles followed a similar trend with very small recovery for the first and last cycles and high recovery during the second and third cycles. However, the condensate recovery trend for the carbonate rock was significantly different with condensate recovery increasing progressively from cycles 1 to 4.

The recovery efficiency of the new technique was also compared to the recovery observed while performing the conventional CO_2 H-n-P injection method on the Berea sandstone core. It was observed that the new technique is able to match the recovery

efficiency achieved for the conventional injection technique but with lesser volumes of CO_2 injected and produced per cycle and cumulatively at the end of the treatment process. At the end of the systematic injection technique, the total gas produced had an 85.9% and a 14.1% hydrocarbon and CO_2 content, respectively. While 49.5% additional condensate recovery was recorded after the H-n-P CO_2 treatment with a cumulative CO_2 storage of 48.6% of the total volume of CO_2 injected. On the other hand, at the end of the conventional injection technique, the total gas produced had a 32.1% and 67.9% hydrocarbon and CO_2 content respectively. 59.1% additional condensate recovery was recorded after H-n-P CO_2 treatment with a cumulative CO_2 storage of 27.3% of the total volume of CO_2 injected. In other words, these results show that the new technique can easily matched the recovery efficiency of the conventional approach but with less CO_2 injected at reservoir conditions. That is, for new technique, a total of 2.1PV of CO_2 was injected at reservoir condition. While, For the conventional technique, a total of 5.1 PV of CO_2 was injected at reservoir condition. The absolute volume of CO_2 stored in conventional approach is approximately 3 times more than the stored CO_2 in new injection technique but with 5.4 times more CO_2 injected. Also, the net amount of CO_2 stored is more in the latter, but the efficiency of storage is poor when compared to the former. Generally, the condensate recovery is 10.5% higher in the conventional approach but this is at the cost of losing 22% of valuable hydrocarbon gas and injecting significantly higher volume of CO_2 relative to the new approach.

A similar comparative analysis was conducted to determine the CO_2 storage efficiency achieved for each rock type. It was observed that the CO_2 storage efficiency declined as both the rock permeability and porosity became lower, again indicating low CO_2-GC interaction. The result from this analysis is presented in Table 4.7.

Table 4.5: Comparison of CO_2 storage efficiency after implementing the proposed H-n-P CO_2 Injection on all Rock Types.

Post-Treatment			
Rock Type	**Permeability, mD**	**Porosity (%)**	CO_2 **Storage Efficiency**
Berea Core	336	18.44	48.6%
Indiana Limestone	3.23	15.3	31.3%
Columbia Carbonate Core	0.03	4.7	22.8%

These results support already established fact that permeability and porosity are very important criteria to consider when selecting potential CO_2 storage sites especially for

reservoirs with low permeability and porosity. These reservoirs are majorly characterised by thin reservoir interval and complex structure that diminishes the injectivity of supercritical CO_2. The obtained results confirm that there is a link between injectivity and storage efficiency of CO_2 in any rock/reservoir type as speculated.

The experimental results presented in this chapter have demonstrated the efficacy of the proposed H-n-P CO_2 injection technique. The findings indicate that this technique offers enhanced condensate recovery, comparable to that achieved with the conventional H-n-P approach. However, it also presents an additional advantage of reducing the volumes of CO_2 required for delivering similar condensate recovery and particularly CO_2 storage as compared to a conventional H-n-P CO_2 injection practice. This is a significant finding as it suggests that the proposed H-n-P CO_2 injection technique can achieve efficient condensate recovery while maximising CO_2 storage, which reduces the environmental impact associated with CO_2 production.

These results also suggest that the vaporising mechanism is the dominant mechanism responsible for the enhanced gas condensate recovery observed when the proposed H-n-P CO_2 injections technique was implemented.

Considering the established fact from the PVT tests CASE-1 & -2 that condensate recovery efficiency was better enhanced by vaporisation when CO_2 was injected at $P<P_{dew}$ rather than by liquid shrinkage where CO_2 was injected at $P> P_{dew}$. For CASE-1, residual condensate fraction of ~3.5% remained in the PVT cell after saturating the system with 80% CO_2. While it took only 60% CO_2 saturation in CASE-2 to completely vaporise the accumulated condensate. Therefore, the injection scenario for the proposed H-n-P CO_2 injections technique was designed to benefit from vaporising mechanism and enhance condensate vaporisation below the dew point pressure of the targeted depleting gas condensate reservoir.

It should also be noted that for this study only the effect of rock permeability and porosity on recovery efficiency was considered. As the decrease in permeability and porosity resulted in declining CO_2 injectivity. It was observed the injectivity of CO_2 had a direct proportionality to the evaluated rock properties. However, the Berea sandstone core with high-porosity was generally favourable for CO_2 injection. It provided ample pore space for CO_2 storage and allowed for efficient CO_2 migration and interaction with resident fluid.

The limestone core had lower permeability and porosity compared to sandstones which may be one of many reasons for the observed decline in recovery. However, CO_2 reaction

with the calcium carbonate in limestone, potentially leading to mineral dissolution or mineral precipitation could have also altered the rock properties significantly and affected CO_2 injectivity, CO_2 – resident fluid interaction and storage capacity.

Finally, the carbonate core had the lowest permeability and porosity of all core samples used in this work and correspondingly the lowest condensate recovery and CO_2 storage potential. Carbonate formations pose other challenges such as mineralogy-reaction and heterogeneity which could have also influenced the CO2-GC fluid interactions during CO_2 injection. Effective CO_2 storage and migration in carbonate formations may require wettability alteration, dissolution of carbonate minerals, which were not considered for the study.

Chapter 5– Numerical Simulation Using Measured Relative Permeability

The CO_2 -GC relative permeability obtained from core flood experiments can be used in large scale reservoir simulation models. For unsteady-state displacement core flood tests, the kr data is calculated by history matching of the pressure profile and production data. To complement and generalise the corresponding core flood experimental results, a preliminary numerical simulation was performed to history match the experimental results of TEST-1 (new H-n-P CO_2 injection technique) on the Berea core. The laboratory PVT test results described in Chapter 3 were used to generate relevant data sets describing the complex changes in phase behaviour of CO_2-GC mixtures. The experimental PVT data were used for tuning the EOS incorporated into the model for describing the phase behaviour of the CO_2/GC system. A compositional simulation approach was performed to simulate the retrograde condensation and formation of condensate bank in the core.

5.1 Model Development

A 1-D cartesian model has been generated replicating the experimental set-up and procedure of the systematic H-n-P CO_2 injection test conducted on the Berea core. The model was designed with the exact length of the core used in the experiment, but the core's circular cross-section was transformed into a square of an equal cross-sectional area. The Berea core was assumed to have homogeneous permeability, porosity, and initial condensate saturation. A well is placed at one end of the model—grid block 102, which acts as an injector or a producer. The static properties of the model are isotropic with an initial water saturation of 0%. The core has a diameter of 5.08 cm and a length of 18.95 cm, while the model has a grid size of 4.5cm x 4.5cm x 18.95 cm, and a grid block dimension of 1 x 1 x 102 blocks, as shown in Figure 5.1 and Table 5.1, which highlight the core properties and initial test conditions implemented in this model.

(a)

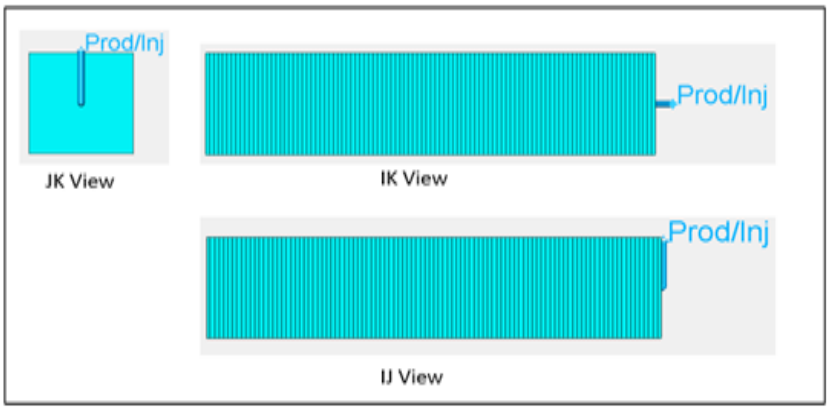

(b)

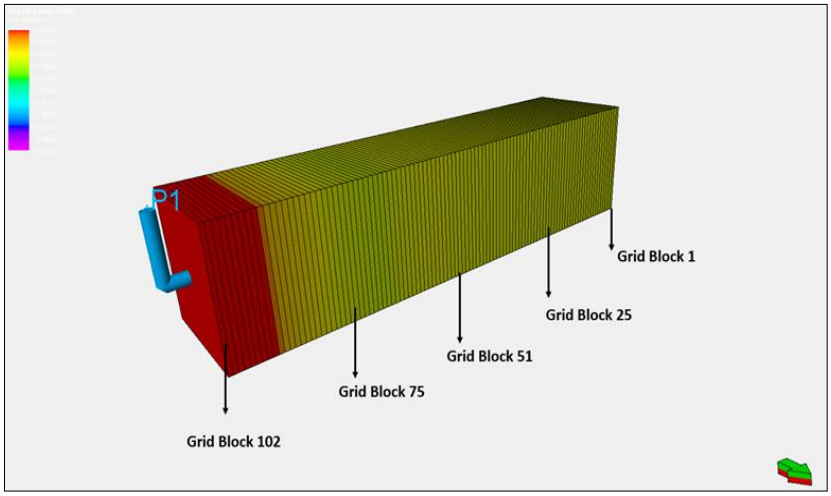

Figure 5.1: [a] Cross-Sectional Views (JK, IK, IJ), [b] Selected grid block distribution of the simulation model used for H-n-P injection.

Table 5.1: Reservoir Properties and Model Input Parameters.

Property	Value	Unit
Effective PERM	336	mD
PORO	18.44	%
Initial Condensate Saturation	29.17	%
Initial Water Saturation	0	%
Initial Core Pressure	5500	psi
Injection Gas	CO_2	cc
Reservoir Temperature	60	^oC
Rock Compressibility	6.7e-5	psi^{-1}

The injection and production constraints mirrored those depicted in Figure 4.4a and the injection was controlled by the reservoir voidage rate, while production was regulated

by the bottom hole pressure. The control mode and constraints employed are illustrated in Table 5.2.

Table 5.2: Well Control Mode and Constraints of the Simulation Model.

	No. of Cycles	Injection + Soak Time/Cycle (hrs)	Injection Control Mode (rcc)	Production Control Mode (psi)	Production Time (hrs)
Test-1	4	2+34	rcc/hr	BHP	11
Test-2	4	0+34	rcc/hr	BHP	11
Test-3	4	2+34	rcc/hr	BHP	11

5.2 Sensitivity Analysis and History Matching of Production Data

The model utilised a set of steady state gas and condensate relative permeability (GC-kr) data which was previously obtained from an experiment conducted at the Heriot-Watt Gas-Condensate Recovery Laboratory, to describe the mobility of gas and condensate through the Berea core. These relative permeability measurements were performed using a binary gas condensate mixture, without the addition of CO_2. A graphical presentation of the original observed GC-kr data for the binary gas condensate fluid without the addition of CO_2 is shown in Figure 5.2.

To enhance the applicability of this GC-kr data for history matching purpose in the simulation model, the measured GC-kr data underwent slight modifications by fitting Corey's model using equations 1 and 2 shown below.

$$K_{rg} = K_{rg\,max}\left(\frac{S_g - S_{gr}}{1 - S_{gr} - S_{or}}\right)^n \ldots\ldots\ldots\ldots\ldots\ldots\ldots\ldots\ldots \quad (5)$$

$$K_{ro} = K_{ro\,max}\left(\frac{1 - S_g - S_{or}}{1 - S_{gr} - S_{or}}\right)^m \ldots\ldots\ldots\ldots\ldots\ldots\ldots\ldots\ldots \quad (6)$$

where that K_{rg} and K_{ro} are the relative permeability of gas and oil, respectively, S_{or} and S_{gr} are residual oil and gas saturation, S_g is the gas saturation, and n and m are Corey constants.

This adjustment enabled easy sensitivity analyses on these GC-kr data and facilitated the history match of the experimental recovery data. In this context, the original GC-kr data obtained from measurements are referred to as PERM-1, while the corresponding Corey-type fitted relative permeability is labelled as PERM-2 and presented in Figure 5.3

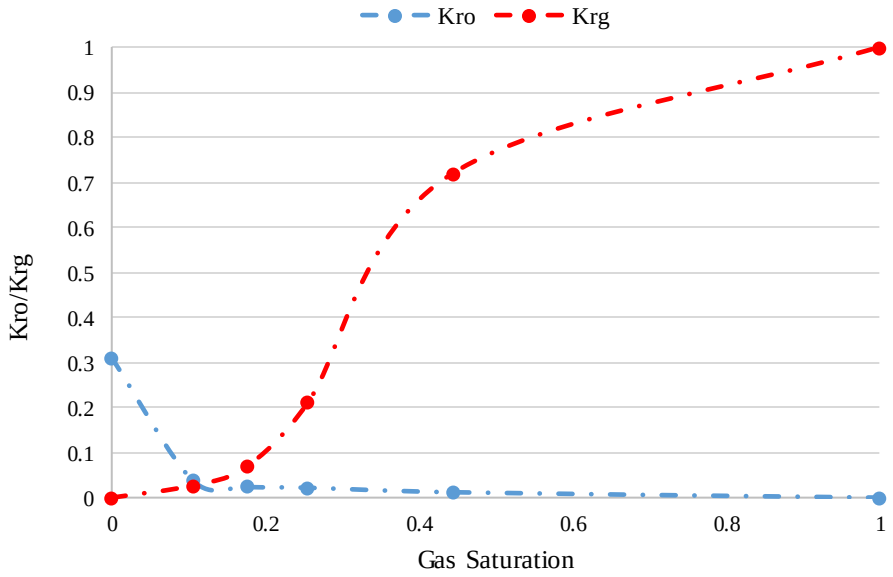

Figure 5.2: PERM-1, Steady-State Gas and Condensate Relative Permeability Curves for the Berea core.

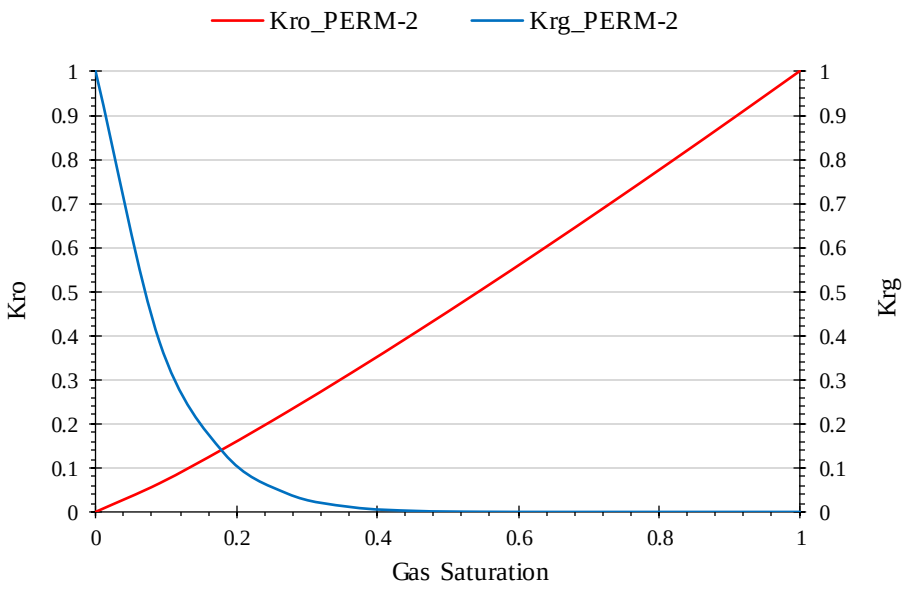

Figure 5.3: PERM-2, Corey Fitted Steady-State Gas and Condensate Relative Permeability Curves for the Berea core.

The production data predicted by the simulation model using PERM-2 data shows significant deviation compared to the corresponding measured gas and condensate recovery data, as shown in Figures 5.4 and 5.5. It is noted that the cumulative gas and condensate production is significantly underestimated by an average error of around 24% and 66%, respectively, across all production cycles. This points out the inability of the model to adequately capture the individual phase flow and mobility even after several parameters were modified.

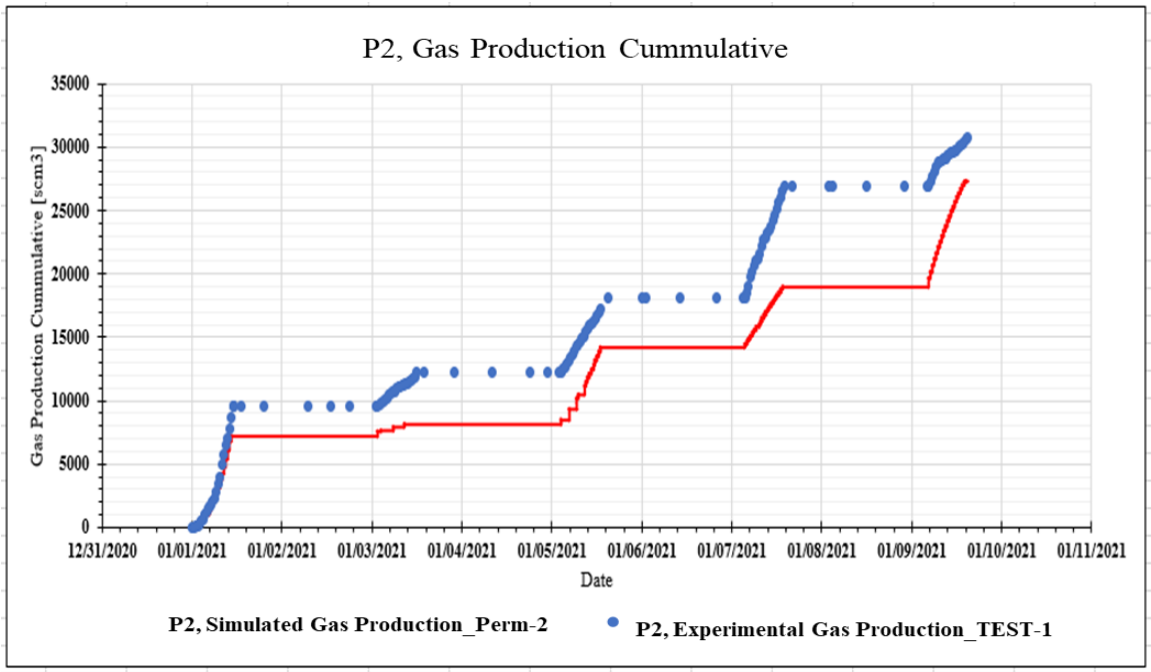

Figure 5.4: Simulated Gas Recovery versus Time Using PERM-2 Compared to the Berea core Experimental Data for TEST-1.

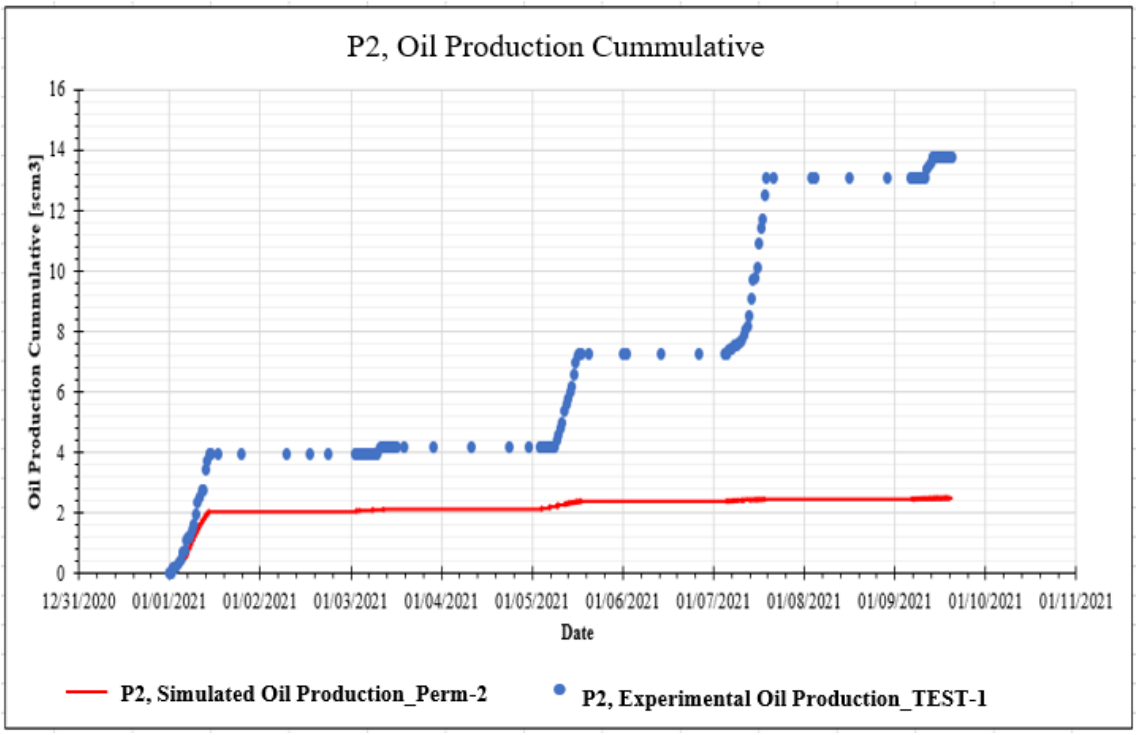

Figure 5.5: Simulated Condensate Recovery versus Time Using PERM-2 Compared to the Berea core Experimental Data for **TEST-1.**

It is important to mention that appropriate experimental CO_2-GC PVT data were already used to tune the employed equation of state. At this stage, sensitivity analysis was performed on the soaking time by increasing the shut-in period to 68 hours to evaluate the impact of more interaction time, which might explain the mismatch. However, no additional condensate recovery was recorded at the end of production for individual cycles. This led to the conclusion that an extended soaking period did not affect the recovery efficiency of the implemented technique. A series of sensitivity and optimization analyses were done on PERM-2 by adjusting specific Corey-kr parameters, including the Corey gas, Corey O/G, and the endpoints for both gas and condensate kr curves. PERM-3 was identified to produce the best obtainable history match of the experimental data from over two hundred GC-kr modification cases. Table 5.3 includes the Corey parameters for PERM-2 and PERM-3 kr data sets. A significant deviation between PERM -1 AND -2 GC-kr curves was observed and Figure 5.6 shows these two kr curves.

Table 5.3: Corey Parameters for PERM-2 and PERM-3 kr data set.

Corey Parameters	**Corey Fitted Rel-Perm (PERM-2)**	**Modified Rel-Perm Values (PERM-3)**
S_{gcr}	0.05	0.05
$Corey\ Gas$	1.140	10.465
$Corey\ Oil/Gas$	10	1
$K_{ro}@S_{omax}$	0.89	0.9
S_{org}	0.05	0
$K_{rg}@S_{org}$	1	0.25

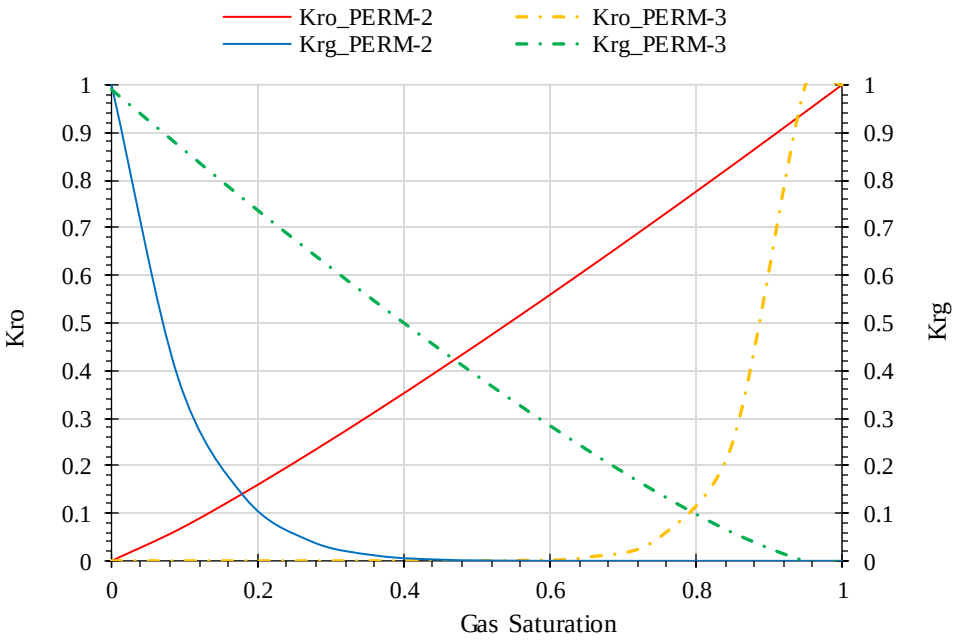

Figure 5.6: PERM-2 and PERM-3, Steady-State Gas and Condensate Relative Permeability Curves, Berea core.

The results for gas and condensate production using PERM-3 are shown in Figures 5.7 and 5.8, respectively. A close agreement between simulated and experimental data is observed for the primary depletion with no CO_2 injection and during the first H-n-P CO_2 injection cycle, where the volume of injected CO_2 (20%) was small relative to the initial condensate volume. There is a mismatch for the second cycle (40% CO_2 injection), third cycle (60% CO_2 Injection), and fourth cycle (80% CO_2 injection) when the volume of CO_2 is increased. The mismatch between the simulated and experimental data for produced gas began from the first CO_2 injection cycle and increased as the volume of CO_2 increased in subsequent cycles. The percent error was estimated to be about 32% for cycle 1 but increased to about 153% at the end of cycle 4. The match was relatively better for condensate recovery, as a mismatch began from cycle 2 with a percent error of 22%, then 88% and 89% for cycles 3 and 4, respectively.

These results show that the PERM-3 kr data can describe the mobility of the gas and condensate phases during the first cycle with a small amount of CO_2 injected. However, they fail to accurately describe the gas and condensate mobility when CO_2-resident fluid interaction effects become more significant. These effects include the re-vaporisation of condensate into the gas phase.

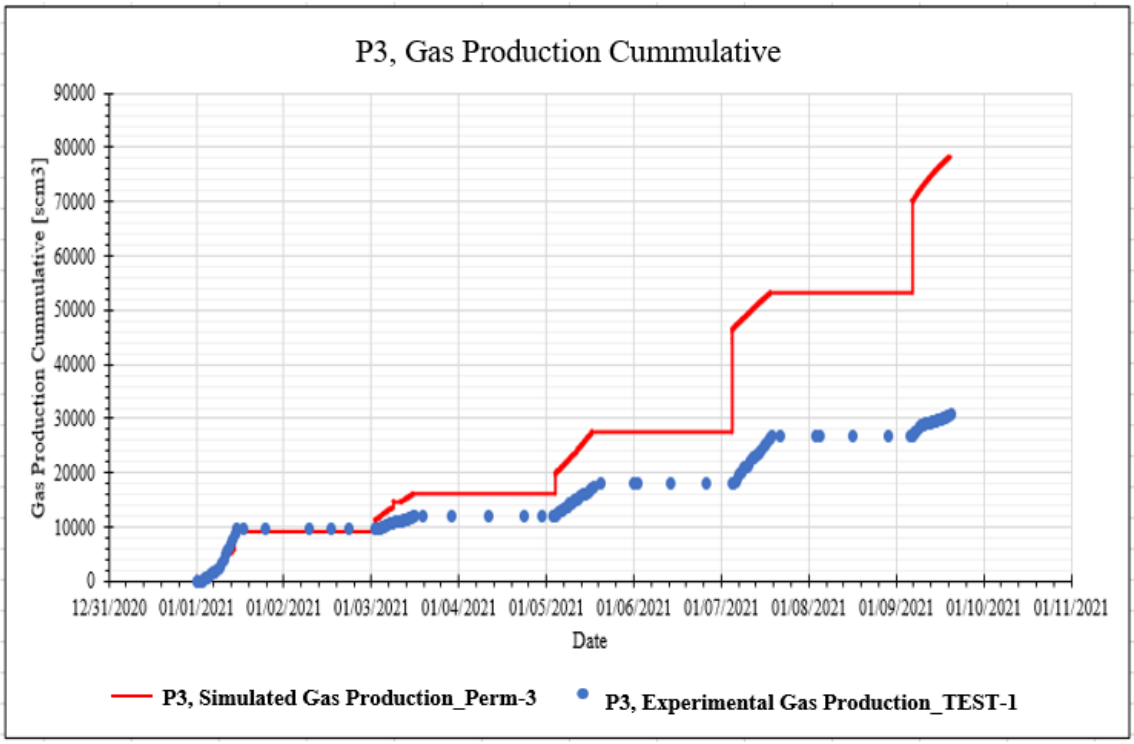

Figure 5.7: Simulated Gas Recovery versus Time Using PERM-3 Compared to the Berea Core Experimental Data for TEST-1.

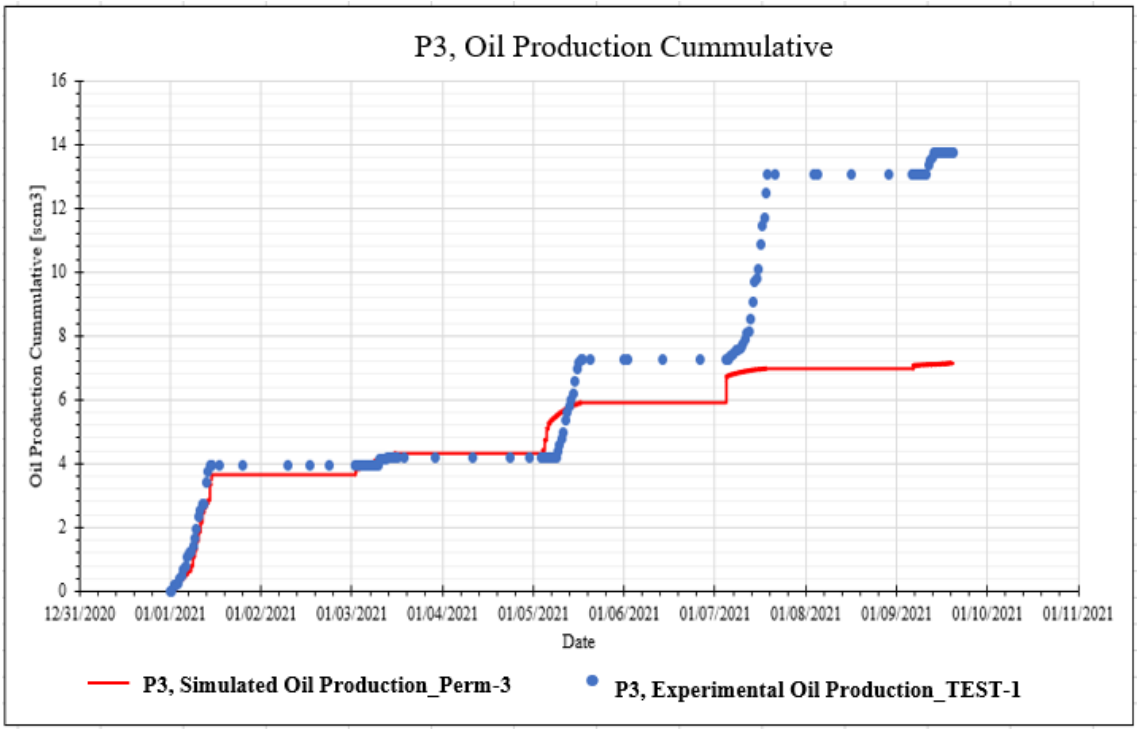

Figure 5.8: Simulated Condensate Recovery Versus Time Using PERM-3 Compared to The Berea Core Experimental Data for TEST-1.

Based on the results obtained thus far, the major conclusions from the simulation runs are:

- Using the previously measured GC-kr data (PERM-1) for gas and condensate prediction provided a good pressure history profile but failed to match the gas and condensate production data.

- The results highlight the inability of the applied gas and condensate relative permeability data to capture the changes that CO_2-GC interactions may have on the mobility of gas and condensate phases.

- Sensitivity analyses were performed on the GC-kr to obtain a match the Berea core experimental production data. However, this was obtained only for the primary depletion and first H-n-P CO_2 cycle confirming the significant impact of compositional changes due to condensate re-vaporisation on the fluid mobility ratio and highlight the importance of measuring and using appropriate CO_2-GC kr data.

5.3 Condensate Saturation, Swelling and Re-vaporisation Analysis.

During the simulation process, a thorough analysis of condensate saturation was conducted at a specific grid block to determine and validate the dominant mechanism responsible for condensate recovery, which was found to be vaporisation. Recall that the model was configured with a single injection/producer well positioned in grid block 102, while grid block 1, situated at the opposite end of the core, served as a sealing point. The examination of saturation primarily focused on two areas: the near well bore region represented by grid block 75, and regions located further away from the injection well, specifically grid blocks 51, 25, and 1. To visualise the distribution of gas and condensate saturation, Figure 5.9 illustrates five individual grid block slices along the core, providing an overview of saturation levels across the entire length of the core. Additionally, Figure 5.10 zooms in on the grid block 75 to specifically display the condensate saturation in that particular area. These figures offer valuable insights into the spatial distribution and behaviour of condensate saturation within the core.

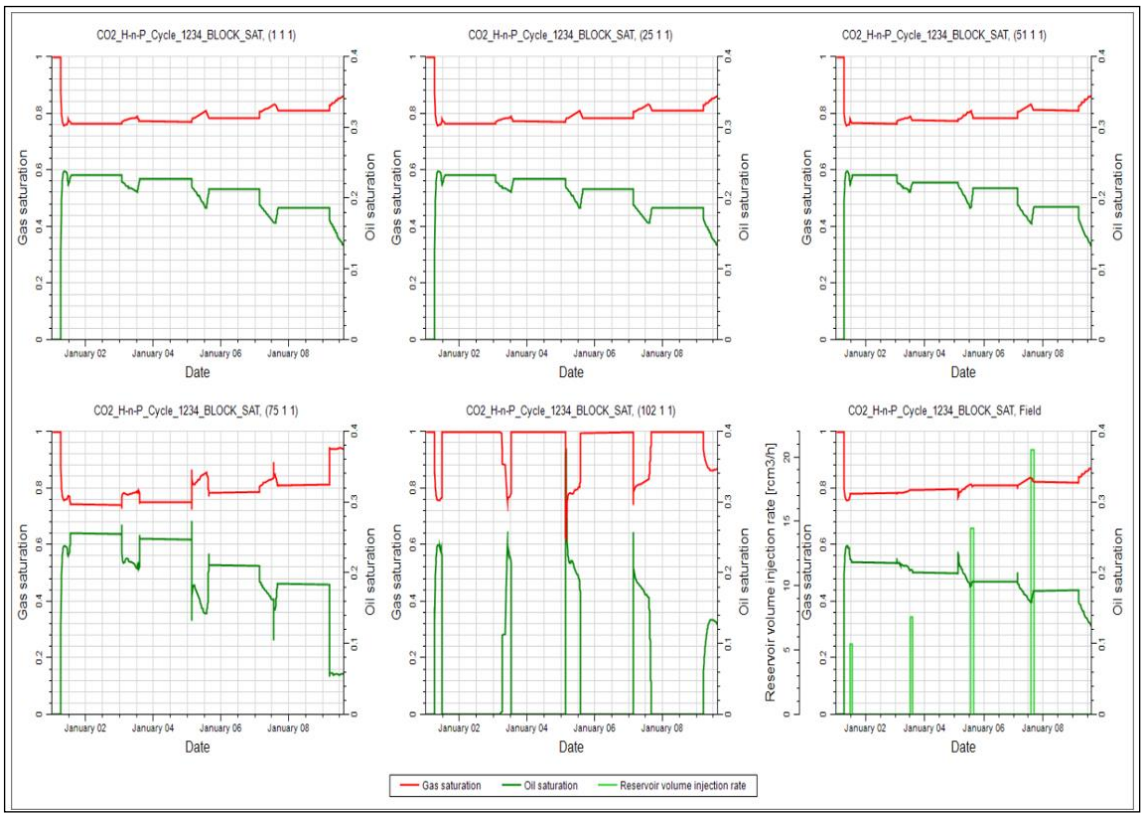

Figure 5.9: Simulated Gas and Condensate saturation versus Time in various grid blocks across the one-dimensional core, showing the presence of Condensate swelling and re-vaporisation, PERM-3 kr and Berea Core Experimental Data of TEST-1.

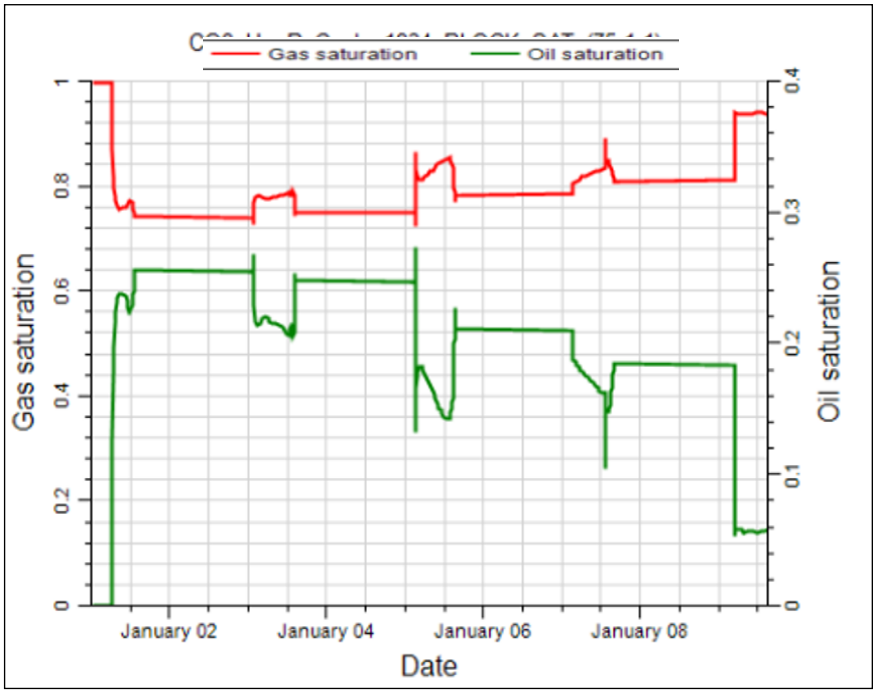

Figure 5.10: Simulated Gas and Condensate saturation versus Time in grid blocks 75, showing the presence of Condensate swelling and vaporisation, Using PERM-3 kr and Berea Core Experimental Data of TEST-1.

The saturation plot for grid block-75 shows an increase of about 11%, 20%, 48%, and 25% in the condensate saturation after each CO_2 injection cycle due to CO_2 dissolution into the condensate (swelling), and then decreases before the production (puff-phase) begins due to condensate vaporisation. This phenomenon is seen to be consistent in all the four analysed grid blocks.

Condensate swelling and re-vaporisation were highest in the grid block-75 as it is closest to the injection well, and CO_2-resident fluid interaction is much higher here compared to grid blocks which are further away. The subplots show a gradual steady decrease in the block's condensate saturation and accordingly an increase in the gas saturation, during the second and third CO_2 injection cycles when the level of gas-condensate and CO_2 interaction is high. Due to the relatively low and high volume of condensate to CO_2 ratio in the core during first and fourth cycles, respectively, the level of CO_2-Condensate interaction is low which limited the amount of recovered condensate. The vapour component mole fraction analysis for grid block 75 is presented in Figure 5.11.

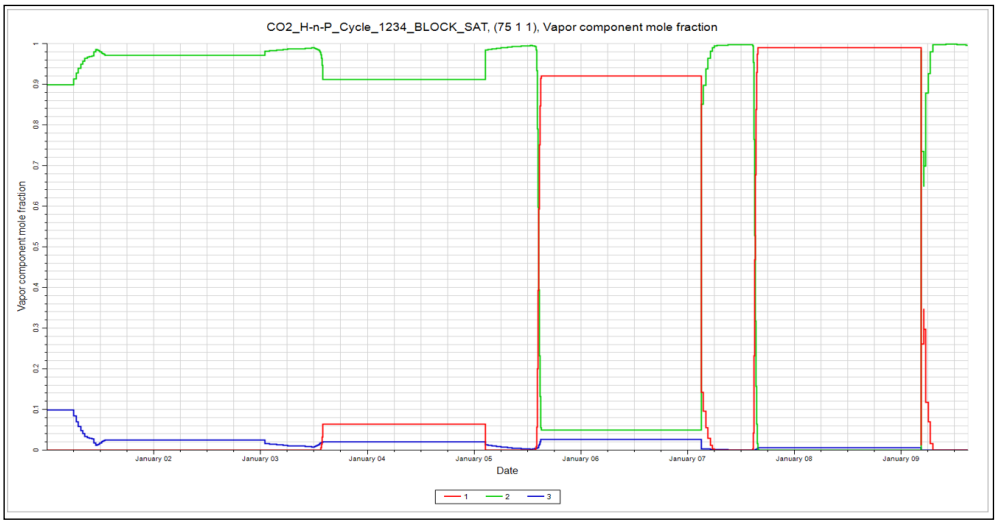

(a)

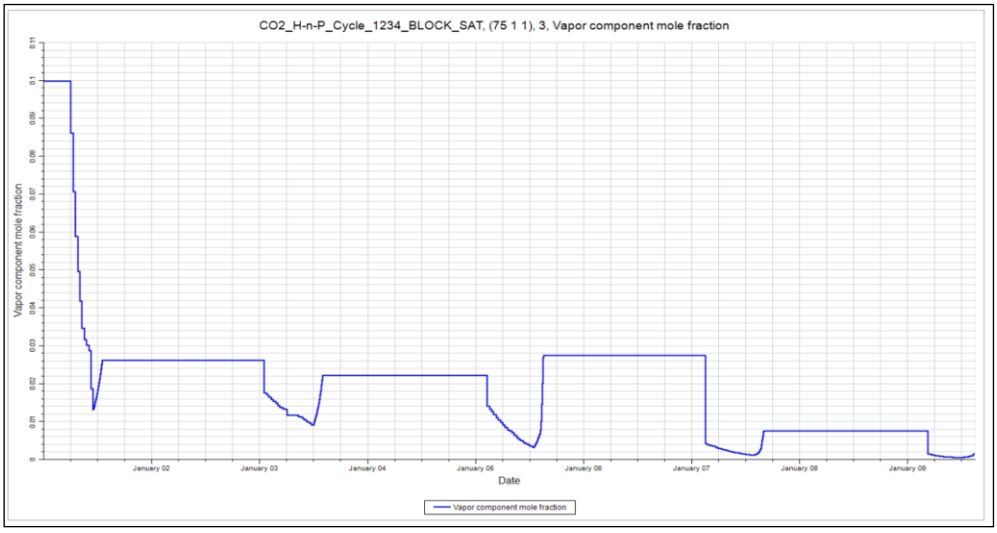

(b)

Figure 5.11: Vapour mole distribution vs time for grid block 75 with a magnified presentation of C8 fraction per cycle using PERM-3 kr data to simulate Berea core experimental data (TEST-1).

For a clearer understanding of the compositional analysis of the gas stream, it is important to recall that the fluid used was a binary mixture of C1 (90%) and C8 (10%), representing the light and heavy components, respectively. The data in Figure 5.11 show a considerable amount of the heavier component re-vaporised back into the gas stream after every Huffing period, i.e., the vapour and liquid mole fractions show increased C8 concentration in the vapour phase. The C8 concentration in the gas phase decreased from 10% to about 1.1% due condensate drop out post-primary depletion but was maintained at an average concentration of 20.9% through the four cycles of incremental CO_2 injection. The highest concentration of C8 in the gas phase was recorded for the third cycle, where the volume of CO_2 injected is comparable to the volume of accumulated condensate. These observations indicate that the numerical simulations are able to demonstrate the more dominant effect of vapouring mechanism.

5.4 Steady State CO_2-GC Relative Permeability Measurement

As mentioned before, series of simulation runs involving condensate saturation analysis and GC-kr modification, showed that the condensate saturation profiles within the core exhibited the expected effects of swelling and vaporising mechanisms. However, these simulations failed to match the experimental production data profile, which was attributed to the effect unrepresentative kr data. To add more value to this work, appropriate CO_2/GC kr data were measured experimentally to capture any effects of presence of CO_2 on the fluid mobility during the more dominant condensate vaporisation

mechanism by the injected CO_2. These data which are lacking in the literature would not only be valuable to test this simulation exercise but also in any studies describing the effects of CO_2-GC interactions.

Therefore, additional high-pressure core flood experiments were conducted using CO_2 saturated gas condensate fluids in the same Berea sandstone cores used during previous core flood experiments to obtain representative steady-state kr data. The aim was to measure the steady-state kr data points across a wide range of condensate-to-gas ratios (CGR), which represents the volume of condensate per unit volume of gas at the test pressure and temperature of 3000 psi and 60C. These test conditions were selected because at this point the original binary gas condensate exhibits maximum liquid saturation and first contact miscibility on contact with injected CO_2. The experimental procedures were carefully designed to ensure that the fluid distribution within the cores accurately represented the conditions prevailing the CO_2 coreflood injection and fluid flow behaviour within gas condensate reservoirs. This was achieved by ensuring that condensate saturation in core was by condensation process rather than by injecting liquid into the core. This is achieved by injecting single phase fluid at high pressure above the dew point and decreasing the pressure down to below the dew point pressure which results in the formation of condensate in the core also referred to as condensation. This was condensate forms uniformly throughout the core in both small and large pores. Then the equilibrated gas and condensate with CO_2 content are injected into the core at pre-defined ratio. The injection continues till full steady-state condition is achieved leading to stable pressure drop and saturation level in the system. Additionally, the hysteresis between drainage and imbibition during the steady-state measurements and the repeatability of the data were also examined.

5.4.1 Experimental Apparatus.

The high-pressure oven is designed to allow a closed loop system for measuring the steady state relative permeability of complex fluid mixtures with CO_2 added. It should be noted that, due to the intricate and time-consuming nature of setting up, plumbing, and operating the closed loop core flooding rig required to measure these data, the steady state relative permeability data for CO_2 gas condensate has not been previously measured experimentally until now. The oven consists of high-pressure pumps with maximum operating pressure of 10,000 psi and a resolution of 0.01 cc, pressure transducers,

graduated sight glass for measuring fluid production within 0.05 cc accuracy, Quartz-dyne transducers for measuring differential pressure across the system, core holder, five high pressure injection and retraction cells, high resolution camera and digital display system. The schematic diagram showing the closed loop oven is presented in Figure 5.11.

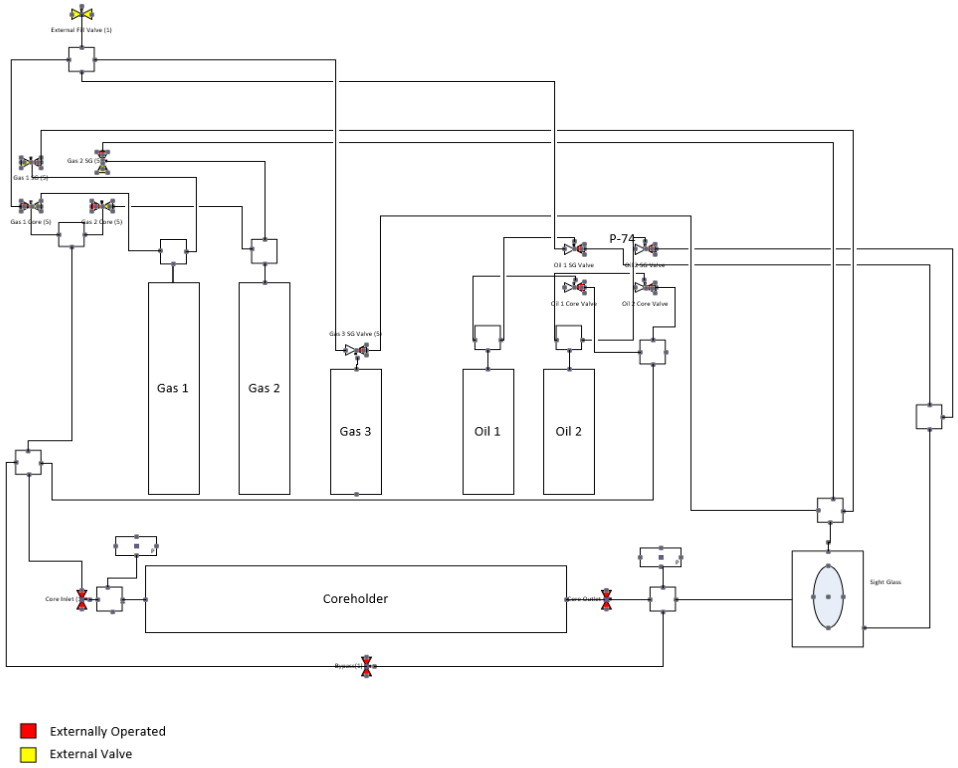

Figure 5.12: A schematic diagram of the closed loop core flood facility used for the steady state relative permeability measurement.

5.4.2 Core Preparation

Prior to beginning the test, the core was cleaned by flushing through with three cleaning agents including toluene, methanol, and acetone respectively at low rates and finally with nitrogen at high rate before vacuuming. The core was the unwrapped and weighed to determine its wet weight, dried and weighed again to confirm no significant weight changes relative to its original weight before any fluid was passed through it. The core was then wrapped, placed in the core holder with an overburden pressure set to 500 psi and vacuumed. Two sets of permeability tests were conducted to confirm the effective permeability of the core prior commencing the steady state relative permeability test. The permeability of the core was tested with Methane and single-phase gas condensate fluid

and results indicated that there has been no damage to the core following previous core flood tests conducted. The measured permeability values were 337 mD and 334 mD to methane and single-phase gas condensate fluid injection, respectively, which were comparable to that of 336 mD that had been measured prior to the previous CO_2 injection experiments.

5.4.3 Test fluid

The test fluid was a ternary mixture Fluid-1 (C1-C8) plus CO_2 in the ratio of 60% to 40% by mol combined at pressure of 5500 psi and room temperature. Due the complex behaviour of CO_2 especially, it was easier handled and safer to transfer at these conditions. This mixture was selected because from experimental PVT and core flood data it was observed that there will still be a maximum liquid drop out of ~20% at 3000 psi (+/- 20) psi. Also, significant condensate recovery began during H-n-P injection cycle 2 when 40% CO_2 was injected. Table 5.4 shows the measured fluid properties of the test fluid.

Table 5.4: Properties of the Ternary mixture used during the steady state relative permeability measurement.

Volume of CO2 added (%)	**Saturation Pressure (psi)**	**LDO_{Max} (%)**	**Swell Factor**
40	3018	19.91	1.58

It is important to mention that the fluid is allowed to stabilize and attain a state of equilibrium at single phase after all components have been added and again after decreasing the system pressure to 3000 psi to establish condensate dropout. Achieving this complete equilibrium state will help in minimizing the effects of mass transfer between the gas and condensate phase when injecting at the selected condensate – gas ratios. This equilibrium state was also checked and maintained at the end of each injection rate consisting of a condensate to gas ratio (CGR) when steady state is achieved. As mentioned before once steady state is achieved at a CGR. CGR is changed which implies the ratio of CO_2 to gas-condensate is different than the original value but at all stages of the test the fluids are ensured to be in equilibrium.

5.4.4 Experimental Procedure and obtained Data.

After the test fluid was prepared, the core was placed into the oven and all line connected and the system flushed with nitrogen, vacuumed and pressure tested to ensure it was leak tight. To condition the system, the core was then saturated with methane and pressured up to 5500 psi and allowed to stabilise. Approximately two pore volumes (about 140 cc) of single-phase gas condensate fluid was injected to displace methane from the core at 5500 psi. The injection cells, Gas 1, 2, 3 and Oil 1,2 were also filled with singe phase fluid before increasing the temperature to 60C. It is important to mention that the system remained connected to an external injection cell, which served as the injection and retraction cell. This cell was required to establish simultaneous pressure depletion both in the core holder and across all the cells to below the dew point ensuring that condensate saturation was established by condensation as opposed to liquid injection. Once the system was stabilised, all valves within the oven were open to ensure communication between the core and cells. The system pressure was decreased gradually over twelve hours from 5500 psi to 3000 psi to achieve a two-phase system of equilibrated gas and condensate as was done during TEST-1. At this stage, the core was shut off by closing both the inlet and outlet valve before bubbling off and collecting the gas and liquid into their respective injection cells. A total of about 860 cc of gas and 74 cc of condensate was recorded at the end of the bubble off separation phase.

To establish a state of steady-state flow in the system, specific condensate-to-gas ratios (CGR) were selected, and the equilibrated gas and condensate fluids were injected into the core following the pre-planned injection pattern. The fluids were continuously displaced through the core until a state of equilibrium was reached, characterised by the CGR at the outlet matching that of the inlet. Once steady-state conditions were achieved at a constant differential pressure, the test was paused, and the core was isolated from the flow system before recording relevant data which includes total volume of condensate and gas injected through the core, volume of condensate in the sight glass and the differential pressure. The gas and condensate flowrate were then ramped up to flowrate corresponding to the next CGR.

Subsequently, the new condensate saturation within the core was determined by calculating the change in the total volume of condensate in the flow system, comparing the final condensate volume to the initial condensate volume in the core. Table 5.5 shows

the selected condensate-to-gas ratio implemented during the steady state relative permeability measurement and the observed differential pressures.

Table 5.5: Properties of the ternary mixture used during the steady state relative permeability measurement.

CGR	Gas Flowrate (cc/hr)	Condensate Flowrate (cc/hr)	Differential Pressure (psi)
0.02	103	2	1.37
0.05	100	5	1.42
0.09	96.5	8.5	1.58
0.1	95.5	9.5	1.64

Kr data of gas and condensate are calculated using Darcy's equation,

$$\boldsymbol{Q_o = \frac{KK_{ro}A}{\mu}\frac{\Delta P}{L}} \ldots\ldots\ldots\ldots\ldots\ldots\ldots\ldots\ldots\ldots\ldots\ldots\ldots\ldots\ldots\ldots\ldots\ldots (7)$$

$$\boldsymbol{Q_g = \frac{KK_{rg}A}{\mu}\frac{\Delta P}{L}} \ldots\ldots\ldots\ldots\ldots\ldots\ldots\ldots\ldots\ldots\ldots\ldots\ldots\ldots\ldots\ldots\ldots\ldots (8)$$

where that $\mathbf{K_{rg}}$ and $\mathbf{K_{ro}}$ are the relative permeability of gas and oil, respectively, **A** is the cross-sectional area of the core, $\boldsymbol{\mu_o}$ **and** $\boldsymbol{\mu_g}$ are the oil and gas viscosity, **ΔP** is the differential pressure, **L** is the length of the core, $\mathbf{Q_o}$ **and** $\mathbf{Q_g}$ are the gas and condensate, and **K** is the effective permeability of the core.

The corresponding gas and condensate relative permeability curves corresponding to selected CGR presented in Table 5.5, core and fluid properties are shown in Figure 5.12. The measured CO_2-GC steady state relative permeability curve will be referred to as PERM-4.

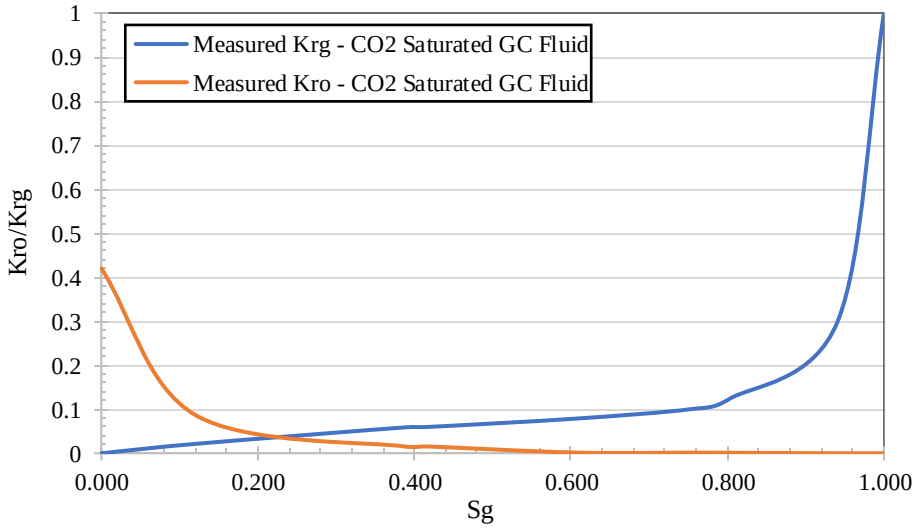

Figure 5.13: Measured steady state gas and condensate kr plot for PERM-4, gas condensate fluid with 40% CO_2 added.

To enhance the applicability of PERM-4 in the simulation model, the measured GC-kr data underwent slight modifications by fitting it to Corey's model using equations 1 and 2 which was applied earlier for curve fitting PERM-1. This untuned Corey fitted kr data was referred to as PERM-5. Just as was done previously, series of sensitivity and optimization analyses were repeated on PERM-5 using PETREL simulator by adjusting specific Corey-kr parameters, including the Corey gas, Corey O/G, and the endpoints for both gas and condensate kr curves and the curve with the best obtainable history match of the experimental data from over two hundred GC-kr modification cases was selected. This set of curves is referred to as PERM-6 and presented in Figure 5.13. Table 5.6 includes the Corey parameters for PERM-6

Table 5.3: Corey parameters for PERM-6 kr data set.

Corey Parameters	**Corey Fitted Rel-Perm (PERM-6)**
S_{gcr}	0.05
$Corey\ Gas$	1.5
$Corey\ Oil/Gas$	11.571

$K_{ro}@S_{omax}$	0.89
S_{org}	0.05
$K_{rg}@S_{org}$	1

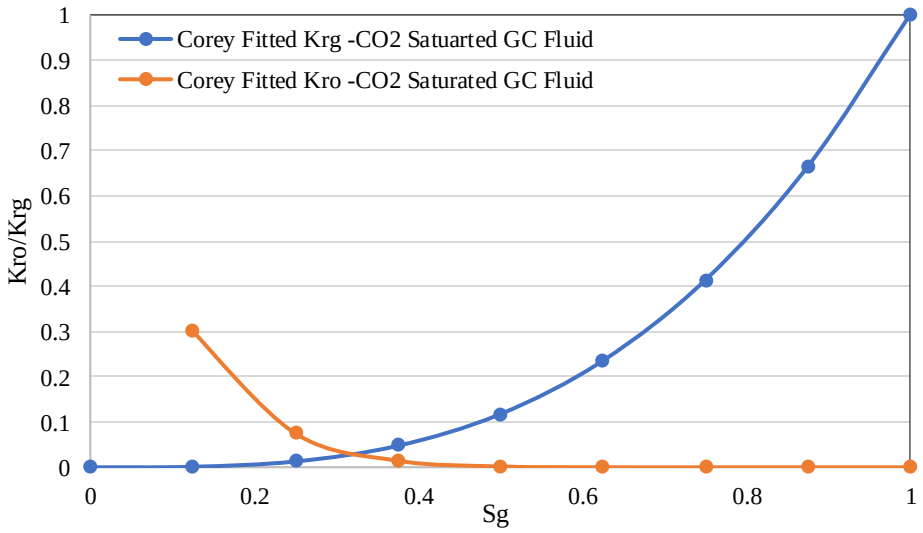

Figure 5.14: Tuned Corey fitted steady state gas and condensate kr plot for PERM-6, using gas condensate fluid with 40% CO_2 added.

PERM-6 kr data was fed into the simulation model and a repeat simulation run completed to predict and match the experimental gas and condensate production profile obtained when the proposed H-n-P CO_2 Injection technique was implemented on the high permeability Berea sandstone core. At the end of the simulation run, a good match was obtained for the gas profile as can be seen in Figure 5.14

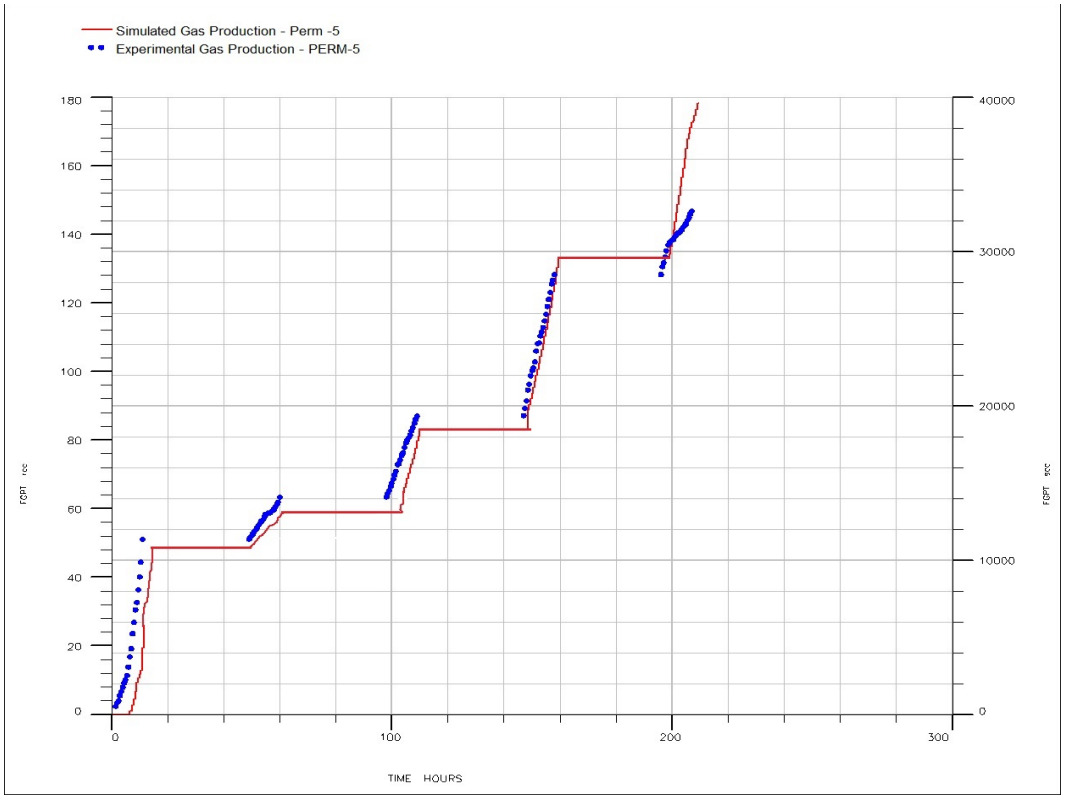

Figure 5.15: Simulated Gas Recovery versus Time Using PERM-5 Compared to Experimental Data for TEST-1.

The results show only ~4% deviation from experimental results compared to a deviation of 24% when PERM-3 (relative permeability without the addition of CO_2 to the original test fluid) was used in the simulation model. On the other hand, the simulated condensate recovery profile did not show significant improvement. Again, showing close prediction for the condensate recovery during the primary depletion stage and Cycle-1 which no CO_2 and 20% CO_2 respectively, but under estimating condensate recovery for Cycles 2, 3 and 4 which has significantly higher saturations of CO_2 by approximately 26%, 54% and 55% respectively. Figure 5.15 shows the plot of cumulative condensate production in (cc) versus time in days for the observed and simulated data. These results show that the complex nature of interactions between CO2 and condensate, which involves multiple factors. The observed discrepancy between predicted and actual condensate recovery may be attributed to several reasons including uncertainty in kr data, porous medium heterogeneity, fluid phase behaviour, capillary pressure effect, saturation and pressure history. It is important to highlight that the simulation model assumes reservoir homogeneity and uniform zero capillary pressure, which is a good assumption for these low IFT systems. The inaccurate condensate recovery prediction may be due to

the variation in reservoir permeability and capillary pressure which has not been adequately captured either during experimental measurements or in the model set up. The assumption of instantaneous equilibrium in phase behaviour applied in EOS models and uniform saturation for the obtained kr data could also play a part for this interactive process.

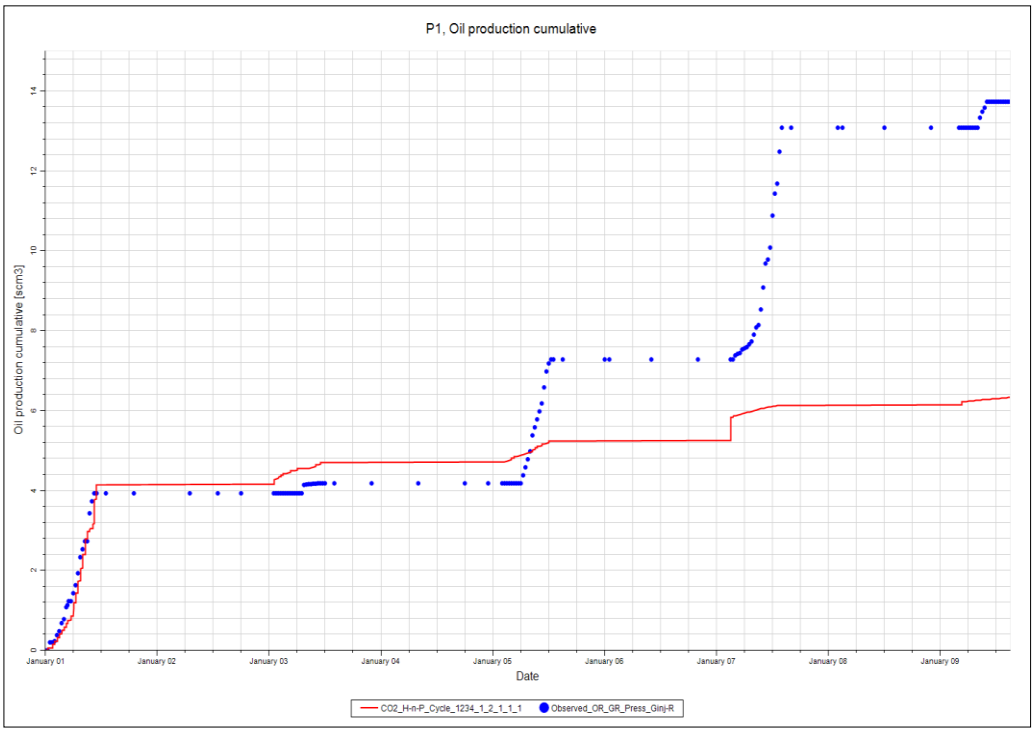

Figure 5.16: Simulated Condensate Recovery versus Time Using PERM-5 Compared to Experimental Data for TEST-1

5.5 Summary and Conclusion

To complement and generalise the corresponding core flood experimental results, a core scale numerical simulation exercise was conducted to history match the experimental results. This simulation exercise examined the effect of main dominant mechanisms.

Based on the results obtained, the major conclusions are:

- Applying PERM-2 (which is the Corey fitted GC-kr data with no added CO_2) in the simulation model for gas and condensate prediction provided a poor match for the gas and condensate recovery by significantly under predicting the cumulative

recovery during the primary depletion phase and across all systematic H-n-P CO_2 injection cycles. On the other hand, applying PERM-3 (which is the sensitised Corey fitted GC-kr data with no added CO_2) in the simulation model only matched the production profile for the primary depletion phase and H-n-P cycle 1 with 0% and 20% CO_2 respectively. However, as the saturation of CO_2 increased across cycles 2, 3 and 4, the predictive capability of the model decreased indicating its inability to capture the effects of increased CO_2-GC fluid flow and phase behaviour interactions leading to improved condensate recovery.

- Appropriate CO_2-GC relative permeability data PERM-4 were obtained by performing steady state relative permeability measurements using CO_2 saturated gas condensate fluid. Corey type model was then fitted to obtain PERM-5, which can allow adequate sensitivity analysis to be performed. A series of Corey parameter tuning were performed on PERM-5 to match the experimental data. At the end of the tuning process, the best match was obtained by applying PERM-6. After attempting to history match the production data using PERM-6 kr data, the simulated gas production profile matched more closely with experimental data compared to that obtained with PERM-3 data. But the condensate recovery profile again showed a mismatch for the H-n-P injection cycles when the volume of injected increase beyond 20% saturation.

- Generally, these results highlight the complexity of the interactive nature of CO_2 and resident fluid and how these may affect fluid flow in the core/reservoir.

The findings from this simulation analysis offer a foundation for assessing the possible advantages of an improved technique for recovering gas and condensate, as well as the need to produce sufficient experimental data on gas and condensate relative permeability especially during CO_2 injection. This data is crucial for testing the simulation model and for studying the impact of mass transfer during CO_2-GC interactions on fluid mobility.

Chapter 6– Summary and Recommendations

6.1 Summary

The injection of CO_2 for enhanced gas condensate recovery (EGCR) in depleting gas condensate reservoirs specifically when considering H-n-P CO_2 injection technique is not a new approach. Several experimental and simulation studies, but limited field pilot tests have been conducted to evaluate the effectiveness of this condensate recovery technique.

Results from literature show that the application of the conventional H-n-P CO_2 injection in depleting gas condensate reservoirs will generally yield approximately 60 - 70% additional condensate recovery. However, this additional recovery requires high volumes of CO_2 injection which ultimately shortens the breakthrough time and increases the volume of CO_2 produced.

The H-n-P CO_2 injection process is governed by several mechanisms including condensate swelling due to CO_2 dissolution and vaporisation of condensate into CO_2. The complex interaction between CO_2 and resident gas condensate fluid must be clearly understood to properly optimise any benefits CO_2 injection can offer. The good performance of any H-n-P CO_2 injection for EGCR is highly dependent on achieving complete miscibility between injected and resident fluid at the given reservoir conditions. The miscibility can be achieved by either the first contact miscibility (FCM) or the multiple contact miscibility (MCM) processes.

It has been proven through several experimental and simulation studies, and field pilot trials that when implementing the conventional H-n-P CO_2 injection for improved condensate recovery in depleting gas condensate reservoirs, the composition of the produced stream becomes significantly important. This is the case because due to the high level of fluid interaction and miscibility, the produced stream could potentially have a high volume of the injected fluid. Due to large volumes of CO_2 injected to repressurise the reservoir and facilitate the efficiency of the vaporising mechanism, high volumes of CO_2 production is usually associated with the recovery process, and this is an unacceptable practice.

Therefore, there is a need to design a new H-n-P CO_2 injection technique that will optimise the volume of injected CO_2 such that lesser volume of CO2 is injected per cycle into the reservoir at specific pressure range and rates. The objective should be to enhance the recovery mechanism and ensure that condensate recovery efficiency is comparable to

the conventional injection technique but with lower volumes of CO_2 injected and produced.

A new approach has been proposed that can match the recovery potential of the conventional H-n-P CO_2 injection technique, but with much lower volumes of CO_2 injected and produced. This proposed technique captures the effects of CO_2-GC interaction including the FCM and MCM processes and achieve optimum condensate recovery when the reservoir pressure is below the dew point.

The work presented here consists of phase behaviour (CCE and shrinkage/swelling), EOS modelling, interfacial tension (IFT) tests, unsteady-state core flood experiments, and CO_2-GC steady-state relative permeability measurements. The emphasis is on the effect of CO_2 on the dew point pressure, liquid dropout, miscibility, swelling, re-vaporisation, and mobility when injected at pressures above and below the measured dew point pressure (Pdew) of gas condensate systems. A combination of experimental and simulation approaches was completed to clearly understand the dominant mechanisms and identify the true potential of CO_2 injection for EGCR and CO_2 storage purposes. The state-of-the-art experimental facility in the GCR laboratory and benefiting from the extensive experience and expertise working on gas-condensate recovery by the team were employed to perform USSD core flood experiments on three core samples with various permeabilities. A commercial compositional reservoir simulator was used to simulate the core experiment's results.

Upon validating the outcomes of the proposed injection techniques through a comparison with results obtained through conventional injection methods in Chapter 4 and utilizing a numerical model in chapter 5 to ascertain and verify the impact of CO_2-GC relative permeability on the recovery efficiency, it has been substantiated that even by injecting five times less CO_2 there is an enhancement in condensate recovery and CO_2 storage efficiency. Based on the experimental results presented in chapters 4 and 5, a new approach for condensate recovery while achieving CO2 storage was developed to enhance the recovery of condensate while injecting supercritical CO_2 which have previously been identified by (Cui et al., 2015) as the best phase to optimise recovery and CO2 storage. The recovery and storage efficiencies of the proposed method was found to be satisfactory.

The results show that although the recovery efficiency of the proposed H-n-P CO_2 injection technique may be reduced by decreasing rock permeability, it was able to closely

match the recovery efficiency achieved by the conventional injection technique when implemented on a high permeability core sample.

Furthermore, the simulation runs for the H-n-P CO_2 injection in high permeability core have shown that measuring appropriate GC-kr data is a very important parameter to consider when designing a simulation model to match and predict future performance during CO_2 injection process.

6.2 Conclusion

This research focused on conducting appropriate experimental CO_2-Gas condensate phase behaviour, unsteady-state core flood, and steady-state relative permeability tests to determine the CO_2-GC interaction level and quantify the vaporising mechanisms governing the recovery process during H-n-P CO_2 injection for EGCR and CO_2 storage. Accordingly, a practically attractive framework to quantify the advantages of CO_2 injection, which helps in screening a suitable target reservoir and is lacking from previous studies, has been proposed and compared to the conventional H-n-P CO_2 technique. The results show that the technique proposed in this research can better improve condensate recovery efficiency relative to the aforementioned techniques.

This research presents a novel approaches for improving condensate recovery which have been duly tested on various rock samples with permeability ranging from high to ultra-low permeability. However, the recovery efficiency of the proposed H-n-P CO_2 injection technique supersedes both the conventional H-n-P CO_2 injection method.

The results obtained from the performed experimental and simulation analysis can be applied to quantify and improve condensate recovery efficiency, enhance the accuracy of forecasting the recovery efficiency of the proposed H-n-P CO_2 injection method for EGCR and CO_2 storage.

Considering the observed results from this study, beginning from the design and implementation of a series of PVT, miscibility, IFT, and core flood experiments which was duly accompanied by developing an appropriate simulation model to replicate the experimental core flood process, the following conclusions can be highlighted:

- Performing appropriate PVT experimental tests to investigate and quantify the level of CO_2-GC interactions to enhance the swelling and vaporising mechanisms above and below the dew point of specific target reservoir is essential. These data include one set of CO_2 -GC phase behaviour, miscibility, swelling, and vaporising tests.

- From PVT CASE-1 (CO_2 injection above P_{Dew}) and CASE-2 (CO_2 injection below P_{Dew}), it has been established that during CO_2 injection for EGCR, condensate recovery is better enhanced by the vaporising mechanism relative to condensate shrinkage. The complies with the results observed by (Nasriani et al., 2014) and (Stpheni et al., 2006). That is, during CASE-2 (involving primarily vaporisation) only 60 mol % of CO_2 injection was required to completely vaporise 19.8 cc of accumulated condensate. On the other hand, during PVT test CASE-1 (involving condensate shrinkage only), after injecting 80 mol % of CO_2 into the system, there was still ~ 3.5% residual condensate saturation.

- Vaporising mechanism has also been identified as the dominant mechanism governing the recovery of condensate during coreflood tests and corresponding numerical simulations when implementing the proposed H-n-P CO_2 injection technique. Previously, it was established that vaporising mechanism was only achievable by increasing the system pressure above the original Pdew of any gas condensate system. However, this study has shown that when implementing this new H-n-P CO_2 injection technique, condensate vaporisation was achieved at pressure below the original Pdew of the selected gas condensate system by optimizing the volume of CO_2 injected and keeping the system pressure above the corresponding Pdew of the CO_2-GC mixture per cycle ensuring that CO_2-resident fluid interaction occurs at the specified pressure boundary before production commences.

- The measured PVT data help in identifying appropriate injection pressure, rate and volume of CO_2 required for implementing the proposed H-n-P CO_2 injection to significantly improve the recovery efficiency of the recovery process.

- Specific but limited PVT experiments and data were required for EOS modelling of the CO_2-GC systems.

- MMP was a vital parameter to consider, as it was observed that at P<MMP, condensate swelling, and vaporisation was significantly reduced irrespective of the volume of CO_2 injected. This phenomenon was initially observed during

PVT CASE-1 experiment and also during the fourth CO_2 injection cycle of the core flood tests where condensate production was small across all three rock types. Hence, maintaining the system pressure above the MMP is vital for obtaining maximum recovery efficiency when implementing the proposed H-n-P CO_2 injection treatment.

- Variation in rock properties can significantly changes the recovery efficiency of the proposed H-n-P Injection technique. More specifically as permeability reduces the benefits of H-n-P reduces. In other words, the results from this work suggest that although the proposed CO_2 H-n-P injection technique can alleviate condensate banking problems in ultra-low and low permeability gas condensate reservoirs, it is more profitable when implemented on high permeable reservoirs.

- The conventional H-n-P CO_2 treatment technique achieved a recovery efficiency of ~80% at the end of four CO2 injection cycles where ~5.1 pore volumes of CO_2 was injected and producing over 70% of injected CO_2. While the proposed H-n-P CO_2 injection technique achieved a recovery efficiency of ~70% at the end of four CO2 injection cycles with just ~2.1 pore volumes of CO2 injected and producing ~51% of the injected CO_2.

- The net amount of CO_2 stored for the conventional H-n-P CO_2 treatment was more, but the efficiency of storage was poorer when compared to proposed H-n-P CO_2 injection technique. The hydrocarbon recovery efficiency in the latter was higher than the former when compared relative to the total volume of hydrocarbon produced from Cycles 1-4.

- CO_2-GC kr data were required especially for developing the H-n-P CO_2 injection simulation model. These data were crucial for testing the simulation model and for studying the impact of CO_2-GC interactions on fluid mobility. Initial simulation runs completed with previously measured GC-kr data could not match the observed gas and condensate production profiles even after several sensitivity analysis and kr data tuning. However, after replacing the

GC-kr data with a newly measure steady state CO_2-GC-kr data, good match was obtained for the gas production profile and fairly good match for the first two cycles of post CO_2 injection.

Generally, the efficiency of an optimised H-n-P CO_2 injection technique has be tested and proven to be efficient from lab scale study and corresponding numerical simulation work was conducted to investigate and confirm vaporisation as the dominant observed recovery mechanism responsible for the additional condensate recovery. This H-n-P CO_2 injection technique provides a combined advantage of improved condensate recovery and CO_2 storage relative to the conventional H-n-P CO_2 injection technique. By implementing the proposed technique, similar additional recovery can be achieved albeit with much lesser CO_2 injected and produced which also results in improved CO_2 storage efficiency. These results not only improve the current understanding of CO_2 injection applications for EGR and storage purposes but also helps to significantly reduce the overhead operational cost and increase the benefits of CO_2 injection making implementation of such a technique more attractive for field applications. These will in turn should help in meeting global energy demands whilst addressing the negative impact of global warming by storing more CO_2 under geological formations, which currently suffer from high operation cost.

6.3 Recommendations

This section presents some recommendations for further consideration following the work carried out in this research. It is important to mention that some simplifying assumptions were made to during the experimental and simulation analysis that can be relaxed.

- In this study, the PVT analysis was conducted initially on a binary mixture and then on a ternary mixture with the addition of hexadecane as the heaviest hydrocarbon component. The phase behaviour analysis when both fluid mixtures were contacted with CO_2 following the proposed injection schedule showed no significant changes in both the dew point pressure and liquid dropout. This should be further investigated by conducting the phase behaviour tests on real fluids at reservoir conditions for more conclusive results.

- In this study, the core flood analysis was performed on three different rock types with different rock properties including permeability, porosity, and pore volume. All three rock samples were assumed to homogenous with uniform permeability and porosity across the entire cross-section of the cores. It proposed to study the effect of reservoir heterogeneity on the proposed recovery technique presented in the work. Also, the effect of wettability alteration, dissolution of carbonate minerals, which were not considered for the study should be thoroughly investigated to evaluate their any potential impact it may present when implementing the proposed injection technique.

- In this study, when conducting the CO_2-GC relative permeability experiment, the test fluid was a mixture of CO_2, C1, and C8 with combination ration of 4.0 5.4, and 0.6 respectively. The test fluid was pre-equilibrated during the kr measurement. This eliminated any effects of mass transfer between phases as fluid flow at the different injection rates. This is in line with the existing EOS modelling approach in compositional numerical simulator that assume instantaneous equilibrium between the two phases. These assumptions be responsible for the poor prediction and history match of the condensate recovery during third and fourth cycles by the simulation model. It is highly recommended to further investigate the effect of these assumptions.

References

AAPG Wiki. (January 2014) https://wiki.aapg.org/File:Petroleum-reservoir-fluid-properties_fig1.png

Afidick, D., Kaczorowski, N. & Bette, S. (1994). Production performance of a retrograde gas reservoir: a case study of the Arun Field. *SPE - Asia Pacific Oil & Gas Conference*

Ahmadi, M., Sharma, M. M., Pope, G. A., Torres, D. E., McCulley, C. A., & Linnemeyer, H. (2011). Chemical treatment to mitigate condensate and water blocking in gas wells in carbonate reservoirs. *SPE Production and Operations*, *26*(1), 67–74.

Ahmed, T., Evans, J., Kwan, R., & Vivian, T. (1998). Wellbore liquid blockage in gas-condensate reservoirs. *Proceedings - SPE Annual Western Regional Meeting*, 119–129.

Al-Abri, A., & Amin, R. (2010). Phase Behaviour, Fluid Properties and Recovery Efficiency of Immiscible and Miscible Condensate Displacements by SCCO 2 Injection: Experimental Investigation. *Transport in Porous Media*, *85*(3), 743–756.

Al-anazi, H. A., Aramco, S., Pope, G. A., & Sharma, M. M. (2002). SPE 77546 Laboratory Measurements of Condensate Blocking and Treatment for Both Low and High Permeability Rocks.

Al-anazi, H. A., Aramco, S., Sharma, M. M., & Pope, G. A. (2004). SPE 90860 Revapourization of Condensate with Methane Flood, 1–7.

Ashwani Kumar. (2020). Experimental setup for CO_2 injection for Enhance Shale Gas Recovery (ESGR) - A Review. *International Journal of Engineering Research And*, *V9*(09), 422–434.

Ayub, M., & Ramadan, M. (2019). Mitigation of near wellbore gas-condensate by CO 2 huff-n-puff injection: A simulation study. *Journal of Petroleum Science and Engineering*, *175*(October 2018), 998–1027.

Bennion, D. B., Thomas, F. B., & Schulmeister, B. (2001). Retrograde Condensate Dropout Phenomena in Rich Gas Reservoirs — Impact on Recoverable Reserves , Permeability , Diagnosis , and Stimulation Techniques Potential Problems Associated with Rich, *40*(12), 5–8.

Chunmei Shi. (2005). Flow Behavoir of Gas-Condensate Wells, (June).

Cui, G., Zhang, L., Ren, B., Zhuang, Y., Li, X., Ren, S., & Wang, X. (2015). Geothermal Exploitation with Considering CO_2 Mineral Sequestration in High Temperature Depleted Gas Reservoir by CO_2 Injection. *Carbon Management Technology Conference*.

Danesh, A., Krinis, D., Henderson, G. D., & Peden, J. M. (1989). Pore-level visual investigation of miscible and immiscible displacements. *Journal of Petroleum Science and Engineering*, *2*(2–3), 167–177.

Danesh, All, Henderson, G. D., & Peden, J. M. (1991). Experimental investigation of critical condensate saturation and its dependence on interstitial water saturation in water-wet rocks. *SPE Reservoir Engineering (Society of Petroleum Engineers)*, *6*(3), 336–342.

Darvish, G., Lindeberg, E., Holt, T., Kleppe, J., & Utne, S. (2007). Laboratory Experiments of Tertiary CO_2 Injection Into a Fractured Core.

Dindoruk, B., Johns, R., & Orr, F. M. (2021). Measurement and modelling of minimum miscibility pressure: A state-of-the-art review. *SPE Reservoir Evaluation and Engineering*, *24*(2), 367–389.

Ding, J., Cao, T., & Wu, J. (2019). Experimental investigation of supercritical CO_2

injection for enhanced gas recovery in tight gas reservoir. In *Carbon Management Technology Conference 2019, CMTC 2019*.

Einstein, M. A., Gerder Castillo, Y. C., & Gil, J. C. (2007). A Novel Improved Condensate-Recovery Method by Cyclic Supercritical CO_2 Injection. *Latin American & Caribbean Petroleum Engineering Conference*.

El Cheikh Ali, N., Zoghbi, B., Fahes, M., Nasrabadi, H., & Retnanto, A. (2019). The impact of near-wellbore wettability on the production of gas and condensate: Insights from experiments and simulations. *Journal of Petroleum Science and Engineering*, *175*(October 2018), 215–223.

El Gohary, M., Al Bairaq, A., Al Hashemi, H. H., Abed, A., Saeed, Y., Torrens, R., & Kumar, A. (2014). Integrated simulation study of a gas condensate field with nitrogen and hydrocarbon recycling. *Society of Petroleum Engineers - 30th Abu Dhabi International Petroleum Exhibition and Conference, ADIPEC 2014: Challenges and Opportunities for the Next 30 Years*, *4*, 3128–3138.

Eshkalak, M. O., Al-shalabi, E. W., Sanaei, A., Aybar, U., & Sepehrnoori, K. (2014). Enhanced Gas Recovery by CO_2 Sequestration versus Re-fracturing. *Spe-172083-Ms*.

Fahimpour, J., Jamiolahmady, M. & Shrabi. M. (2012). A Combined Experimental and Theoretical Investigation on Application of Wettability Modifiers in Gas-Condensate Reservoirs. *SPE Annual Technical Conference and Exhibition, San Antonio, Texas, USA, October 2012*.

Fahimpour, J., & Jamiolahmady, M. (2014). Impact of gas-condensate composition and interfacial tension on oil-repellency strength of wettability modifiers. *Energy and Fuels*, *28*(11), 6714–6722.

Fahimpour, J., & Jamiolahmady, M. (2015). An improved understanding of performance of wettability alteration for condensate banking removal under steady-

state flow conditions. *Society of Petroleum Engineers - Abu Dhabi International Petroleum Exhibition and Conference, ADIPEC 2015*, 1–18.

Fevang, Ø., & Whitson, C. H. (1996). Modelling Gas-Condensate Well Deliverability. *SPE Reservoir Engineering (Society of Petroleum Engineers)*, *11*(4), 221–230.

Gachuz-Muro, H., Gonzalez Valtierra, B. E., Luna, E. E., & Aguilar Lopez, B. (2011). Laboratory Tests with CO_2, N_2 and Lean Natural Gas in a Naturally Fractured Gas-Condensate Reservoir under HP/HT Conditions. *SPE EOR Conference*.

Ghahri, P., Alatefi, S., & Jamiolahmady, M. (2015). A new, accurate and simple model for calculation of horizontal well productivity in gas and gas condensate reservoirs. *Europec 2015*, (June), 720–749.

Ghahri, Panteha, Jamiolahmadi, M., Alatefi, E., Wilkinson, D., Sedighi Dehkordi, F., & Hamidi, H. (2015). A new and simple model for the prediction of horizontal well productivity in gas condensate reservoirs. *EUROPEC 2015*, *223*, 431–450.

Ghaleb Al Habsi, SOheil Ghanbarzadeh, Motealleh, S., & Badar Al Busafi. (2019). Hydraulic Fracturing: Best Remedy for Condensate Banking Effects in Tight Gas-Condensate Reservoirs. *SPE*.

Hassan, A., Mahmoud, M., Al-Majed, A., Alawi, M. B., Elkatatny, S., BaTaweel, M., & Al-Nakhli, A. (2019). Gas condensate treatment: A critical review of materials, methods, field applications, and new solutions. *Journal of Petroleum Science and Engineering*, *177*(February), 602–613.

Hassanzadeh Khadar, R., Aminshahidy, B., Hashemi, A., & Ghadami, N. (2013). Application of gas injection and recycling to enhance condensate recovery. *Petroleum Science and Technology*, *31*(10), 1057–1065.

Henderson, G. D., Danesh, A., Tehrani, D. H., Al-Shaidi, S., Peden, J. M., & Heriot-Watt, U. (1996). Measurement and Correlation of Gas Condensate Relative Permeability by the Steady-State Method. *SPE Reservoir Engineering (Society of Petroleum Engineers)*, *1*(2), 134–139.

Henderson, G. D., Danesh, A., Tehrani, D. H., Al-Shaidi, S., Peden, J. M., & Heriot-Watt, U. (1998). Measurement and Correlation of Gas Condensate Relative Permeability by the Steady-State Method. *SPE Reservoir Engineering (Society of Petroleum Engineers)*, *1*(2), 134–139.

Herderson, G. D., Danesh, A., & Tehrani, D. H. (2001). Effect of positive rate sensitivity and inertia on gas condensate relative permeability at high velocity. *Petroleum Geoscience*, *7*(1), 45–50.

Høier, L., & Whitson, C. H. (1998a). Miscibility variation in compositionally grading reservoirs. *Proceedings - SPE Annual Technical Conference and Exhibition*, *1999-Septe*(February).

Høier, L., & Whitson, C. H. (1998b). Miscibility variation in compositionally grading reservoirs. *Proceedings - SPE Annual Technical Conference and Exhibition*, *1999*.

Holm, L. W., & Josendal, V. A. (1982). Effect of Oil Composition on Miscible-Type Displacement by Carbon Dioxide. *Society of Petroleum Engineers Journal*, *22*(01), 87–98

Honari, A. (2016). Enhanced Gas Recovery By Carbon Dioxide Sequestration : Elucidating the Physics of Mixing Between Carbon Dioxide and Methane in, (March).

Hou, D., Xiao, Y., Pan, Y., Sun, L., & Li, K. (2016). Experiment and Simulation Study on the Special Phase Behaviour of Huachang Near-Critical Condensate Gas Reservoir Fluid. *Journal of Chemistry*, *2016*, 1–10.

Husiyandi Husni, & Jamiolahmady, M. (2017). *Chemical Treatment to Alleviate Condensate Banking*. *MSc Project Report*.

Iddphonce, R., Wang, J., & Zhao, L. (2020). Review of CO_2 injection techniques for enhanced shale gas recovery: Prospect and challenges. *Journal of Natural Gas Science and Engineering*, *77*(April 2019), 103240.

Jamiolahmady, M., Ghahri, P., Victor, O. E., & Danesh, A. (2007). Comparison of vertical, slanted and horizontal wells productivity in layered gas-condensate reservoirs. *69th European Association of Geoscientists and Engineers Conference and Exhibition 2007: Securing The Future. Incorporating SPE EUROPEC 2007*, *6*, 3808–3814.

Jamiolahmady, M., Mahdiyar, H., Ghahri, P., & Sohrabi, M. (2011). A new method for productivity calculation of perforated wells in Gas condensate reservoirs. *Journal of Petroleum Science and Engineering*, *77*(3–4), 263–273.

Jamiolahmady, M., Sohrabi, M., Ghahri, P., & Ireland, S. (2010). Gas/condensate relative permeability of a low permeability core: Coupling vs. inertia. *SPE Reservoir Evaluation and Engineering*, *13*(2), 214–227.

Jamiolahmady, M., Sohrabi, M., & Ireland, S. (2009). Gas condensate relative permeability of low permeability rocks: Coupling versus inertia. *SPE Middle East Oil and Gas Show and Conference, MEOS, Proceedings*, *2*, 522–535.

Jamiolahmady, M., Sohrabi, M., Ireland, S., & Ghahri, P. (2009). A generalised correlation for predicting gas-condensate relative permeability at near wellbore conditions. *Journal of Petroleum Science and Engineering*, *66*(3–4), 98–110.

Jamiolahmady, Mahmoud, Danesh, A., Tehrani, D. H., & Sohrabi, M. (2006). Variations of gas/condensate relative permeability with production rate at near-wellbore conditions: A general correlation. *SPE RE-Engineering*, *9*(6), 688–697.

Jessen, K., & Orr, F. M. (2004). Gas cycling and the development of miscibility in condensate reservoirs. *SPE Reservoir Evaluation and Engineering*, *7*(5), 334–341.

Jia, Y., Shi, Y., Exploration, P., Huang, L., Yan, J., Exploration, P., & Sun, L. (2019). SPE-195493-MS The Feasibility Appraisal for CO_2 Injection and Storage in Condensate Gas Reservoir : Mechanism Studies and Case Analysis.

Khan, C., Amin, R., & Madden, G. (2013). Carbon dioxide injection for enhanced gas recovery and storage (reservoir simulation). *Egyptian Journal of Petroleum*, *22*(2), 225–240.

Khazam, M. M., Abu Grin, Z. Y., Elhajjaji, R. R., & Sherik, A. A. (2017). The Impact of Condensate Blockage on Gas Well Deliverability - Part 1, (November), 2–4.

Kumar, A., Gohary, M. E., Pedersen, K. S., & Azeem, J. (2015). Gas Injection as an Enhanced Recovery Technique for Gas Condensates. A comparison of three Injection Gases. *Abu Dhabi International PEC*, (2014), 1–13.

Kumar, V., Bang, V., Pope, G. A., & Sharma, M. M. (2006). SPE 102669 Chemical Stimulation of Gas / Condensate Reservoirs. *SPE Annual Technical Conference and Exhibition Held in San Antonio, Texas, U.S.A., 24–27 September 2006.*

Kusumawati, I., & Jamiolahmady, M. (2009). Alleviation of Condensate Banking by CO2 Injection in Gas Condensate Reservoir.

Leeuwenburgh, O., Neele, F., Hofstee, C., Weijermans, P. J., De Boer, H., Oosthoek, P., Gutierrez-Neri, M. (2014). Enhanced gas recovery - A potential "U" for CCUS in the netherlands. *Energy Procedia*, *63*, 7809–7820.

Linderman, J., Al-Jenaibi, F., Ghori, S., Putney, K., Lawrence, J., Gallet, M., & Hohensee, K. (2008). Substituting nitrogen for hydrocarbon gas in a gas cycling project. *Society of Petroleum Engineers - 13th Abu Dhabi International Petroleum*

Exhibition and Conference, ADIPEC 2008, *2*, 986–995.

Liu, B., Shi, J., Sun, B., Shen, Y., Zhang, J., Chen, X., & Wang, M. (2015). Molecular dynamics simulation on volume swelling of CO_2-alkane system. *Fuel*, *143*, 194–201.

Mahdiyar, H., Jamiolahmady, M., & Sohrabi, M. (2009). Optimization of hydraulic fracture geometry. *Society of Petroleum Engineers - Offshore Europe Oil and Gas Conference and Exhibition 2009, OE 2009*, *1*(2002), 125–147.

Marokane, D., Logmo-Ngog, A. B., & Sarkar, R. (2002). Applicability of Timely Gas Injection in Gas Condensate Fields to Improve Well Productivity. *Proceedings - SPE Symposium on Improved Oil Recovery*, 244–259. https://doi.org/10.2523/75147-ms

Meng, X., Meng, Z., Ma, J., & Wang, T. (2019). Performance evaluation of CO_2 huff-n-puff gas injection in shale gas condensate reservoirs. *Energies*, *12*(1).

Meng, X., & Sheng, J. J. (2016a). Experimental and numerical study of huff-n-puff gas injection to re-vapourise liquid dropout in shale gas condensate reservoirs. *Journal of Natural Gas Science and Engineering*, *35*, 444–454.

Meng, X., & Sheng, J. J. (2016b). Experimental Study on Revapourization Mechanism of Huff-n-Puff Gas Injection to Enhance Condensate Recovery in Shale Gas Condensate.

Meng, X., Sheng, J. J., & Yu, Y. (2015). Evaluation of enhanced condensate recovery potential in shale plays by huff-n-puff gas injection. *SPE ERM*, *2015-Janua*.

Meng, X., Yu, Y., Sheng, J. J., Watson, M., & Mody, F. (2015). An experimental study on huff-n-puff gas injection to enhance condensate recovery in shale gas reservoirs. *Society of Petroleum Engineers, URTeC 2015*.

Miller, N., Nasrabadi, H., & Zhu, D. (2010). On Application of Horizontal Wells to Reduce Condensate Blockage in Gas Condensate Reservoirs. *International Oil and Gas Conference and Exhibition in China*, (McCain 1990), 1–15.

Mithani, A. H., & Jamiolahmady, M. (2018). MSc (Petroleum Engineering) Project Report 2017 / 2018 Aijaz Hussain Mithani Condensate Bank Removal Using Hydrocarbon Gases and CO_2 in a Real Gas Field in Africa School of Energy Geoscience Infrastructure and Society Institute of Petroleum Engineering.

Mogbo, O. (2011). SPE 150752 CO_2 EOR and Sequestration in a Depleted Gas-condensate Reservoir: UKNS Case Study. *Work*.

Mohamadi-Baghmolaei, M., Azin, R., Osfouri, S., & Zendehboudi, S. (2019). Evaluation of mass transfer coefficient for gas condensates in porous systems: Experimental and modelling. *Fuel*, *255*(May), 115507.

Mohammed, N., Abbas, A. J., Enyi, G. C., Suleiman, S. M., Edem, D. E., & Abba, M. K. (2020). Alternating N2 gas injection as a potential technique for enhanced gas recovery and CO_2 storage in consolidated rocks: an experimental study. *Journal of Petroleum Exploration and Production Technology*, *10*(8), 3883–3903.

Mohsin, A., Abd, A. S., & Abushaikha, A. (2021). Modelling Condensate Banking Mitigation by Enhanced Gas Recovery Methods.

Monger, T. G., & Khakoo, A. (1981). Phase Behaviour Of CO_2 - Appalachian Oil Systems. In *Society of Petroleum Engineers of AIME, (Paper) SPE*.

Monger, T. G., Ramos, J. C., & Thomas, J. (1988). Light oil recovery from cyclic CO_2 injection: influence of low pressures, impure CO_2, and reservoir gas, (February).

Monger, Teresa G., & Coma, J. M. (1988). Laboratory and field evaluation of the CO_2 huff "n" puff process for light-oil recovery. *SPE Reservoir Engineering (Society*

of Petroleum Engineers), *3*(4), 1168–1176.

Moses, P. L., & Wilson, K. (1981). Phase Equilibrium Considerations in Using Nitrogen for Improved Recovery From Retrograde Condensate Reservoirs. *JPT, Journal of Petroleum Technology*, *33*(2), 256–262.

Narinesingh, J., & Alexander, D. (2014). CO2Enhanced gas recovery and geologic sequestration in condensate reservoir: A simulation study of the effects of injection pressure on condensate recovery from reservoir and CO_2 storage efficiency. *Energy Procedia*, *63*, 3107–3115.

Nasiri Ghiri, M., Nasriani, H. R., Sinaei, M., Najibi, S. H., Nasriani, E., & Parchami, H. (2015). Gas Injection for Enhancement of Condensate Recovery in a Gas Condensate Reservoir. *Energy Sources, Part A: Recovery, Utilization and Environmental Effects*, *37*(8), 799–806.

Nasriani, H. R., Borazjani, A. A., Sinaei, M., & Hashemi, A. (2014). The effect of gas injection on the enhancement of condensate recovery in gas condensate reservoirs: A comparison between a synthetic model and PVT cell results. *PST*, *32*(5), 593–601.

Nekoeian, S., Aghajani, M., & Alavi, S. M. (2019). Experimental study of gas phase mass transfer coefficients in gas condensate reservoirs. *Journal of Petroleum Science and Engineering*, *173*(September 2018), 1210–1221.

Odi, U. (2012a). Analysis and potential of CO_2 Huff-n-Puff for near wellbore condensate removal and enhanced gas recovery. *Proceedings - SPE Annual Technical Conference and Exhibition*, *6*, 4877–4896.

Odi, U. (2012b). Analysis and Potential of CO_2 Huff-n-Puff for Near Wellbore Condensate Removal and Enhanced Gas Recovery. *SPE Annual Technical Conference and Exhibition*, (October), 8–10.

Reis, P. K. P., & Carvalho, M. S. (2022). Pore-scale analysis of gas injection in gas-condensate reservoirs. *Journal of Petroleum Science and Engineering*, *212*, 1–34.

Renner, T. A., Metcalfe, R. S., Spencer, M. F., & Yellig, W. F. (1987). Displacement of a rich gas condensate by nitrogen: laboratory corefloods and numerical simulations.

Sadooni, M., & Zonnouri, A. (2015). The effect of nitrogen injection on production improvement in an iranian rich gas condensate reservoir. *Petroleum Science and Technology*, *33*(4), 422–429.

Samuel, R. (2020). Transient Flow Modelling of Carbon Dioxide (CO_2) Injection into Depleted Gas Department of Chemical Engineering, (October 2019).

Sanger, P. J., Bjornstad, H. K., & Hagoort, J. (1994). Nitrogen injection into stratified gas-condensate reservoirs. *Proceedings - SPE Annual Technical Conference and Exhibition*, *Sigma*(pt 2), 507–511.

Sayed, M. A., & Al-Muntasheri, G. A. (2014). Liquid bank removal in production wells drilled in gas-condensate reservoirs: A critical review. *SPE - European Formation Damage Conference, Proceedings, EFDC*, *1*(1), 425–449.

Sayed, M. A., Company, A. S., Al-muntasheri, G. A., & Company, A. S. (2016). SPE-168153-PA.pdf, (May).

Sayed, M., Liang, F., & Ow, H. (2018). Novel surface modified nanoparticles for long-lasting mitigation of water and condensate blockage in gas reservoirs. *In Proceedings of the AOTC* (Vol. 6, pp. 4571–4585).

Seteyeobot, I., Jamiolahmady, M., & Jaeger, P. (2021). SPE-206117-MS An Experimental Study of the Effects of CO_2 Injection on Gas / Condensate Recovery and CO_2 Storage in Gas-Condensate Reservoirs.

Seteyeobot, I., Orodu, O. D., Anawe, P. A. L., Enaworu, E., & Onuh, C. (2016). Modelling the effect of composition change during condensate dropout in a horizontal gas well. *Society of Petroleum Engineers - SPE Russian Petroleum Technology Conference and Exhibition 2016*, (January).

Sheng, J., Sheng, J. J., & Li, L. (2016). A comparison study on huff-n-puff gas injection and chemical relative permeability modification to mitigate condensate blocking in fractured shale gas condensate reservoirs. *Society of Petroleum Engineers - SPE Low Perm Symposium*.

Shtepani, E. (2006). CO_2 sequestration in depleted gas/condensate reservoirs. *Proceedings - SPE Annual Technical Conference and Exhibition*.

Shtepani, E., Thomas, F. B., & Energy, H. (2006). an Experimental Approach of CO_2 Sequestration in Gas Condensate Reservoirs. *Carbon*, 1–12.

Siregar, S., Hagoort, J., & Ronde, H. (1992). Prototype gas. *Spe*, *SPE 22360*(paper was prepared for presentation at the SPE International Meeting on Petroleum Engineering held in Beijing, China, 24-27 March 1992,), 281–291.

Soltan Sleiman, Jamiolahmady, M., & seteyeobot Ifeanyi. (2021). Master of Science Thesis Impact of addition of N_2 , CO_2 and CO_2 / N_2 combination on Gas-Condensate fluids phase behaviour Author : Supervisor : A thesis submitted in fulfilment of the requirements for the MSc degree . in the, (March).

Su, Z., Tang, Y., Ruan, H., Wang, Y., & Wei, X. (2017). Experimental and modelling study of CO_2-Improved gas recovery in gas condensate reservoir. *Petroleum*, *3*(1), 87–95.

Subero, C. L. (2009). *Numerical modelling of nitrogen injection into gas condensate reservoir*. West Virginia University Follow.

Todd Hoffman, B., & Reichhardt, D. (2020). Quantitative evaluation of recovery mechanisms for huff-n-puff gas injection in unconventional reservoirs. *SPE/AAPG/SEG, URTeC 2020*, 1–15.

Vijayvargia, U., Jamiolahmady, M., Nakhli, A. R., & Yi, N. K. (2019). Clean-up efficiency of multiple fractured horizontal wells enhanced by reactive chemicals in tight gas homogeneous & naturally fractured reservoirs. *SPE Middle East Oil and Gas Show and Conference, MEOS, Proceedings*, *2019-March*.

Vo, H. X., & Horne, R. N. (2016). Compositional Variation Study for Improving Recovery in Gas-Condensate Reservoirs. *Proceedings of the 4th Unconventional Resources Technology Conference*.

Wang, Z., Zhu, S., Zhou, W., Liu, H., Hu, Y., Guo, P., … Ren, J. (2018). Experimental research of condensate blockage and mitigating effect of gas injection. *Petroleum*, *4*(3), 292–299.

Wheaton, R. J., & Zhang, H. R. (2000). Condensate banking dynamics in gas condensate fields: Compositional changes and condensate accumulation around production wells. *SPE Reservoir Engineering (Society of Petroleum Engineers)*, (B), 153–166.

Zhang, A., Fan, Z., & Zhao, L. (2020). An investigation on phase behaviours and displacement mechanisms of gas injection in gas condensate reservoir. *Fuel*, *268*(January), 117373.

Zhang, Y. P., Sayegh, S. G., Huang, S., & Dong, M. (2004). Laboratory investigation of enhanced light-oil recovery by CO_2/flue gas huff-n-puff process. *Canadian International Petroleum Conference 2004, CIPC 2004*, (3), 1–13.

Zhengyuan, S., Yong, T., Hongjiang, R., Yang, W., & Xiaoping, W. (2017). Experimental and modelling study of CO_2 - Improved gas recovery in gas condensate reservoir. Advanced Research Evliving Science (Petroleum), 87-95.